NUMERICAL MODELING AND PARAMETRIC STUDY OF NATM TUNNELS SUPPORTED BY UMBRELLA ARCH

by

Hakkı Erman Ergincan

B.S., Civil Engineering, Middle East Technical University, 2020

Submitted to the Institute for Graduate Studies in
Science and Engineering in partial fulfillment of
the requirements for the degree of
Master of Science

Graduate Program in Civil Engineering
Boğaziçi University

2024

To my sister and my mother,
who will never be able to read this;
and to the workers who lost their lives in tunnels.

ACKNOWLEDGEMENTS

First of all, I owe my thesis supervisor Assist. Prof. İrem Zeynep Yıldırım a debt of gratitude, for her courage, and unwavering support. Neither starting nor proceeding nor finishing this thesis would have been possible without her close interest, meticulous guidance, and devoted effort. I feel very lucky since I have had the opportunity to become her student.

I am also indebted to my thesis co-supervisor Assist. Prof. Tolga Yılmaz Özüdoğru for his noble consent to accompany us throughout the studies. I would like to thank him for sparing his valuable time. This work has been catalyzed by his patience, understanding, wise guidance and magical touches.

I would like to thank Prof. Özer Çinicioğlu, and Assist. Prof. Mustafa Hatipoğlu for their kind acceptance to serve on my thesis committee and generous feedback to clarify the thesis.

I would also like to thank all of my workmates who provide a nice environment to study in, and in particular,my chiefs Tuğçe Perveroğlu Şat, Emirhan Selçuk and Orhan Koca for their helpfulness in sharing their experience and knowledge that feeds this study.

Most of all, I am grateful to Fazıl Sungun Ergincan. He, not only as a father but also as a chief, made me the luckiest person in the world with his firm trust and endless support. His presence is enough to be strong, vigorous, and brave while struggling, studying, and working. I hope that I do not disappoint him throughout my life and can make him proud with this academic study.

I would like to acknowledge my friends who have motivated and tolerated me during the challenges of life, going simultaneously in the aspects of academic, political, professional, and social. I extend my special thanks to my long-time pal Yiğit Talas, who has always shared his support using every means available.

Also, I would like to acknowledge İstanbul Metropolitan Municipality Rail System Department Anatolian Side Rail Systems Directorate for the official allowance to use the information and data relevant to Çekmeköy-Sancaktepe-Sultanbeyli Metro Line project in this study. For some parts of this work, I am also glad to be financially supported by Boğazici University within the frame of Scientific Research Projects (BAP) numbered 16961.

Last but not least, thanks to the heroic Turkish people is a must for me. Whatever I have been able to contribute with this work is thanks to their devoted lives to defend the land, save independence and sovereignty, found the republic, provide public education, and bring the progressive generations up.

ABSTRACT

NUMERICAL MODELING AND PARAMETRIC STUDY OF NATM TUNNELS SUPPORTED BY UMBRELLA ARCH

In this numeric study, the behaviors of tunnels supported by the umbrella arch method were investigated parametrically through two-dimensional (2D) finite element models. Firstly, the numerical modeling concept was validated principally by comparing the results of the models with the real measurements taken from two different twin tunnel sections excavated with the New Austrian Tunnel Method (NATM) and supported by the umbrella arch (UA) located in the Çekmeköy-Sancaktepe-Sultanbeyli Metro Line project. For the validation, the models were created with three different approaches called plate (P), dummy plate (DP), and individual pipe (IP) in the literature, and their appropriateness was evaluated. All three approaches succeeded in predicting the surface settlement with an acceptable error margin. In comparison with the two others, DP approach predicted the real site data more precisely, and it was adopted to proceed with the parametric studies. Based on the validation study, by using constant deconfinement ratios, a total of 162 models were created for the parametric study with and without UA as a combination of three tunnel diameters, three overburden depths, three clear distance ratios between twin tunnels, and three soil conditions. These models were analyzed comparatively in terms of forces and displacements. The results indicated that maximum vertical displacement governs the maximum resultant displacement in tunnels, and surface volume loss (V_S) increases as inner tunnel volume loss (V_L) increases, and V_L increases as ground conditions worsen. Their ratio (V_S/ V_L) decreased with the reduction in tunnel diameter (D) or overburden depth (C). The results showed that the twin tunnels converge differently due to geometry and ground conditions, and this difference causes asymmetric settlement profiles, which may also include two peaks as the distance between tunnels increases and C/D decreases. In the aspect of forces on support elements, the factor of safety increases as tunnel diameter gets smaller, overburden depth gets shallower, clear distance gets larger, and ground condition gets better. The results implied the importance of deconfinement ratio to simulate UA effect in 2D.

ÖZET

BORU KEMER YÖNTEMİYLE DESTEKLENEN NATM TÜNELLERİN SAYISAL MODELLEMESİ VE PARAMETRİK ÇALIŞMASI

Bu sayısal çalışmada, şemsiye kemer yöntemiyle desteklenen tünellerin davranışları iki boyutlu (2D) sonlu eleman modelleri aracılığıyla parametrik olarak incelenmiştir. İlk olarak, sayısal modelleme konsepti, modellerin sonuçlarının Çekmeköy-Sancaktepe-Sultanbeyli Metro Hattı projesinde yer alan Yeni Avusturya Tünel Yöntemi (NATM) ile kazılan ve şemsiye kemer (UA) ile desteklenen iki farklı ikiz tünel kesitinden alınan gerçek ölçümlerle karşılaştırak ilkesel olarak doğrulanmıştır. Doğrulama için literatürde plaka (P), suni plaka (DP) ve tekil boru (IP) olarak adlandırılan üç farklı yaklaşımla modeller oluşturulmuş ve uygunlukları değerlendirilmiştir. Her üç yaklaşım da kabul edilebilir bir hata payıyla yüzey oturmasını tahmin etmede başarılı olmuştur. Diğer iki yaklaşımla karşılaştırıldığında, DP yaklaşımı gerçek saha verilerini daha hassas bir şekilde tahmin etmiş ve parametrik çalışmalara devam etmek için benimsenmiştir. Doğrulama çalışması temelinde, sabit gevşetme oranları kullanılarak, üç tünel çapı, üç örtü kalınlığı, ikiz tüneller arasındaki üç temiz açıklık oranı ve üç zemin koşulunun kombinasyonu olarak UA'lı ve UA'sız parametrik çalışma için toplam 162 model oluşturulmuştur. Bu modeller kuvvetler ve yer değiştirmeler açısından karşılaştırmalı olarak analiz edilmiştir. Sonuçlar, maksimum düşey yer değiştirmenin tünellerdeki maksimum bileşke yer değiştirmeye hükmettiğini, tünel içi hacim kaybı (V_L) arttıkça yüzey hacim kaybının (V_S) arttığını ve zemin durumu zayıfladıkça V_L arttığını göstermiştir. Bunların oranı (V_S/ V_L) tünel çapındaki (D) veya örtü kalınlığındaki (C) azalmayla düşmüştür. Sonuçlar, ikiz tünellerin geometri ve zemin koşulları nedeniyle farklı şekilde kapandığını, bu farklılıkğın tüneller arasındaki mesafe arttıkça ve C/D azaldıkça iki tepe noktası da içerebilen asimetrik oturma profillerine neden olduğunu göstermiştir. Destek elemanları üzerindeki kuvvetler açısından, tünel çapı küçüldükçe, örtü kalınlığı sığlaştıkça, açıklık mesafesi arttıkça ve zemin durumu iyileştikçe güvenlik faktörü artmaktadır. Sonuçlar, UA'nın 2D'deki etkisini simüle etmek için gevşeme oranının önemini ortaya koymuştur.

TABLE OF CONTENTS

ACKNOWLEDGEMENTS iv
ABSTRACT vi
ÖZET vii
LIST OF FIGURES x
LIST OF TABLES xv
LIST OF SYMBOLS xvii
LIST OF ACRONYMS / ABBREVIATONS xix
1. INTRODUCTION 1
1.1. General 1
1.2. Objectives 3
1.3. Scope 4
2. LITERATURE REVIEW 6
2.1. Tunnels 6
2.2. Tunneling Methods 6
2.3. Support Systems 9
2.3.1. Umbrella Arch 20
2.4. Tunnel Analyzing Methods 25
2.4.1. Empirical Methods 25
2.4.2. Analytical Methods 26
2.4.3. Numerical Methods 29
2.4.3.1. Finite Difference Method (FDM) 30
2.4.3.2. Finite Element Method (FEM) 30
2.5. Effecting Parameters 31
2.5.1. Improvement Zone 32
2.5.2. Overburden Depth 36
2.5.3. Tunnel Diameter 37
2.5.4. Ground Conditions 37
2.5.5. Distance Between Twin Tunnels 39
3. VALIDATION STUDY 41
3.1. FEM Model 41

3.1.1. FEM Modeling Approaches for UA Application 42
3.1.1.1. Plate (P) Approach 44
3.1.1.2. Dummy Plate (DP) Approach 44
3.1.1.3. Individual Pipe (IP) Approach 44
3.2. Instrumented Case Studies Investigated for the Validation Study 45
3.2.1. Assumptions 48
3.2.2. Excavation Stages 49
3.3. Results of the Validation Studies 52
3.3.1. Results of the Analysis for the Instrumented Studies 52
3.3.2. Discussion of the Comparative Findings 55
4. RESARCH METHODOLOGY FOR THE PARAMETRIC STUDY 56
4.1. Approach for the Parametric Study 56
4.2. Parameter Selection for the Numerical Analysis 60
4.2.1. Geometric Parameters 60
4.2.2. Soil and UA Material Properties 61
5. RESULTS AND DISCUSSION OF THE PARAMETRIC STUDY 65
5.1. Umbrella Arch Application 65
5.2. Settlement Profiles 68
5.3. Maximum Settlement Value (S_{max}) and Its Coordinate (skewness) 73
5.4. Volume Loss in Tunnels and on Surface 77
5.5. Convergence 84
5.6. Forces on Support Elements 89
6. CONCLUSION AND RECOMMENDATIONS 96
REFERENCES 100
APPENDIX A: DATA USE PERMISSION FOR ACADEMIC PURPOSES 114
APPENDIX B: VISUAL REUSE PERMISSION 115

LIST OF FIGURES

Figure 2.1. A tunnel example from İstanbul, constructed with the cut-and-cover method. 7

Figure 2.2. A special tunnel example from İstanbul, performed with TBM method. 8

Figure 2.3. Ground reaction curve and support reaction curve graph exported from RocSupport Tutorial 1 (modified from RocScience, 2004). 13

Figure 2.4. Excavation and lining sequence of the “old” Austrian tunneling method. 14

Figure 2.5. The view of metro pedestrian tunnels constructed and operated in İstanbul without permanent concrete lining. 16

Figure 2.6. Correlation chart (modified after Karahan, 2010; Barış & Mahmutoğlu, 2018; Türköz, 2023). 19

Figure 2.7. UA applied longitudinal tunnel section sketch simplified from Çekmeköy-Sancaktepe-Sultanbeyli Metro Project located in İstanbul, Türkiye. 21

Figure 2.8. Enlarging cross-section of UA application sketch simplified from Çekmeköy-Sancaktepe-Sultanbeyli Metro Project located in İstanbul, Türkiye. 22

Figure 2.9. Adoption reasons for injected steel pipe umbrella method (modified after Muraki, 1997). 24

Figure 2.10. Beam model approaches (modified after Marotta, 2013). 28

Figure 3.1. The sketches of the evaluated approaches for the validation study: (a) Plate Approach (P), (b) Dummy Plate Approach (b), (c) Individual Pipe Approach (P) (modified after Ergincan et al., 2024). 43

Figure 3.2. The plan views of the specified inspection areas for validation study (a) Case1 (modified after Ergincan et al., 2023) and (b) Case2 (modified after Ergincan et al., 2024). 46

Figure 3.3. The numerical modeling phases appointed for the UA applied twin NATM tunnel sections in the validation studies (adopted from Ergincan et al., 2024). 51

Figure 3.4. The settlement profile obtained from the numerical modeling for Case1 and its comparison with the field measurements shown with settlement bolts (modified after Ergincan et al., 2023). 54

Figure 3.5. The settlement profile obtained from the numerical modeling for Case2 and its comparison with the field measurements shown with settlement bolts (modified after Ergincan et al., 2024). 55

Figure 4.1. The numerical modeling phases appointed for the UA applied twin NATM tunnel sections in the parametric study. 58

Figure 4.2. A mesh view of a model used in the parametric study. 59

Figure 4.3. Model views belonging to D10_C30_O3_S2_T1 case representing (a) full section, (b) zoomed in section for twin tunnels, and (c) zoomed in section for the left tunnel. 64

Figure 5.1. Effect of UA application on settlement profiles of extreme cases. 66

Figure 5.2. Effect of UA application on average volume loss (V_L) of twin tunnels in extreme cases. 67

Figure 5.3. Effect of UA application on average volume loss (V_L) of twin tunnels in D08_O2 cases. 67

Figure 5.4. Surface settlement profiles of D10_T1 cases for (a) O1, (b) O2, (c) O3. 70

Figure 5.5. Surface settlement profiles of D08_T1 cases for (a) O1, (b) O2, (c) O3. 71

Figure 5.6. Surface settlement profiles of D06_T1 cases for (a) O1, (b) O2, (c) O3. 72

Figure 5.7. Maximum surface settlement (S_{max}) of the UA applied tunnels with respect to overburden depth for (a) D10, (b) D08, and (c) D06 cases. 74

Figure 5.8. Maximum surface settlement (S_{max}) of the UA applied tunnels with respect to clear distance for C30 cases. 75

Figure 5.9. Coordinate of the maximum surface settlement (skewness) of the UA applied tunnels for D10 case. 75

Figure 5.10. Coordinate of the maximum surface settlement (skewness) of the UA applied tunnels for D08 case. 76

Figure 5.11. Coordinate of the maximum surface settlement (skewness) of the UA applied tunnels for D06 case. 76

Figure 5.12. Average volume loss percentage (V_L %) of the UA applied tunnels with respect to overburden depth for (a) D10, (b) D08, and (c) D06 cases. 79

Figure 5.13. Average volume loss percentage (V_L %) of the UA applied tunnels with respect to tunnel diameter for O1 case. 80

Figure 5.14. Surface volume loss (V_S) of the UA applied tunnels with respect to overburden depth. 80

Figure 5.15. Volume loss reflection ratio (V_S/V_L) of the UA applied tunnels for (a) D10, (b) D08, and (c) D06 cases. 81

Figure 5.16. Average volume loss percentage (V_L %) of the UA applied tunnels with respect to clear distance to tunnel diameter ratio (C/D) normalization for (a) O1, (b) O2, and (c) O3 cases. 82

Figure 5.17. Average volume loss percentage (V_L %) of the UA applied tunnels with respect to clear distance to tunnel area ratio (C/A_T) normalization for (a) O1, (b) O2, and (c) O3 cases. 83

Figure 5.18. Maximum vertical displacement ($u_{y,max}$) of UA applied tunnels with respect to overburden depth for (a) D10, (b) D08, and (c) D06 cases. 86

Figure 5.19. Maximum horizontal displacement ($u_{x,max}$) of UA applied tunnels with respect to overburden depth for (a) D10, (b) D08, and (c) D06 cases. 87

Figure 5.20. Maximum resultant displacement (u_{max}) of UA applied tunnels with respect to overburden depth for (a) D10, (b) D08, and (c) D06 cases. 88

Figure 5.21. Maximum resultant displacement (u_{max}) of UA applied tunnels for O1 cases. 89

Figure 5.22. Maximum axial force on bolts of UA applied twin tunnels throughout the construction ($N_{bolt,max}$) with respect to overburden depth for (a) D10, (b) D08, and (c) D06 cases. 91

Figure 5.23. Maximum axial force on linings of UA applied twin tunnels throughout the construction ($N_{lining,max}$) with respect to overburden depth for (a) D10, (b) D08, and (c) D06 cases. 92

Figure 5.24. Maximum axial force on linings of UA applied twin tunnels throughout the construction ($N_{lining,max}$) with respect to tunnel diameter for O1 cases. 93

Figure 5.25. Maximum shear force on linings of UA applied twin tunnels throughout the construction ($V_{lining,max}$) with respect to overburden depth for (a) D10, (b) D08, and (c) D06 cases. 94

Figure 5.26. Maximum bending moment on linings of UA applied twin tunnels throughout the construction ($M_{lining,max}$) with respect to overburden depth for (a) D10, (b) D08, and (c) D06 cases. 95

Figure A.1. Official permission to use of the project data for academic purposes. 114

LIST OF TABLES

Table 2.1. Chronological development of the NATM (modified after Sauer, 1988; Sauer & Gold, 1989; Kahyaoğlu, 1998; Karakuş & Fowell, 2004; Schubert & Lauffer, 2012). 11

Table 2.2. Subcategorized classification (modified after ÖNORM B 2203-1, 1994). 18

Table 2.3. Supporting actions to stabilize the tunnel excavation (modified after Lunardi, 2000). 20

Table 3.1. Idealized soil profile of Case1 selected for validation study (adopted from Ergincan et al., 2023). 47

Table 3.2. Idealized soil profile of Case2 selected for validation study (adopted from Ergincan et al., 2024). 47

Table 3.3. Calculated properties of the improved zone in Case1 (adopted from Ergincan et al., 2023). 47

Table 3.4. Calculated properties of the improved zone in Case2 (adopted from Ergincan et al., 2024). 48

Table 3.5. Displacement and volume loss results of Case1 (adopted from Ergincan et al., 2023). 53

Table 3.6. Displacement and volume loss results of Case2 (adopted from Ergincan et al., 2024). 54

Table 4.1. Soil and rock parameters used in the parametric study. 61

Table 4.2. The fixed parameters of improved zones according to ground conditions. 62

Table 4.3. Calculation example for the elastic modulus and unit weight of improved zone. 62

Table 4.4. The varied parameters of improved zones according to ground conditions. 63

LIST OF SYMBOLS

A_p	Area of the parabola
A_T	Tunnel area
A	Cross-sectional area
b	Width of the tunnel cavity
B	Settlement bolt
c'	Effective cohesion
C/A_T	Ratio of overburden depth to tunnel area
C/D	Ratio of overburden depth to tunnel diameter
D	Tunnel diameter
D_{eq}	Equivalent tunnel diameter
E	Elastic modulus
E'	Effective elastic modulus
E_{50}^{ref}	Secant stiffness in standard drained triaxial test
EA	Axial stiffness
EI	Bending stiffness
E_{oed}^{ref}	Tangent stiffness for primary oedometer loading
E_{ur}^{ref}	Unloading/reloading stiffness
f	Strength factor
F_s	Factor of safety
h	Height of the parabola
I	Moment of inertia
K_0	Lateral earth pressure at rest
$M_{lining,max}$	Maximum bending moment on linings of twin tunnels during construction
M_{stage}	Total multiplier that controls the staged construction process
$N_{bolt,max}$	Maximum axial force on bolts of twin tunnels during construction
$N_{lining,max}$	Maximum axial force on linings of twin tunnels during construction

R_{inter}	Interface strength reduction factor
S_{max}	Maximum surface settlement
u_{max}	Maximum resultant displacement
$u_{x,max}$	Maximum horizontal displacement
$u_{y,max}$	Maximum vertical displacement
v	Poisson ratio
V_L	Volume loss
V_S/V_L	Volume loss reflection ratio
$V_{lining,max}$	Maximum shear force on linings of twin tunnels during construction
V_S	Surface volume loss
v_{ur}	Poisson's ratio for unloading - reloading
γ	Unit weight
γ_{sat}	Saturated unit weight
$\sum V_L$	Total volume loss in the twin tunnels
ψ	Dilatancy angle
ϕ	Angle of shear strength

LIST OF ACRONYMS / ABBREVIATONS

2D	Two-dimensional
3D	Three-dimensional
AASHTO	American Association of State Highway and Transportation Officials
B.C.	Before Christ
C10	Code used in the parametric study to describe the 10-m overburden depth
C20	Code used in the parametric study to describe the 20-m overburden depth
C30	Code used in the parametric study to describe the 30-m overburden depth
CAD	Computer aided drawing
D06	Code used in the parametric study to describe the 6-m tunnel diameter
D08	Code used in the parametric study to describe the 8-m tunnel diameter
D10	Code used in the parametric study to describe the 10-m tunnel diameter
DP	Dummy plate
DSI	DYWIDAG System International
FDM	Finite Difference Method
FE	Finite Element
FEM	Finite Element Method
FHWA	Federal Highway Administration
FpdGUA	Double Forepole Grouted Umbrella Arch
FpGcUA	Forepole Grouted Continuous Umbrella Arch
FpGdcUA	Forepole Double Continuous Grouted Umbrella Arch
FpGoUA	Forepole Open Grouted Umbrella Arch
FpGUA	Forepole Grouted Umbrella Arch
HC	Hard clay

HWR	Highly weathered rock
IMM	İstanbul Metropolitan Municipality
IP	Individual pipe
ITA	International Tunnelling Association
NATM	New Austrian Tunneling Method
O1	Code used in the parametric study to describe the one-time-diameter-distance between twin tunnels
O2	Code used in the parametric study to describe the two-times-diameter-distance between twin tunnels
O3	Code used in the parametric study to describe the three-times-diameter-distance between twin tunnels
ÖNORM	Austrian Standards
Q-System	Rock Mass Quilty System
P	Plate
RMR	Rock Mass Rating
RQD	Rock Quality Designation
RSR	Rock Structure Rating
S1	Code used in the parametric study to describe the first ground condition representing hard clay
S2	Code used in the parametric study to describe the first ground condition representing highly weathered rock
S3	Code used in the parametric study to describe the first ground condition representing weathered rock
SHJG	Sub-Horizontal Jet-Grouting
T0	Code used in the parametric study to describe the nonexistence of umbrella arch
T1	Code used in the parametric study to describe the existence of umbrella arch
TBM	Tunnel Boring Machine
UA	Umbrella Arch
UAM	Umbrella Arch Method
UASC	Umbrella Arch Selection Chart

UNESCO	United Nations Educational, Scientific and Cultural Organization
W.P.	Weighted Percentage
WR	Weathered rock

1. INTRODUCTION

1.1. General

The history of underground excavations goes a long way back. Its development is deeply rooted in mankind. The tunnels have been constructed for centuries to meet various human needs, such as shelter and transportation. The demand for tunnels increased with the varying needs of human beings. Thereby, tunnel construction started playing a vital role both in passing steep and curvy geographies and in reaching the ore in deeply formed mines. Tunnel construction then also started to provide sustainable solutions for the demands of urban life, such as inner-city railway and highway facilities. Tunnels serve as an alternative to relieve highly congested traffic and improve the speed, comfort, and reliability of transportation. In construction of such tunnels, nowadays, tunnel boring machines (TBMs) are mainly preferred as their speed and stability are advantageous features in construction. However, before the relatively recent invention of modern TBMs, New Austrian Tunneling Method (NATM) has been the most common tunneling method used throughout the world. Today, even though TBMs are commonly utilized in urban projects, their use is not always feasible due to the restrictions related to cost and geometry. In these cases, to this day, NATM has become an obligation rather than a preference. Once NATM is selected as the tunnel construction method, its safety has to be ensured. This becomes especially tricky very frequently in urban tunneling when weak ground conditions are encountered in the construction of wide tunnel sections. Generally, the strength of soil and rock typically increases with depth, contrariwise the urban tunnels are shallow with low overburden. In addition to tunnel face stability problems, settlement-sensitive critical infrastructures and superstructures are commonly present above or around the tunnel sections in urban areas. Accordingly, these challenging conditions are frequently encountered in urban tunneling.

NATM principally attempts to transfer the load on the tunnel to the ground (soil or rock) by recreating the stress distribution as the ground deforms, in essence using the arching principle. This principle works well in relatively strong ground conditions with high stiffness. However, there are cases in which the excavation period without support is short due to ground conditions, or there is a risk of collapse in the tunnel due to excessive

convergence or on the surface due to excessive settlement. In these scenarios, either the soil or weak rock around the NATM tunnels should be improved or the tunnel support system should be strengthened. This additional support requirement can be carried out before or after the face excavation.

Umbrella arch method is one of these additional support measurements used with NATM. Unlike the well-known support techniques of NATM, such as shotcrete, steel girders, and anchoring, the umbrella arch method (UAM) is applied before performing the excavation advancement; therefore, it is considered as one of the pre-support techniques. UAM increases the resisting capacity of the support system both in radial and longitudinal directions. It is cheaper and easier to apply when compared to other pre-support techniques such as ground freezing, pipe jacking, or horizontal jet grouting. As a precaution to ensure tunnel excavations, umbrella arch method (UAM) both improves the ground and strengthens the support system. Thus, while excavating the face, UAM helps to provide safety by holding the ground material above the excavation roof. Applying UAM also decreases the volume loss of the tunnel and its reflection to the surface. Volume loss is a frequently used expression in tunnelling to indicate the difference between the displaced area and the original area of the tunnel in terms of volume per meter (m^3/m), or its ratio to the original tunnel area in terms of percentage (%).

With its proven success in the last decades, it is widely used around the world with NATM. Since surface deformation is very critical in urban areas compared with rural areas, UAM is specifically preferred in urban tunneling projects located in poor ground conditions to eliminate the structural failure of settlement-sensitive infrastructures or superstructures.

At the beginning of the projects, the deformations induced by excavations are estimated and the stability of the structures are analyzed together with their possible failure modes. To observe excavation-induced ground movements, near-surface sensors are placed on the structures located around the tunneling and continuous measurements are taken and recorded during the tunneling projects. These measurements are compared with the predicted results continuously to manage risks of collapse and to take preventive actions when necessary. As a consequence, predicting tunnel-induced deformations plays a key role in the tunnel designing process as the design is altered when needed. The behavior of underground

openings is affected by many factors, such as openings dimensions, overburden depth, its excavation and supporting method, material properties of the ground, and also the distance between excavations. Therefore, it is not easy to predict the deformations comprehensively and precisely using analytical and empirical calculations. For this reason, finite element method based numerical analysis offers effective solutions for engineers. Thanks to the built-to-order software, tunnel excavations can be simulated in construction stages and the expected result at the end of each construction stage can be obtained. Although tunnel excavation is a three-dimensional (3D) problem, modeling the complex geometry and stages of a tunnel excavation is challenging in 3D, as both modeling and calculation phases require extensive time and computational effort. Therefore, after appropriate assumptions and simplifications, in the majority of the tunneling projects, two-dimensional (2D) models are still frequently used by engineering companies. Several researchers developed approaches that can be used to model the UAM in 2D. The effects of openings dimension, overburden depth, material properties of the ground, and also the distance between excavations are not well known in UAM supported NATM tunnels. A parametric study backed by instrumented validation cases is required to reveal the effect of various parameters on behavior and to aid in the design of NATM constructed with UAM efficiently.

1.2. Objectives

The tunneling works are large-scale projects that include various parameters that vary along the path, such as overburden depth, properties of the ground, loads on the surface, groundwater level above the tunnel, support, and excavation sequences. It is hard to conduct experimental studies that include physical model tests. For this reason, unfortunately to this date, past experiences and empirical approaches dominate the design and construction of tunnels. Technological advancements facilitated numerical studies that gave an opportunity to predict the tunnel behavior for safer construction. Since tunneling has a 3D effect, in essence, the direction perpendicular to the excavation face also shows variations. Consequently, in reality, it is ideal to perform a 3D analysis. On the other hand, the required time to both create and analyze 3D models is extensive. Accordingly, with adopting some assumptions and simplifications, 2D finite element models are still frequently used to predict

surface displacements and support forces in the design of NATM tunnels, both in research and engineering.

Despite its known practical success, in the literature, studies that focus on the parametric analysis of tunnels with UAM are scarce. This study aims to evaluate the reliability of the 2D modeling approach for the tunnel sections supported by UAM based on two instrumented case studies and to better understand the behavior of these types of tunneling sections under various parameter combinations.

In order to evaluate the reliability of the UAM modeling approaches, two separate sections from Çekmeköy-Sancaktepe-Sultanbeyli Metro Line project located in İstanbul, Türkiye were modeled with their excavation phases using a finite element method based software, and the results of the numerical analyses were compared with the field data obtained from site measurements as a validation study. Upon the completion of the validation study, the sections of circular twin tunnels, which are accordant with the combinations of the factors affecting the behavior, were created for the parametric study. For the parameter combinations, three diameters (6m, 8m, 10m), three overburden depths (10m, 20m, 30m), three clear distance ratios depending on tunnel diameter (1D, 2D, 3D) were analyzed. All sections were analyzed with and without UAM application for three ground parameter sets determined for hard clay, highly weathered rock, and weathered rock. Thus, a total of 162 numerical models covering these combinations were analyzed. To understand the effects of various factors on the tunnel deformation behavior, the results of numerical analyses were investigated comparatively for the forces and moments on support elements, as well as for the displacements of the tunnel lining and at the surface.

1.3. Scope

This thesis is structured into five main chapters and is presented in the following sequence. In Section 1, the thesis is introduced with its goals and scope. Section 2 explains the development history of the tunneling support systems, sheds light on the umbrella arch terminology in tunneling, briefly describes the analysis methods, and gives information about the parameters that impact the behavior of tunnel excavations. The validation study,

which was conducted using two instrumented case studies, is comprehensively clarified in Section 3 with the obtained results from the case studies. In Section 4, the research methodology for the parametric study is explained with the parameter selection. Section 5 contains the results of the parametric study that are discussed in detail. Finally, Section 6 presents the summary of the study and concludes the findings obtained from the validation and parametric studies.

2. LITERATURE REVIEW

2.1. Tunnels

Underground excavations are deeply rooted in the development of mankind, dating back to the era of Neanderthals, who were the first known to dig the ground manually. This implies that the history of underground excavations is as ancient as the history of mankind itself. The digging activities of humankind were not limited to cave excavations or small-scale mining operations. As the techniques used by humans improved, the size and complexity of excavations increased. Thus, the excavations reached a formation that can be called tunnels having at least two open ends, i.e., an entrance and an exit. The earliest known tunnel, dating back to 2200 B.C., was constructed in Babylonia to connect the palace and the temple. Over the years and centuries, tunnel excavations have been undertaken in order to meet various human needs, such as irrigation, transportation, and sewage. Moreover, tunnels have served military and housing purposes, as evidenced in Cappadocia, located in Nevşehir, Türkiye. Thanks to the techniques developed over the years, the construction of tunnels has spread around the world, and their purposes have varied. These widened purposes led to the need to tackle challenging conditions and restricting requirements, and to find comprehensive engineering solutions for larger, longer, and better tunnels.

2.2. Tunneling Methods

One of the main reasons for the need for tunneling is the rapidly increasing urbanization of the world. The primary tunneling methods are surface tunneling (such as open trench or cut-and-cover structures), mechanized tunneling (typically fully faced via tunnel boring machines, rarely partially faced via roadheader or digger type machines), and conventional tunneling (typically partially faced via basic excavating machines or explosives). In cases where the tunnel is underwater instead of underground, then subaquatic tunneling (immersed tube) can be included in the method list. In addition, a relatively newer method named water jet tunneling can be listed, but it is very rarely; therefore, cannot be considered a primary method. Furthermore, submerged floating tunneling can be mentioned

as another approach for subaquatic conditions; however, it has not gone beyond the proposal and design stages yet.

The cut-and-cover method relies on the excavation of the ground from the surface by digging a trench and covering the depth of the burden after the tunnel lining in the opened volume has been constructed. Thus, it offers advantages in constructing sections with corners, such as rectangles. On the other hand, it causes the closure of the construction area located on the surface and often causes relocating of infrastructures in urban areas. Consequently, this method introduces problems in areas having critical roads and facilities on the ground. Additionally, its depth leads to problems since the costs strikingly escalate with increasing depth. Moreover, in comparison with the other two methods, the transportation and recycling of the excavated material presents larger challenges in this method. Besides these, noise, dust, visual and light pollution risk is higher in comparison with the other methods. Therefore, it is typically limited to shallow tunnels, and due to its nature, the cut-and-cover method is more associated with deep excavation and slope stability problems rather than tunneling problems. A cut-and-cover tunnel example photographed in İstanbul is presented in Figure 2.1.



Figure 2.1. A tunnel example from İstanbul, constructed with the cut-and-cover method.

In the context of tunneling, full-face excavation, or fully mechanized excavation, generally refers to tunnel boring machines (TBMs). The TBMs are highly efficient for excavating long paths thanks to their effective mechanization techniques, such as shield, slurry, or earth pressure balance. In comparison with conventional tunneling, mechanized tunneling has advantages in terms of lower ground deformation, automated support, and faster advancement rate. However, they are constrained by the circular geometry of the machines. At times, its complex electro-mechanical structure can become disadvantageous due to breakdowns that need long repair times. In addition to that, since they use hydraulic forces to excavate the ground, it becomes difficult when they are faced with hard rocks. Resistance of high-strength rocks against the hydraulic force causes deceleration of TBMs and excessive abrasion of cutter heads. Also, due to their high initial investment, operating, and maintenance expenses, they are not cost-effective unless the tunnels to be excavated are sufficiently long. In spite of the fact that TBMs are commonly used in tunneling and could be regarded as conventional anymore, they are not referred to as such. The conventional method refers to the cyclic (sequential) advancement of the excavations rather than the continuous advancement of TBMs. A rare but good to see example of a TBM photographed from outer perspective, due to construction scheduling constraints, in İstanbul is presented in Figure 2.2.



Figure 2.2. A special tunnel example from İstanbul, performed with TBM method.

On the other hand, conventional tunneling methods, despite their disadvantageous characteristics in terms of ground disturbance, hazardous working conditions, and longer construction times, make it possible to design tunnels with shapes other than circular ones, in addition to being more cost effective and requiring shorter maintenance durations. Portals or vertical shafts provide sufficient access to the tunnel, thus requiring less excavation from the surface to tunnel depth compared to cut-and-cover and TBMs. Conventional tunneling provides flexibility for partial excavation of the tunnel face and allows for modifications to the supporting design, thus avoiding overdesign and reducing costs. Depending on the ground conditions, drilling and blasting can be employed to advance the excavations. Also, during the excavations, it is possible to benefit from heavy machinery such as drillers, breakers, excavators, roadheaders, loaders, erectors, and sprayers, alongside manpower. The partial face excavations are often referred to by nation names like German, English, Italian, Belgian, Swiss, and Austrian, based on where they were adopted and frequently used. These methods predominantly utilize timber support elements and manual labor. They are not very suitable for mechanization due to their very small excavation face areas, manpower requirements for the support system, and limited working spaces because of the closely braced vertical, horizontal, and cross bar support elements. Even though these manpower-based excavation methods are not frequently used in the twenty-first century, some of their principles are still used in modern tunneling works.

2.3. Support Systems

Opening a cavity under the ground causes the redistribution of the stresses initially present. This stress redistribution results in ground deformation. Therefore, obviously, it should be ensured that the balance of stress and deformation must be satisfied for every underground opening by an appropriate method.

On this basis, the arching effect of ground material helps to stabilize the tunnel. This effect relies on shearing resistance due to the relative movement between the yielding and remaining parts of the soil. Terzaghi (1943) defines the function of this resistance as keeping the yielding mass in its original position by reducing the pressure on the yielding part of the support and increasing the pressure on the adjoining stationary part. The arching effect is

described by Zelger (2012) as the rotation of the principal stress directions that causes the creation of an arch over the unsupported length by redistributing vertical loads proportionally to the lining and the undisturbed ground ahead of the face.

When the properties of the ground are insufficient to resist the redistributed stress conditions, the openings must be supported by auxiliary elements. Although the strength of the ground may be adequate to resist the induced stresses, auxiliary support elements may still be necessary to reduce deformation or mitigate problems related to block discontinuity, water flow and earthquakes.

According to Sauer (1990), New Austrian Tunneling Method (NATM) can be defined as creating an underground space by using all available means to develop the maximum self-supporting capacity of the rock or soil to ensure the stability of the opening. The self-supporting capacity of the ground and its evolution have a long history. The chronological evolution of this method, which will be named as the New Austrian Tunneling Method and abbreviated as NATM subsequently, has been listed in Table 2.1.

Table 2.1. Chronological development of the NATM (modified after Sauer, 1988; Sauer & Gold, 1989; Kahyaoğlu, 1998; Karakuş & Fowell, 2004; Schubert & Lauffer, 2012).

Years	Developments
1818	Circular shield for soft ground tunneling patented by Sir Marc Isambard Brunel (British patent no.4204)
1848	Fast-setting mortar has been started to use instead of timber at Wejwanow coal mine in Czechia
1848-1854	Curved tunnel sections have been designed and constructed by Carl Ritter von Ghega in Austria for the Semmering Pass, a UNESCO World Heritage Site
1872	Rhiza's replacing proposal for steel support instead of timber
1881	Engesser's theoretical investigation on letting deformation to reduce the loads
1911	Akeley patented shotcrete spraying machine by improving his invention in 1907
1914	The first use of shotcrete in underground works
1926	Schmid presented analytical solution by improving the Engesser's theory
1944	Rabcewicz's studies on pressures around tunnels
1948	Rabcewicz's dual lining system proposal
1954	Anton Bruner's proposal to use shotcrete as immediate support instead of timber or steel; thereafter, it was patented
1954-1956	Rabcewicz's experience gathering in the tunnels of Prutz-Imst Hydroelectric Power Project and his development on the systematic ground anchoring with shotcrete
1956	First use of systematic anchoring with shotcrete as the only means of support (in the La Cabrera Tunnel which is a highway tunnel in Venezuela)
1960	Prof. L. Müller's development to effectively measure the time dependent deformation around the tunnel opening
1962	Creation of the New Austrian Tunneling Method term by Professor L. von Rabcewicz in a lecture to the XIII Geomechanics Colloquium in Salzburg
1963	Pacher's study to produce deformation curves under controlled pressure relaxation
1963-1965	Gaining popularity of NATM with its successful application in Massenberg Tunnel (a road tunnel in Austria) and Schwaikheim Tunnel (a rail tunnel in Germany) guided by Prof. Rabcewicz, Prof. Müller, and Prof. Pacher.
1969	The first urban NATM application in soft ground conditions located in Frankfurt Metro project and its leading to series of scientific investigations and model tests
1980	Redefinition of NATM, due to conflict existing in the literature, by the Austrian National Committee on Underground Construction of the International Tunnelling Association (ITA)

Since this support system has evolved over the years by the contributions of engineers and researchers from various nations as aforementioned, its content is highlighted by some sources rather than being referred to by the name of a specific nation. Therefore, this support system is also called the Shotcrete Methods, Sprayed Concrete Lining, Sequential Excavation Method, Sequential Support Method, or Observational Tunneling Method. However, the success of contributions made by three Austrians, (Professor Ladislaus von Rabcewicz, Professor Leopold Müller, and Professor Franz Pacher) resulted in the widespread recognition of the method with the name New Austrian Tunneling Method, meritedly. Also, it is obvious that the Austrian contributors had to differentiate it from the older Austrian tunneling method. Even though other terminology is also used for the same method, New Austrian Tunneling Method with the NATM abbreviation is the most common one, and will be used in this thesis moving forward.

First of all, NATM provided flexibility to meet the greater underground demand of society. By implementing shotcrete in tunnel excavations, it reduced the potential for disintegration, spalling and loosening of excavation surfaces. In addition, it provided deceleration in dimension of support elements and acceleration in operability and advancement rate. Also, it facilitated better contact between the radial surface of the excavation and the support elements, enhancing stress transfer and redistribution. Furthermore, by benefitting from the self-supporting capacity of the ground, it reduced the construction costs. NATM, by employing every technique at hand to increase maximal potential, allowed for the use of alternative solutions and materials in tunneling. Especially, thanks to the superlative contributions of Prof. Rabcewicz on dual lining, Prof. Müller on monitoring, and Prof. Pacher on ground reaction curve, NATM has gained widespread adoption worldwide with its effectiveness in durability and cost, particularly in poor ground conditions.

Pacher (1963) investigated the reaction of the ground when subjected to excavation-induced forces. He conducted his research on galleries by testing the effects of combined factors such as strength and deformation behavior of the rock mass, the state of stress in the unworked rock mass, the cross-section, the time, and the properties of the lining. Thus, he observed the characteristic load-deformation-curves of rock masses from the moment of excavation to a new equilibrium state. Afterwards, this research led to the development of

the convergence-confinement method. The graph generated in RocSupport software (RocScience Inc., 2004) is projected to visualize the interaction between the ground and support in Figure 2.3.

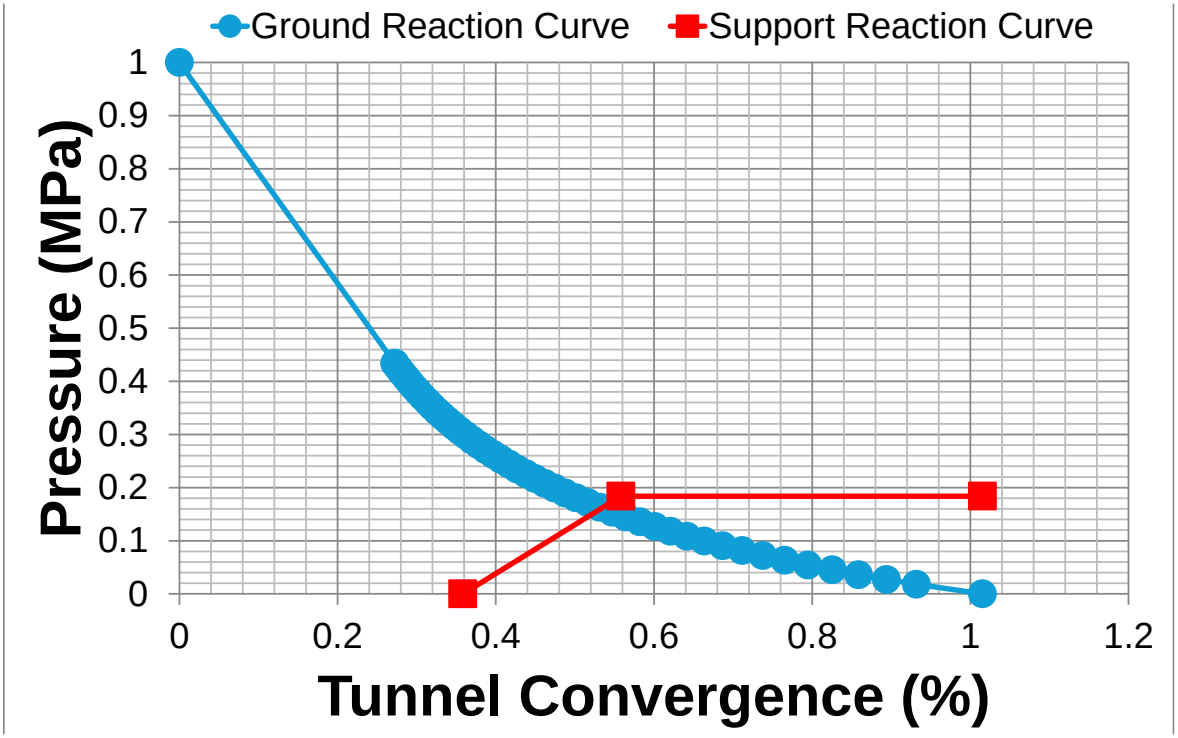


Figure 2.3. Ground reaction curve and support reaction curve graph exported from RocSupport Tutorial 1 (modified from RocScience, 2004).

In the conventional tunneling methods, the excavation sequences and support systems are generally similar, with minor variations. In the German method, excavation starts from the bottom sides of the section, and bottom sides are lined while the excavation is continued with centered small roof opening. Subsequently, the upper sides are excavated and lined while the excavation is continued with center of bench. The left bottom core is removed at the end. In the Belgian, British, Swiss, and Austrian methods, on the other hand, excavation starts from the bottom core of the section, and progresses upward before it is widened to the sides and lined. Maidl et al. (2013), Schubert (2015), and Birincioğlu (2017) describe the specific partition for excavation and support sequence of the "old" Austrian tunneling method, which distinguishes it from the others, as shown in Figure 2.4. Initially, the bottom part is excavated and supported; afterwards, the narrower section reaching the roof is advanced. Subsequently, the roof is opened, and then this top part is widened both left and

right. Later, the excavation is carried forward from the roof to the shoulder and then from the shoulder to the bottom. Finally, the completion of the entire cross-section excavation is followed by the lining process from bottom to top along the radial surface. Since it relies on using dressed stone or brick as lining and timber as support element, it has disadvantages in poor ground conditions, such as lengthy advancement time to complete the masonry lining, loose backfilling, and potential for irreparable damage. Rabcewicz (1964a, b; 1965) explained these drawbacks of the old Austrian tunneling method and proposed using shotcrete and steel support elements with auxiliary arch (invert) and systematic anchoring if necessary for the temporary support and constructing inner lining after deformations cease.

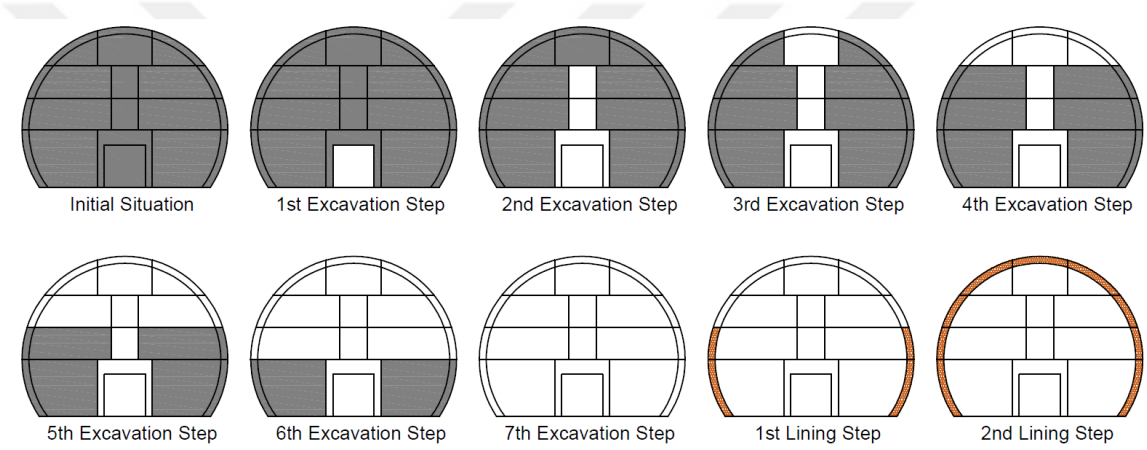


Figure 2.4. Excavation and lining sequence of the “old” Austrian tunneling method.

The twenty-two principles of NATM (after Müller and Fecker, 1978) are summarized as follows:

1. The ground is the primary support source to bear the load induced by excavation.
2. The ground surrounding the opening should not lose its strength.
3. Since loosening in surrounding ground causes strength reduction, it should be preserved.
4. Preventing uniaxial and biaxial stress environment protects the ground as its strength decreases.
5. The formation of the protective zone must be carefully supervised and guided.
6. Support should be constructed neither too early nor too late, and neither too rigid nor too flexible.

7. The application time of support elements should be designated properly since the behavior of the rock depends on the timing of the protective zone creation.
8. The characteristic time factor is determined thanks to convergence and deformation measurements during construction and laboratory tests before construction. This provides the determination of very important parameters such as rock classification, standing time and deformation rate.
9. The surface of the excavation is reinforced by bonding it with shotcrete and anchors.
10. The temporary lining shells should be thin and flexible.
11. The temporary lining should be formed with wire mesh, anchors, and steel girders, providing necessary flexibility, and anchoring it to the ground instead of thickening the shell.
12. The supporting time and elements should be designated by monitoring because measuring of deformation and stresses permits to determine the behavior of the rock during application.
13. The tunnel should be considered as a composite closed system consisting of protective zones and temporary lining.
14. In order to close the system, invert excavation and support should be completed after top heading and bench works.
15. An incomplete lining system can lead to ground yielding and decreased bearing capacity.
16. The unsupported span length should be kept as short as possible.
17. A covering inner shell layer can be applied on the steel supports to prevent torsional moments and fractures by making the inner and outer shells thin.
18. The strength of the inner and outer shells can be increased not by thickening but by bracing, by way of decreasing the spacing between bolts or increasing their lengths.
19. During the construction process, continuous convergence and deformation measurements along the tunnel provide guidance and determine whether supporting is required, ensuring the stability and safety of the whole system.
20. Stress measurements between the shell and surrounding ground are necessary for sizing the outer shell.
21. The aim of the permanent lining is to enhance safety and provide architectural appearance.

22. Drainage pipes should be installed around the opening to drain water pressure transmitted from the surrounding to the shell.

With the worldwide spread of NATM, the Austian National Committee on "Underground Construction" of the International Tunnelling Association (1980) redefined it as follows: "The New Austrian Tunnelling Method (NATM) is based on a concept whereby the ground (rock or soil) surrounding an underground opening becomes a load bearing structural component through the activation of a ring–like body of supporting ground." With the flexibility brought by NATM, sometimes there is even no need for permanent concrete lining during operation, as photographed in Figure 2.5.



Figure 2.5. The view of metro pedestrian tunnels constructed and operated in İstanbul without permanent concrete lining.

Despite its flexibility in poor ground conditions with shotcrete, steel girders and anchors, these measures may not suffice for some projects. Because the support system design must ensure a safe construction process for displacement-sensitive infrastructures, such as pipelines around the section or superstructures like buildings on the surface as well as for the tunnel itself. Moreover, it should offer economic solutions for the owners and contractors. Soil conditions with low strength instead of rock, or shallow overburden with low deformation limitations due to sensitive structures located in the effect zone of the tunnel rarify constructability. Suchlike challenging situations require additional precautions to

advance the tunnel safely and economically; thus, it is tended to modify the original NATM supportive components.

In tunnel design, there are three main approaches named observational, empirical, and analytical. NATM serves as a good example for the observational approach with its nature based on monitoring. While the empirical approach relies on experience and engineering judgement, the analytical approach takes complex mathematical equations and comprehensive analysis into consideration. Advances in technology have made analytical approaches more usable. It can be said that all these design approaches begin with the classification of the media where the tunnel will be excavated. In tunneling works, it is critical to characterize the media since the material to be excavated has a lot of uncertainties. At that point, rock mass classifications are helpful to form an opinion about the support needs of the case and to guide the design of the underground structure.

Bieniawski (1990) lists six classifications in his work including Terzaghi's rock load classification, Lauffer's classification, Deere's rock quality designation (RQD), the rock structure rating (RSR) concept, the geomechanics classification or rock mass rating (RMR), and rock mass quality (Q-System); and underlines that the last three are used in modern tunneling by presenting user guides. The RSR concept, developed by Wickham et al. (1972), primarily depends on geologic parameters such as rock type and joint properties and construction parameters such as tunnel size, tunnel advancement direction, and method of excavation. The RMR system, developed by Bieniawski (1973), classifies rock masses based on their intact rock uniaxial compressive strength, RQD, discontinuity spacing, discontinuity orientation, discontinuity condition, and groundwater condition. The Q-System, developed by Barton et al. (1974), summarizes the overall rock mass quality with the parameters of RQD, joint set number, joint roughness number, joint alteration number, joint water reduction number, and stress reduction number. These classification systems guide the engineers not only for rocks but also for fully weathered, decomposed materials like soil. Especially, the RMR system notes a uniaxial compressive strength of 150 psi (approximately 1 MPa) as the boundary for defining the material as soil or rock rather than its weathering. Therefore, it is clear from the evaluation parameters for classifying rock masses that all these three approaches focus on similar factors such as rock strength and its reduction due to

discontinuities and water conditions. Based on these similarities, Bieniawski (1976) proposed a correlation between RMR and Q-System, formulated as

$$RMR = 9 \ln Q + 44; \quad (2.1)$$

additionally, Rutledge and Preston (1978) proposed correlations among three of them as

$$RMR = 13.5 \log Q + 43, \quad (2.2)$$

$$RSR = 0.77\, RMR + 12.4, \quad (2.3)$$

$$RSR = 13.3 \log Q + 46.5. \quad (2.4)$$

Another classification system, known as the NATM classification, was released by Austrian Standards ÖNORM B 2203-1 (1994). It guides contractual issues and defines rock masses into three main groups: stable to over-breaking (A), friable (B), and squeezing (C). Table 2.2 shows its subcategories along with the proposed support elements. In addition to that, a frequently used correlation chart between Q, NATM, and RMR classification systems is presented in Figure 2.6, as referred by Karahan (2010), Barış & Mahmutoğlu (2018), Türköz (2023).

Table 2.2. Subcategorized classification (modified after ÖNORM B 2203-1, 1994).

Class	**Rock mass behavior**	**General excavation requirements**	**General support requirements**
A1	Stable rock	Full face	No support
A2	Over-breaking	Full face or top heading-bench	Roof support
B1	Friable	Top heading-bench	Roof support
B2	Very friable	Top heading-bench	Roof and wall support
B3	Rolling	Top heading-bench-invert	Roof and wall support, and invert support if required
C1	Rock bursting	Top heading-bench-invert	Roof, wall, and invert support
C2	Squeezing	Top heading-bench-invert	Roof, wall and invert support, and face support if required
C3	Heavily squeezing	Top heading-bench-invert	Roof, wall, invert, and face support if required
C4	Flowing	Top heading-bench-invert	Special support requirements
C5	Swelling	Top heading-bench-invert	Special support requirements

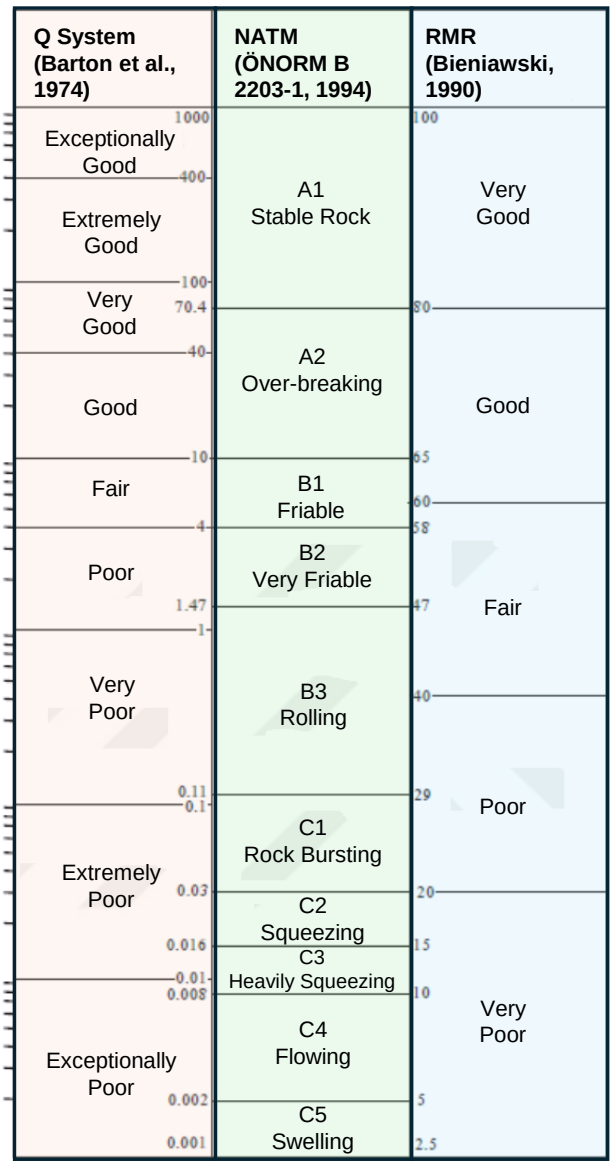


Figure 2.6. Correlation chart (modified after Karahan, 2010; Barış & Mahmutoğlu, 2018; Türköz, 2023).

The deformations become larger and more difficult to control when the excavation is performed in poor ground conditions and sensitive environmental conditions. Although the use of support elements, especially pre-support elements, means a principal modification of NATM since it relies on self-supporting, additional support techniques may become an obligation for safe construction in such conditions. Lunardi (2000) categorizes these stabilization actions on the basis of pre-confinement, confinement, and pre-support as shown in Table 2.3. Forepoling, injection, draining, freezing, anchorage and pressurizing can be listed under these precautions.

Table 2.3. Supporting actions to stabilize the tunnel excavation (modified after Lunardi, 2000).

Basis of Stabilization Action	Stabilization Technique
Pre-confinement	Traditional injections
	Freezing
	Sub-horizontal jet-grouting
	Mechanical precutting
	Drainage pipes
	Reinforcement of the ground around cavity and of the core using fiber glass structural elements
Confinement	Shotcrete
	Mechanical pressure shield
	Earth pressure balanced shield and hydro-shield
	Full length anchorage
	End anchorage
	Creating invert
	Open face shields
Pre-supporting	Forepoling

2.3.1. Umbrella Arch

Umbrella arch (UA) is one of the forepoling methods and is different from spiles, which is another forepoling method. The early examples of spiles presented by Proctor & White (1946) show that spiles are generally wooden cantilevers and rarely steel elements. Although spiles have evolved over the years, the early examples of spiles did not include a grouting process; therefore, they acted individually without providing any ground improvement. On the other hand, UA combines forepoling, grouting, and arch beam. In the umbrella arch method (UAM), to create this supportive combination, angled holes are first drilled above the roof part of tunnel sections. After the drilling, perforated steel pipes are inserted into the holes. Sometimes, due to the converging trend of the holes, pipes are driven while drilling, and the drilling bit is left in the ground when the drilling rod is withdrawn. Then, grout is injected into the pipes. Since the pipes are perforated, the grout injection fills

not only the inside of the pipes but also the void between the outer diameter of the pipes and the inner diameter of the holes. Thanks to the injection pressure the injected grout also improves the ground surrounding the pipes. Thus, an artificial arch beam is created on the roof part of the tunnel, allowing safe excavation underneath it. Since the method is applied at an angle, the excavation section area enlarges while the excavation proceeds. Therefore, the initial excavation cross-section does not remain the same; correspondingly, the curved steel beams (lattice girders or profile girders) buffering the radial surface of the excavation with shotcrete and wire mesh also enlarge. When the set of steel beams is completed, the excavation sequence starts again with the initial section geometry having the smallest cross-section. This creates a forehead area on the excavation face. New angled holes for the umbrella pipes are drilled from this forehead area. As a result, the artificial roofs partially overlap in the longitudinal direction, depending on the set number, advancement length, pipe length, and drilling angle. As an example, a longitudinal section of UA application is presented in Figure 2.7. The enlarging cross-sectional nature of this method due to inclined pipe insertion is sketched in Figure 2.8.

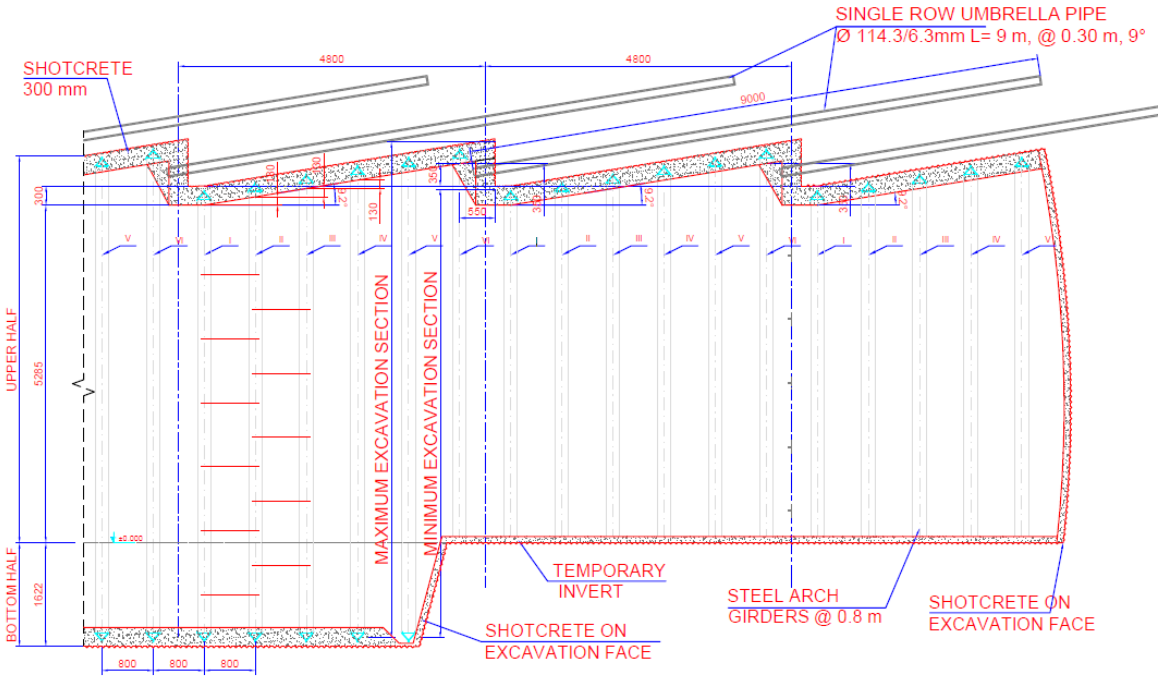


Figure 2.7. UA applied longitudinal tunnel section sketch simplified from Çekmeköy-Sancaktepe-Sultanbeyli Metro Project located in İstanbul, Türkiye.

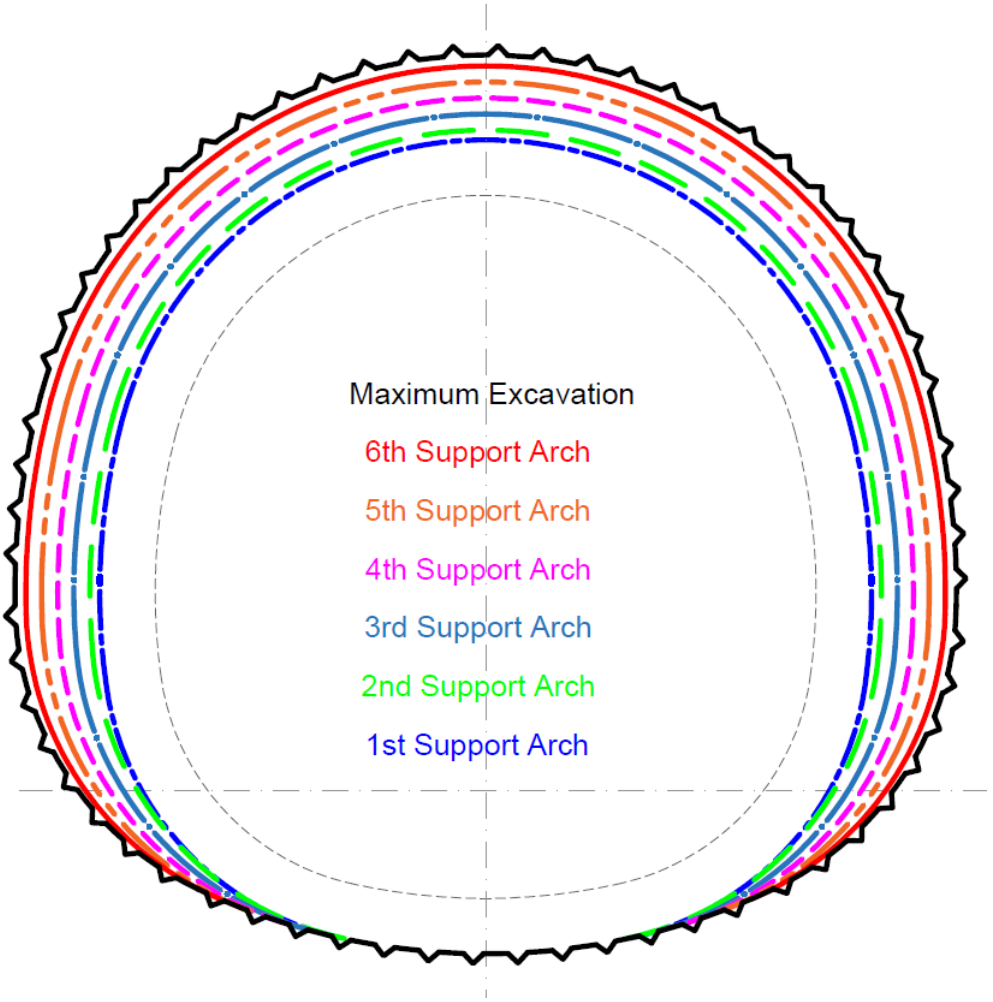


Figure 2.8. Enlarging cross-section of UA application sketch simplified from Çekmeköy-Sancaktepe-Sultanbeyli Metro Project located in İstanbul, Türkiye.

For the first application of umbrella arch, Selçuk (2016) refers to Paris Metro, which was under construction in the late 1970s, although no specific date is provided. Carrieri et al. (1991) identify 1975 in Italy as the first use of angled steel pipe based forepoling. Rostami et al. (2016) marks the early 1960s and Antwerp subway station in Belgium for the first use; however, it is debated due to the development chronology of conventional tunneling. Also, Tan (2005) indicates pipe jacking instead of umbrella arch for the Antwerp Metro and dates the project back to the early 1970s. Although this method is commonly called the umbrella arch method in the literature, there is also diversity in UAM nomenclature as addressed for NATM nomenclature. With its application variations, there are some other denotations such as “Steel Pipe Umbrella” by Pelizza & Peila (1993), “All Ground Fasten” by Tanaka (1996) and Miwa & Ogasawara (2001), “Forepole Umbrella” by Hoek (2001), “Steel Pipe Canopy”

by Gibbs et al. (2002), “Long- Span Steel Pipe Fore-Piling” by Miura (2003), “Canopy Technique” by Croce et al. (2004), “Grouted Pipe-Roofing Reinforcement” by Bae et al. (2005), “Pipe Roof Umbrella” by Bauer et al.(2005), “Pipe Arch Canopy” by Nitschke et al. (2009) and Jenkins et al. (2011), or “Canopy Tube” by Ghee et al. (2011).

Oke (2016) presents a nomenclature study for umbrella arch and splits it into three main categories as spiles, grouted, and forepoles. The spiles category refers to the longitudinal bars that differs from forepoles in being shorter than the tunnel height, and generally not pipe-shaped. In his work, the main categories are broken down into 11 subcategories. Even though some subcategories of the spiles and forepoles may consist of some amount of grouting, the grouted main category refers to the predominant use of grout as the primary support element. According to this nomenclature study, the first instance of a forepole grouted UA was in Saint Bernardino, Italy, dating back to the late 1970s. It has been used commonly in Italy and Japan in its first years. By referring to this nomenclature, this thesis deals with the forepole umbrella arch category and its grouted subcategories. These include FpGUA, meaning forepole grouted umbrella arch (with FpdGUA indicating double-layered forepoles), FpGcUA, meaning forepole continuous grouted umbrella arch (with FpGdcUA indicating double-layered forepoles), and FpGoUA, meaning forepole open grouted umbrella arch, as outlined in the umbrella arch selection chart (UASC) developed by Oke et al. (2014a). If grout is not employed, spiles and forepoles are confined by the ground itself. On the other hand, in the cases of FpGUA and FpdGUA, the grout fills only the voids inside the pipes and between the pipes and their drilling holes. Thus, the ground improvement in the arch section is limited, but it is replaced with stiffer forepole elements in patches. On the contrary, in FpGoUA, grouting fills the voids and penetrates out of drilling holes without reaching adjacent forepoles, leading to partial but discontinuous ground improvement in the arch section. Conversely, in FpGcUA and FpGdcUA, the grouting fills the voids and the grout penetration reaches neighboring forepoles. Consequently, the ground in the arch section is completely improved and the connection between forepoles is provided. The studies in this thesis primarily focus on forepole continuous grouted umbrella arch (FpGcUA).

While the techniques applied after excavation advancement are resisting mainly against the radial displacement around the excavation border, UAM increases the resisting

capacity against both radial and longitudinal displacement by its nature advancing ahead of the excavation face. Thus, UAM provides advantages to reduce ground settlement, especially in the longitudinal direction, to decrease the working risks in front of the face by enhancing face stability, to optimize other support requirements, and to enlarge the workability area of machines and personnel. Additionally, it acts as a barrier against water inflow. Muraki (1997) investigates 24 case studies related to the umbrella method by accepting sub-horizontal jet-grouting (SHJG), injected steel pipe umbrella, and pipe roof methods as the types of it. The majority of the investigated cases are from tunnels in Japan and Italy, where UAM has been widely used for many years, and they are generally located in urban areas. In his work, the purposes to adopt those methods are presented and some cases include multiple reasons. The purposes to adopt the injected steel pipe umbrella method (consistent with the focus of this thesis) are shown in Figure 2.9. Also, the provided statistics in his work show that the most common reason for adopting the pipe roof method is to reduce surface settlement, whereas it is the least common reason for adopting SHJG. Among the investigated cases, the pipe roof method has not been used for slope or landslide failure mitigation; however, both SHJG and injected steel pipe umbrella methods are used for all three purposes. SHJG is aligned with the grouted main category in the UASC proposed by Oke et al. (2014a). While the grouted category covers various types of grouting, even though they are rarely applied, SHJG specifically refers to jetted type of grouting. In addition, the grouted category generally refers to only using the grouting independently, whereas Muraki adds the alternative use of SHJG by reinforcing with steel pipe.

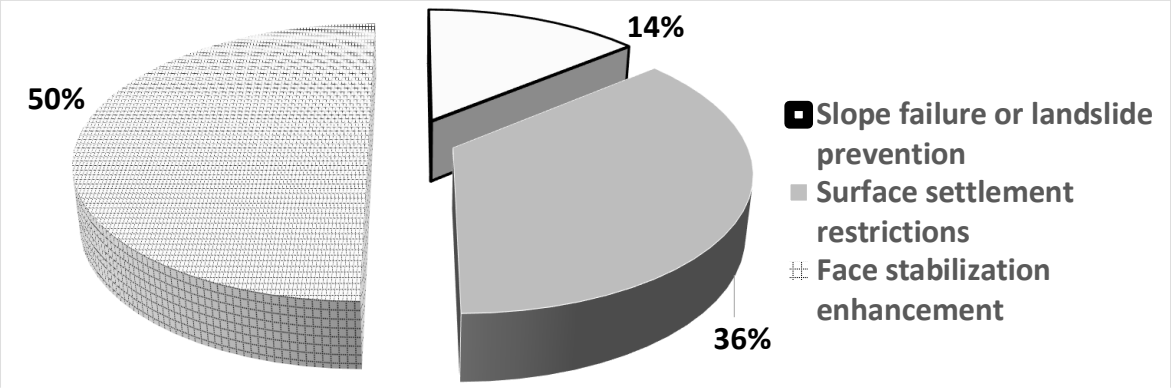


Figure 2.9. Adoption reasons for injected steel pipe umbrella method (modified after Muraki, 1997).

2.4. Tunnel Analyzing Methods

Tunnel analysis relies on mainly three methods. They are analytical, empirical, and numerical methods. In this thesis, numerical methods are the preferred choice for conducting a parametric study.

2.4.1. Empirical Methods

Maiko Tunnel in Kobe is extensively studied by many authors. Harazaki et al. (1998) evaluated the field measurements in the tunnel to describe the behavior of the ground and realized that the reaction of pipes in UA application resembles that of beams. They found that this support method is beneficial to improve the ground conditions and enhance tunnel face stability.

Volkmann and Schubert (2007) utilized inclinometer chains to evaluate the behavior of sections supported with UA application. Thanks to this instrumentation, the system behavior could have been observed ahead of the face and movements could have been recorded from the beginning of the excavation process, not after the instruments were positioned.

Shin et al. (2008) conducted a large-scale experimental study to investigate the reinforcing mechanism of the UA in granular soil. Their study focused on the reinforcing pattern. In an instrumented soil tank, influences of excavations without reinforcement, with crown reinforcement, with face reinforcement, and with both face and crown reinforcement were observed in terms of settlement and stress changes. The results indicated that UA application which acts like embedded beams, enhances longitudinal load transfer ahead of the face, leading to decreased deformation and increased face stability. Also, a three-dimensional numerical study has been conducted as a supplement to that empirical work.

Another experimental study has been conducted by Yeo et al. (2010) in a heavily compressed kaolin clay to model UA application using half symmetrical pipe inserted setup subjected to a centrifugal test. The study showed that the collapse pattern of the non-reinforced setup is different from the reinforced ones. In addition, the experiment focused

on the effect of varying pipe lengths and revealed that the effective length of pipes is between 1 to 2 times of the tunnel diameter.

Additional study was done by Juneja et al. (2010) to understand the effect of the unlined portion of tunnel advancement and the embedment length of pipes. According to the findings through six centrifuge tests, the success of UA in settlement mitigation has been reemphasized. The authors suggested that tunnel stability is influenced not only by unsupported length but also by forepoling length.

Another centrifuge test study was made by Le and Taylor (2016) to examine the effect of UA application on the surface settlement. Overburden depth, embedment length, and filling angle (i.e. the angle that was covered along the tunnel boundary by the pipes) were the variables of the tests conducted in clay. The settlement and tunnel support pressure graphs obtained from the experimental results demonstrated comparable findings in terms of UA presence and showed significant contribution of the UA application to reduce surface settlements in both deep and shallow tunnels. It is found that the UA application is more effective in shallow tunnels in terms of tunnel stability and improvement efficiency increases with greater embedment length. Additionally, the ratio of cover to depth is a factor in soil mobilization and it concentrates on the crown of relatively shallow tunnels.

2.4.2. Analytical Methods

Analytical methods mainly rely on the prediction of loads above the tunnel and the resisting mechanism of the support elements against these loads. In these methods, due to its forepoled nature, UA is assumed as beams in the ground. Muraki (2007) explains the mechanism underlying UA, comparing the longitudinal tunnel sections with and without forepoling. The vertical stress arises at the two ends of the unsupported span in the case without forepoling. Contrarily, the vertical stresses at the ends are smaller when UA is installed and the load on the supported but unlined span is transferred through these UA beams. Thus, the increment in major principal stress is reduced and the Mohr circle is detracted from the Mohr-Coulomb failure envelope.

Terzaghi (1946) incorporates the load above the tunnel into his analysis based on the rock condition and geometric dimensions of the tunnel. Therefore, his rock classification accounts for rock load calculations and includes supporting remarks. While the rock condition deteriorates, the load taken into consideration increases due to the enlargement of the arching zone. It considers the load in cross-sectional, not in longitudinal manner; therefore, the support elements to bear the load are radial arch supports rather than forepoles.

Széchy (1970) explains Protodyakonov's parabolic theory and its similarity with Terzaghi's theory in terms of specific pressure. The arching zone expands as the ground condition worsens. The height of the parabola is formulated as

$$h = \frac{b}{2f} \tag{2.5}$$

where b is the width of the tunnel cavity and f is the strength factor which is less than 1 for loose, granular, and plastic soils. Thus, the height of the required zone for arching becomes greater than the width of the tunnel in these types of ground conditions. If vertical pressure is considered only, then the area is calculated as

$$A_p = \frac{2bh}{3} = \frac{b^2}{3f} \tag{2.6}$$

thanks to the simple area of parabola by substituting the h with the equation above (Eq. 2.5). Therefore, the pressure corresponds to the multiplication of the area and the specific weight of the ground in the arching zone.

In terms of forepoling, Marotta (2013) reviewed various design approaches used for the beam assumption, as shown in Figure 2.10. One of the approaches models the pipes as a beam by considering the unsupported span length and the partially embedded length having negligible resistance. Thus, the beam is pinned to the arch support of the tunnel at one end and supported by ground in pinned or fixed conditions at the other end. The other approach models the pipes as a simply supported beam that considers only the advancement length of the tunnel and a pinned beam on two consecutive arch supports of tunnel behind the face. Another approach models the pipes as propped cantilever beams by considering partial loading of the beams. Here, the unsupported span length is loaded and pinned at one end, while the embedded length is not loaded and fixed at the opposite end. Additionally, there is another approach, known as the beam on multiple supports that employs Winkler's springs to support a fully loaded beam. In this approach, the embedded length of the beam is

supported by springs mimicking the stiffness properties of the ground. On the other hand, the advanced length can either be linked with springs on arch supports or pinned to them. Last but not least, there is an approach called the beam on Pasternak elastic foundation. It considers the beam is loaded along the advancement length and effective embedment length; on the other hand, it is supported continuously by the primary lining or ground except for the unsupported span length.

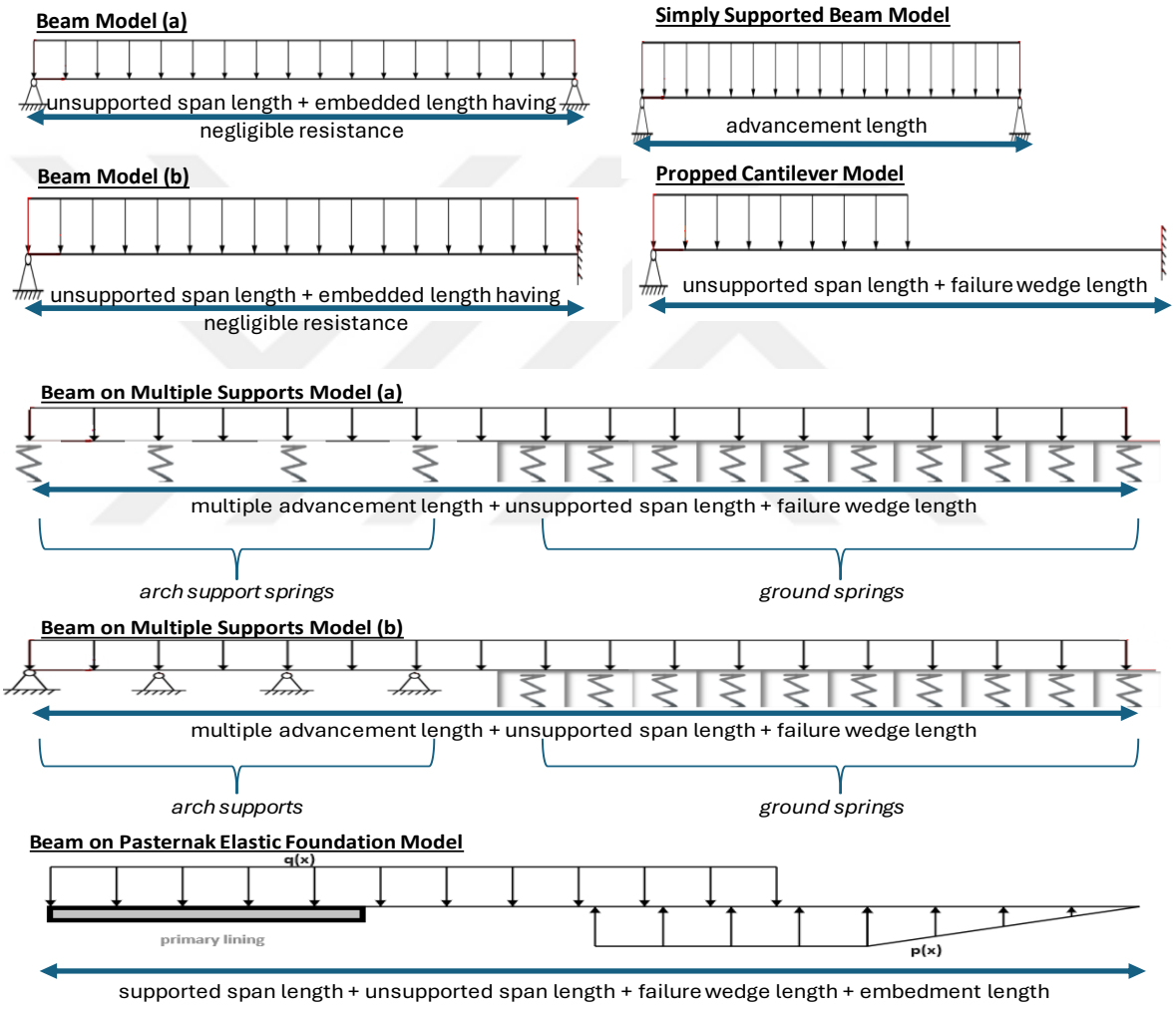


Figure 2.10. Beam model approaches (modified after Marotta, 2013).

Wang et al. (2009) studied to solve the differential equations and subsequently compared the analytical solutions of Winkler and Pasternak beam approaches with the field measurements in Erlangshan tunnel in Chuanzang Highway. The study showed that Pasternak approach gives much closer results to the field measurements in terms of longitudinal strain of UA pipes. Moreover, it indicated that the UA application is effective

in limiting surface settlement ahead of the tunnel face, decreasing deformation and increasing face stability.

Peila et al. (2017) conducted a comparative study between analytical and numerical models of the tunnels in Apennine Mountains in Italy. The Winkler beam on multiple supports was adopted for the analytical approach. The results showed that the three-dimensional numerical model presents sufficient agreement with the analytical ones. Replacing the fixed connection on arch girders with yielding springs in the analytical model led to better alignment with the numerical model. Also, reducing the stiffness of springs just ahead of the face helps to increase the coherence between analytical and numerical models.

Zhang et al. (2020) conducted an analytical study based on the limit equilibrium method and the strength reduction technique in order to investigate the role of face bolts and umbrella arch in improving stability. The proposed model was compared with other analytical models and numerical studies, demonstrating good agreement. As a case study, Yenikapı - Unkapanı Tunnel located in İstanbul, Türkiye is investigated in terms of stability. The results showed the practicality of the proposed analytical model. Furthermore, the results obtained by the proposed model showed the high efficiency of UA in improving the stability of unsupported spans. On the other hand, effectiveness of UA in improving face stability was found to be limited; therefore, it was suggested using bolts to improve face stability.

2.4.3. Numerical Methods

Due to the complexity of tunnel engineering problems, the analytical methods often fall short in solving them and predicting accurate results. Therefore, the necessity of numerical methods has emerged. The success of numerical methods in predicting accurate results and the advancement in computer technology have accelerated the use of numerical methods in engineering disciplines, including geotechnical engineering. In addition to these advantages, numerical methods are also useful in conducting parametric studies. Among various numerical methods, finite difference and finite element methods are widely used to obtain approximated solutions for analyzing tunnels.

2.4.3.1. Finite Difference Method (FDM). Principally, the finite difference (FDM) method relies on discretizing the continuum of the problem into discrete particles. It aims to replace the differential equations with approximate algebraic equations by way of finite difference equations at specific nodes. The approximated results are obtained for discretized nodes and interpolation can be used for intermediate points. In tunnel design, FDM-based software is frequently used as well as finite element method based software.

2.4.3.2. Finite Element Method (FEM). Like the FDM, the finite element method (FEM) relies on discretizing the continuum of the problem into definite particles in terms of geometry and dimensions. Each discretized element consists of nodes. These elements form the mesh of the problem domain. The behavior of the elements is prescribed by constitutive models such as Mohr-Coulomb, strain hardening, cam clay, and elastic model for geomechanical problems. Thus, the relationship is defined between elements and algebraic representation of the problem is formed. Boundary conditions are applied, and the algebraic formulation is simplified. The problem is then post-processed to predict the results of unknowns. The approximated results are obtained for the elements with polynomial functions. Implementing FEM is more complex than FDM, but thanks to these functions, it can be said that FEM generally provides higher accuracy than FDM. One of the most commonly used geotechnical software, PLAXIS, is a FEM-based software and it is the software used in this thesis.

For tunnel problems, finite element analysis models can be created in two-dimensional or three-dimensional formats. The three-dimensional modeling is useful to see the mechanistic behavior of forepoles and the effects depending on tunnel advancement. For example, the 3D numerical studies conducted by Özer (2011), Bagherzadeh et al. (2020) and Pashaye et al. (2021) show that the application of forepoling before excavation helps to mitigate displacements and increase tunnel stability. Also, numerical modeling is useful to find the optimum properties for support elements. On the other hand, axisymmetric or plane strain conditions are available for two-dimensional models. In the axisymmetric models, generally the tunnel is modeled in longitudinal section, and it is rotated to satisfy the axisymmetric conditions. As stated by Çeçen (2007), to eliminate the effect of rotation under these conditions, the initial stress distribution can be arranged by utilizing high K_0 coefficients. However, it is not suitable to model sequential excavation and forepoling. In

plane strain models, the tunnel can be modeled in transverse or longitudinal sections. The longitudinal models are not suitable to observe the stresses on the tunnel lining and the settlement distribution in lateral direction since the curved geometry cannot be modeled. Also, it does not allow modeling twin tunnels. Instead, the forepoling elements can be modeled as embedded beams. On the other hand, cross-sectional modeling shows the stress and settlement distribution in lateral direction, but it does not indicate settlement occurrence in tunnel advancement direction. The full geometry of the tunnel can be projected, and it is appropriate to model more than one tunnel in the same problem. To implement the forepoling elements into the model, creating a homogenized improved zone is suggested by Hoek (2004). There are various homogenization approaches that can be applied and Oke et al. (2012) states that modeling the forepole elements as a homogenous region is empirically acceptable even though it has deficiencies to reflect the mechanistic behavior.

2.5. Effecting Parameters

Numerous numerical studies focused on tunnels supported with umbrella arch. Aksoy and Onargan (2010) conducted case studies belonging to İzmir Metro Tunnels located in Türkiye. The tunnels were supported with UA and bolts implemented on both radial and face surfaces of the excavation. The inner tunnel convergence results obtained from 3D FEM analysis showed good agreement with the field measurements. Furthermore, based on these validated results, the convergence was predicted by numerical analysis for the case of without umbrella arch and bolts. The comparison of results of these two cases revealed, as expected, the deformation in the tunnel supported with UA was less than in the tunnel not supported with UA.

Elyasi et al. (2016) conducted case studies belonging to an adit tunnel to access the Zagros Tunnel located in northwest Iran. The tunnel support system was designed with UA and 3D FDM analysis was performed for both supported and unsupported cases. The comparison showed that the plastic zone around the tunnel and displacement in the crown of the tunnel decreased when UA was applied. Also, the results of numerical analysis closely matched with the readings obtained from field measurement instruments.

Zarei et al. (2019) conducted case studies belonging to Sabzkooh Tunnel located in Iran. The tunnels were supported with UA and bolts implemented on both radial and face surfaces of the excavation. The comparison based on the 3D FDM analysis performed for both supported and unsupported cases showed that the vertical displacement and surface settlement along the excavation direction decreased when pre-supports were applied. Thereupon, they focused on the optimization of UA pipe characteristics such as diameter, angle, and spacing.

In the literature, numerous parameters have been investigated to reveal their effects on the behavior of the UA-supported tunnels. For this thesis, parameters affecting the pipe characteristics have not been focused on due to 2D modeling, but five main factors in terms of geometry and conditions are determined for the parametric study. These are UA improvement zone, overburden depth, clear distance, diameter, and properties of the surrounding ground. In this framework, the parameters are defined, and they are considered in combination, resulting in the creation and calculation of 162 numeric models.

2.5.1. Improvement Zone

Since the method relies on the strength of the pipes and grout, in order to increase the effective area of the UAM, steel pipes sometimes can be applied in double rows and the grouted area can be enlarged. For example, Kim (2008) shares his experiences regarding different support measurement examples applied in Seoul Subway Line construction and underlines the application of double-layered and reinforced horizontal jet grouting columns in a low cohesive alluvial deposit under shallow overburden depth and high ground water level conditions located in Line 9 Lot 912. By stating varied support measurements along the route, Krenn et al. (2008) gives an example from Austria where double-layered UA was applied in the shallow sections under unstable gravel conditions. Similarly, Trunk and Winkler (2013) present the support system of the Ceneri Base Tunnel located in Switzerland as an example for double-row horizontal jet grouting columns under loose rock and shallow overburden depth conditions. In another example, the case study of Tonon (2011) is listed as FpGdcUA by Oke (2016) since steel reinforcement is used in sub-horizontal jet grouted columns in this case and the grouted main category is limited by the use of only grout according to nomenclature. However, this categorization should be corrected due to the

confusion arising from frequent overlapping (doubling or even tripling) of pre-support elements in the cross-section of Cassia Twin Tunnel. Also, the main categorization should be considered as grouted for the Cassia Twin Tunnel since they are performed essentially by jet-grouting and reinforced by steel as noted by Muraki (1997). A similar example in the list is the work of Da Via et al. (2006). This case study explains the redesigning of the support system with reinforced double-layered sub-horizontal jet grouting and its successfully implementation in Hukou tunnel after two major collapses occurred in the project, where single row UA had been applied before the failure. Therefore, the other author of the same case study, Marotta (2013) in his thesis, mentions this pre-supported section as triple layered, indicating that the overlapped regions of single row UA have resisted more against the collapse. A parametrical study has been conducted in his thesis over the simple analytical – empirical and semi-empirical approaches proposed for longitudinal pre-supports and another model has been suggested by the author, which did not include the double-layered pre-supports. As can be seen, double layering is generally associated with horizontal jet grouting and is applied rarely, typically only when the overburden is shallow or the ground conditions are unstable.

Though limited, there are also examples of double row applications in forepoling. For example, Küçük (2011) investigated the effect of ground water in a case study and stated that even though the tunnel had been surrounded with double-layered UA, it was insufficient to resist the challenging geomechanical conditions weakened by dynamic water flow. On the other hand, DSI (2014) stated that the second row was applied for the metro tunnel located in Hong Kong, China, when the first row became insufficient to support the tunnel crown consisting of highly weathered rock. Aygar and Gökceoğlu (2020) suggested using the second row while passing a collapsed tunnel zone to benefit from the inclination of pipes in order to reach deeply into the collapse zone and to fill the potential voids at the tunnel ceiling. Another example for the double layered pre-supporting in that list is Dulles Corridor passing under an overburden of approximately 2.1 to 4.5 meters at Tyson Corner. According to Jenkins et al. (2011), where the overburden rises, the double-layered grouted forepoling umbrella arch application was abandoned, and the project was employed with single row. In addition to the contractor company, Gall et al. (2011), contributing as the consultancy company for the same tunnel, implied very shallow overburden and critical utilities above and around the tunnel path as the reasons to adopt double layer. Furthermore, they explained

the adjustments due to disadvantages of double-layered forepoling, such as reduced overburden and less overlapping. Moreover, they created a 2D model to assess the tunnel induced deformation and tunnel structural design, though it did not include UA elements. Additionally, a 3D model was created to supply the two-dimensional model and assess the performance of UA; however, it has been prepared for only single tunnel and single row UA since modeling twin tunnels with double layered UA is more complex and time-consuming. Again, it is seen that the double layering with forepoling is a very rare application and it is applied only when the overburden is thin, single row is insufficient, or critical structures are located around the tunnel.

Increasing the number of forepoling rows to increase the area of the improved zone is a practical solution in challenging conditions. However, the works in the literature beyond the case studies are too limited to reveal its success and to demonstrate its superiority over single row. It is especially hard to point out its effect in numerical modeling studies, particularly in two-dimensional models. Klotoé and Bourgeois (2019) studied on a double forepole grouted umbrella arch case by modeling it in three dimensions; however, the obtained settlement results in the longitudinal direction between the unsupported case and the case with umbrella arch were very similar. In addition, Bizjak and Petkovsek (2004) explain the landslide that occurred in the tunnel portal of Golovec Tunnel, which is the first three-lane and two-tube highway tunnel in Slovenia, and they present this failure as the reason for adopting double-layered UA. They also created a 2D numerical model of the excavation and succeeded in getting good agreement between the numerical simulation results and site measurements of surface settlement. Furthermore, thanks to their three-dimensional finite difference approach, Yang et al. (2008) achieved a good fitting between the numerical analysis results and site observations of a tunnel portal construction. They found up to 50% reduction directly above the tunnel crown in terms of surface settlement when they compared the results of the double-layered model with the unsupported model. Thus, they proposed to adopt the double-layered UA while passing through tunnels under critical structures. Oke et al. (2014b) also observed the beneficial effect of the double layer UA to reduce the maximum surface settlement using 3D modeling. Miwa and Ogasawara (2005) conducted a case study located in Japan where the tunnel has passed under the national road, adopting double-layered UA and performing numerical analysis before the excavation. However, when the excavation was completed, the tunnel crown displaced more

than estimated. The authors attributed the discrepancy between the actual and predicted displacements to the variation of soil properties in layers and insufficient bearing capacity of the ground where the steel supports were implemented. Despite the challenges in modeling and computing, the contribution of double-layered UA compared to single-layer remains unclear. The results presented by Perveroğlu Şat et al. (2023) in a case study show no significant differences in terms of surface settlement between the single-layer and double-layer UA models. According to the results, they imply the insufficiency of 2D modeling to reveal the potential benefits of double-layer UA in mitigating surface settlements. Therefore, in the parametric study of this thesis, double-layered UA modeling is not prioritized. Instead, the result comparison is framed more broadly to understand the overall contribution of UA systems in comparison with no pre-support, rather than focusing solely on surface settlement.

Ağbay (2019) conducted case studies on twelve forepoled twin tunnel sections belonging to Eurasia Tunnel project located in Türkiye. These studies covered various ground conditions and as forepoling technique, six of the sections have been supported by spiles, two of them have been supported by umbrella arch, and spiles are used for one tunnel while umbrella arch is applied for the other tunnel in the remaining four twin tunnel sections. The improvement zones were created according to the weighted average of the materials in the zone. In their parametric study, the properties of the improved layers were adjusted by changing the forepole spacings used for ground improvement. The tabulated results presented for the maximum surface settlement (S_{max}) with respect to pipe spacing indicated that increasing the elastic modulus in the improvement zone by decreasing the spacing between forepoles has a limited impact on reducing S_{max}.

Li et al. (2020) conducted a parametric study based on the case studies belonging to the triple tunnels located at Badaling Great Wall Underground Station in China. The improvement zone was defined to simulate the forepoled area in 3D modeling. Its equivalent elastic modulus and equivalent density are calculated with respect to the change in pipe diameter in the range of 0 – 186 mm. According to the parametric optimization study, the effect of pipe diameter on mean crown settlement was not prominent for diameters larger than 108 mm.

2.5.2. Overburden Depth

Song et al. (2013) conducted a parametric study with 3D models to investigate the effect of overburden depth in the range of 10 – 40 m under different UA application conditions, including pipe diameter and pipe spacing. The results revealed that the factor of safety against shear force and bending moment decreases as overburden depth increases. Another parametric study with 3D models was conducted by Wang et al. (2020) in order to investigate the effect of overburden depth in the range of 1.6 – 11.6 m under the same support conditions. The results indicated that settlement increases as overburden depth increases.

Sarıgül (2018) conducted case studies belonging to Terzili and Ulubey Tunnels located in Türkiye in order to analyze the swelling effect. Although the models did not include swelling directly, the swelling condition was accounted for by applying additional stresses on the tunnel lining. Comparing the no-swelling stages for the Terzili Tunnel under 10 m and 30 m overburden depths, it is seen that the primary stress and deformation increase as the overburden depth increases. However, this trend was not observed for Ulubey Tunnel, suggesting that overburden depth is not the only parameter affecting tunnel deformation; other parameters such as ground conditions and distance between tunnels should also be considered.

The overburden depth was taken into consideration as the multiples of the tunnel diameter in the 2D parametric study in longitudinal section conducted by Çeçen (2007). Since the model is in longitudinal direction, the maximum displacement was calculated on the face, not on the radial surface of tunnels. Therefore, maximum horizontal displacement was measured in that study. According to the results, the maximum horizontal displacement on the tunnel face increases as overburden depth increases.

Kamal et al. (2021) investigated the effect of overburden depth on the straining actions of twin tunnels. According to static analysis in their study, the change in overburden depth is investigated in the range of 2D to 5D. The study showed that displacements and axial forces increase as overburden depth increases along the range. However, shear force decreases up to 2.5D and starts to increase up to 5D by changing its direction. On the other

hand, bending moments oscillate along the range by increasing their amplitude while the tunnel's depth gets deeper.

2.5.3. Tunnel Diameter

Sojoudi (2015) conducted a study for TBM tunnels having varied tunnel diameters by using the same software used in the present thesis. and in the software. The study, which maintained a fixed contraction ratio, showed that the maximum settlement on the surface and the maximum vertical displacement in the tunnel increase as tunnel diameter increases.

In the study conducted by Kanik (2019), the tunnel shape and size were altered, resulting in changes to the equivalent diameter of the tunnel. The investigation focused on the yielding depth of the tunnels. According to the results, as the tunnel gets larger, the yielding depth decreases, which means the support elements of larger tunnels reach the yielding stress levels at shallower depths compared to smaller tunnels.

2.5.4. Ground Conditions

Tan (2005) conducted case studies belonging to Maiko Tunnel located in Japan, which covered two different zones in terms of ground conditions. Both zones were underlain by Kobe formation consisting of sandstone and shale. However, the top layer was an alluvial fill consisting of gravel with clay in Zone A and it was Osaka formation consisting of clayey gravel in Zone B. The differences were represented by variations in elastic modulus and cohesion values. As expected, Zone B, which was stiffer and more cohesive, exhibited less settlement than Zone A. Additionally, by conducting a parametric study for Zone A in terms of the elastic modulus of the ground, it was found that the surface settlement profile shifts downward and S_{max} increases as elastic modulus decreases.

The lateral earth pressure at rest (K_0) is taken into consideration as a ground condition parameter in the study conducted by Çeçen (2007). As mentioned before, since the study was conducted in the longitudinal section, the maximum horizontal displacement values were measured from numerical analysis. The results marked that horizontal displacement

increases as K_0 increases and its effect becomes more distinguishable with greater overburden depth.

The study conducted by Song et al. (2013) also investigated the effect of ground conditions. The tunnels having identical geometry and support conditions were analyzed by changing the ground conditions representing weathered rock, highly weathered rock, and weathered soil. The results show that safety factors in terms of shear force or bending moment decrease as ground conditions worsen. Similarly, another parametric study with 3D models was conducted by Wang et al. (2020). In order to investigate the effect of ground conditions, four different soil sets were used and the results revealed that the settlement increases as ground conditions worsen.

Kaya and Bulut (2017) conducted case studies belonging to Cankurtaran Tunnel located in Türkiye. The studies covered four zones in terms of ground conditions. Three zones were classified as poor according to RMR classification, very poor according to Q classification, B3 (rolling) according to NATM classification. One zone was classified as very poor according to RMR classification, extremely poor according to Q classification, and C1 (rock bursting) according to NATM classification. Numerical modeling was used to analyze the support systems defined by RMR and Q empirical classification systems. It was concluded that the support system proposed by Q classification for the zone having extremely poor conditions was insufficient. On the other hand, the support systems proposed by RMR and Q classification systems for the zones having poor and very poor conditions, respectively, were sufficient for two of the three zones but insufficient for one. Therefore, the authors recommended checking empirical designs by performing numerical analyses and observing them during construction.

With the case studies conducted by Ağbay (2019) for twelve forepoled twin tunnel sections, it was found that ground condition is the dominant factor on the maximum surface settlement. Additionally, a sensitivity analysis was conducted in that study by varying the ground parameters. This analysis showed that S_{max} increases dramatically as ground conditions worsen due to reduction in elastic modulus. The study, which used Mohr-Coulomb failure criterion, also implied that Poisson's ratio has a great impact, but angle of shear strength and cohesion parameters have limited impact.

2.5.5. Distance Between Twin Tunnels

Karakus and Fowell (2000) conducted a parametric study based on a validated approach for the Heatrow Express Trial Tunnel in London, United Kingdom. The validation study has been conducted for a single tunnel with different excavation sequences to detect the best approach by comparing the numerical analysis results with field measurements. Upon this validation, the distance between twin tunnels, which is referred to as pillar width in that study, is investigated with spacings of 0.5D, 1D, and 2D. It was observed that the S_{max} increases as the spacing decreases, and the settlement profile gets narrower and deeper with reduced spacing.

Kaya and Bulut (2013) conducted case studies belonging to Cankurtaran Tunnel located in Türkiye. The studies aimed to compare the empirical and numerical stability analyses of tunnels. The case involves twin tunnels; however, empirical methods consider the tunnels as singular entities and give identical results for different tunnel tubes under the same ground and geometry conditions. On the other hand, it differs in FEM analysis due to tunnel construction stages, even though they are under the same conditions. Their study reflected this situation by tabulating different factors of safety results for left and right tubes. Since the results depend on stress distribution, it was indicated that tunnel behavior is influenced by the construction order and the distance between the twin tunnels. Differences between left and right tubes in terms of stress distribution were also observed in another study conducted by Kaya and Bulut (2017).

Kaya and Bulut (2019) continued their work on Cankurtaran Tunnel, aiming to propose appropriate primary support designs for the tunnel along the route by dividing it into 15 segments. The performed two-dimensional and three-dimensional numerical analyses showed differences in twin tunnels located in the same segments. Therefore, they recommended conducting numerical analyses over empirical methods for twin tunnels, in order to capture these differences accurately.

The studies conducted by Ağbay (2019) belonging to the twin tunnels with forepoling found that in addition to the ground conditions, the distance between tunnels, also affects the surface settlement significantly. It is noticed that the S_{max} in the former tunnel section located

at the beginning of the excavation is higher than the latter one located at the end of the path since the distance between the tunnels increases as the section is excavated. In addition, according to the maximum settlement tables presented in that study, it can be inferred that the volume loss of the secondly excavated tunnel in the same section is higher than the firstly excavated one when the center-to-center distance of twin tunnels ranged between 1.58 to 2.45 times the tunnel diameter.

Li et al. (2020) conducted a case study on the Badaling Great Wall Underground Station located in China. The platform level of the station has triple tunnels, where the two tunnels on the sides have the same geometric properties. In that study conducted by installing pressure cells on the steel frames in the primary lining to monitor the excavation, the surrounding rock pressure graphs of the side tunnels show that the pressure developed around the secondly excavated tunnel is higher than the firstly excavated one when the supporting stages of two tunnels were completed. Also, it is implied that decreasing the distance between the tunnels causes more severe weakening of the pillar.

Wijaya et al. (2021) conducted a three-dimensional finite element analysis to compare the cases involving single and twin tunnels supported with umbrella arch method. Based on the geometric and geotechnical conditions of Cisudawu Tunnel, which is the first tunnel supported with UA in Indonesia, the numerical results are compared in terms of the maximum roof displacement of the tunnel, the maximum lateral displacement of the tunnel, and the maximum surface settlement. As expected, due to interaction distance, all the compared results showed that the values in the case involving twin tunnels are higher than the case involving a single tunnel. Also, due to the same reason, the location of the maximum surface settlement was observed between the tunnels.

According to the static analysis results of the study conducted by Kamal et al. (2021), the displacements, shear force, and bending moment decrease while the distance increases within the range of 1 to 3 times of tunnel diameter. On the other hand, axial forces are not affected significantly due to changes in distance

3. VALIDATION STUDY

In this research study, a series of numerical analyses were conducted on the tunnel models supported by UA using a FEM based 2D software to better understand the factors effecting the tunnel deformation behavior. Before initiating a parametric study, the modeling principles and their suitability to use in the parametric study should have been determined. Therefore, in the initial part of this research, a validation study was conducted using two instrumented case studies. The main goal of this validation study was to model UA application with different approaches available in the literature to determine the effects of approach differences on numerical analysis results. The results obtained from the numerical analysis were compared with the measurements obtained from the sensors located in the field. The site data obtained from Çekmeköy – Sancaktepe – Sultanbeyli Metro Project located in İstanbul, Türkiye has been instrumental in this research phase. The further details of these two case studies used for the validation are explained in Ergincan et al. (2023) and Ergincan et al. (2024). After completion of the validation, the methodology was finalized using the modeling approach selected. A parametric study was conducted to understand the effects of various parameters (overburden depth, tunnel diameter, tunnel clear distance, ground conditions, and the existence of an improved zone representing UA application) on the behavior of NATM tunnels.

This chapter summarizes the modeling approaches investigated, the methodology, the selected cases for the validation study, and the results obtained from the study. The methodology used in the parametric study, which was developed based on the validation study, is presented in the next chapter.

3.1. FEM Model

The tunnel sections were created and analyzed using PLAXIS 2D, a widely used finite element (FE) analysis software of Bentley System's (2022) in geotechnical practice, throughout this research study. This software allows for the modeling of UA supported tunnels in both longitudinal and transversal cross-sections.

The studies by Çeçen (2007) and Ocak & Selçuk (2017) apply longitudinal modeling with elastic beam theory to study the effects of tunneling in the advancement direction. However, this approach is not suitable to investigate the effects of tunneling in the transverse direction. Therefore, in the validation study, transversal cross section is selected following Tan (2005), Ağbay (2019), Norouzi (2020), and Güneş (2021). In these studies, the UA application is typically defined as an improved zone above the tunnel crown, and the model is analyzed in plain strain conditions.

3.1.1. FEM Modeling Approaches for UA Application

In order to simulate the improved zone and the temporary lining supports in UA applied tunnels, three (3) main modeling approaches were taken into consideration. One of them is the *plate approach* used in the studies of Tan (2005), Ağbay (2019), and Norouzi (2020). The second approach is the *dummy plate* used by Güneş (2021). The last one is the *individual pipe*, which is another approach used in Hefny et al. (2004) and Tan (2005).

All of these approaches rely on creating a lining support around the tunnel and an improved zone above the tunnel crown. The properties of this improved zone are defined mainly by using the weighted average of the properties of the utilized materials present in the zone. In these calculations, the area covered by each material in this zone is considered; however, there are variations in each approach with respect to how each component and its properties are defined. Thus, the same section was modeled with three different approaches to evaluate the most suitable approach for the analysis of the UA applied tunnel sections in this research work. For this purpose, the numerical results obtained from the analysis of FEM models created with different UAM modeling approaches were compared with the results obtained from field measurements. The sketches of the evaluated UAM modeling approaches are shown in Figure 3.1.

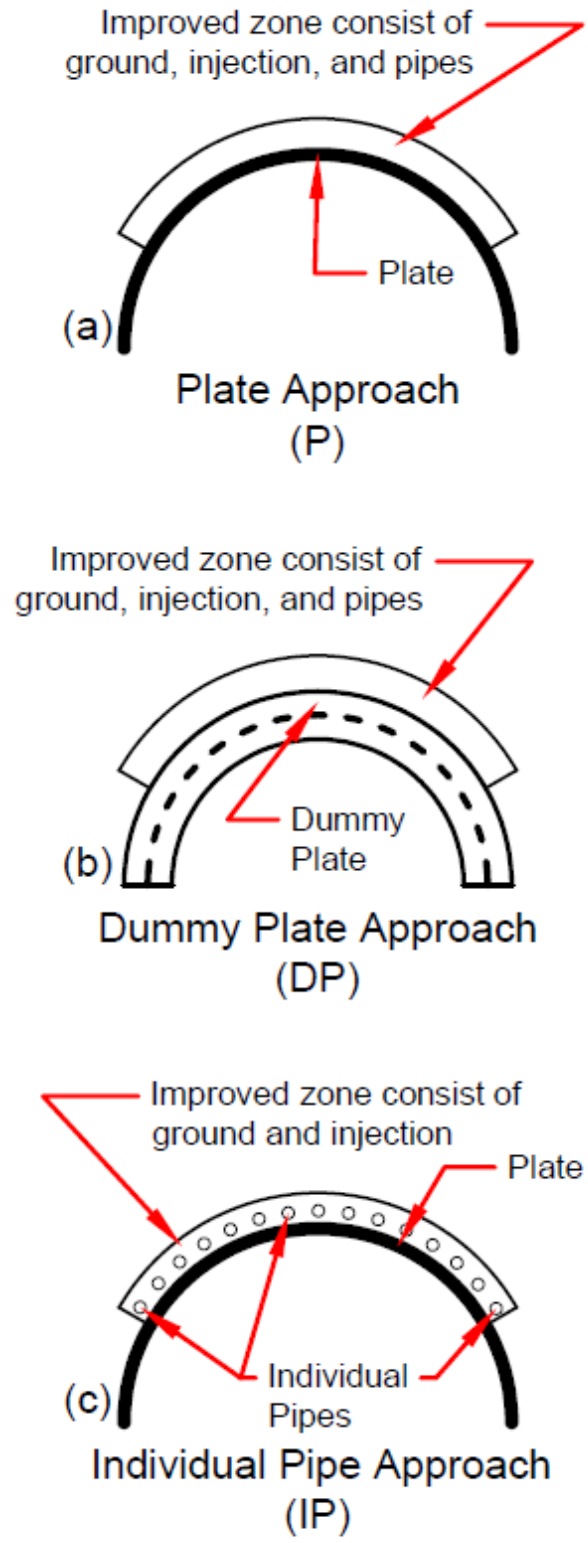


Figure 3.1. The sketches of the evaluated approaches for the validation study: (a) Plate Approach (P), (b) Dummy Plate Approach (b), (c) Individual Pipe Approach (P) (modified after Ergincan et al., 2024).

3.1.1.1. Plate (P) Approach. In the plate (P) approach, the *improved zone* consists of the original ground surrounding the tunnel before the UA application, the injected grout that fills the voids, and steel pipes inserted into drilled holes for UA application. The elastic modulus (E) of this improved zone is calculated according to the weighted average of the elastic moduli of these three materials (see Figure 3.1a). In this approach, the lining is modeled as a plate element. The plate element has bending stiffness and axial stiffness defined by EI ($kN.m^2/m$) and EA (kN/m), respectively. In this definition, I is the moment of inertia, and A is the cross-sectional area of the plate elements.

3.1.1.2. Dummy Plate (DP) Approach. Similar to the P approach, in the dummy plate (DP) approach, the improved zone consists of the original ground surrounding the tunnel before the UA application, the injected grout that fills the voids, and steel pipes inserted into drilled holes for UA application. The elastic modulus (E) of this improved zone is calculated according to the weighted average of the elastic moduli of these three materials. In this approach, the lining is modeled as a volume element (i.e. soil layer). Along the centerline of this volume element, an impotent plate element is inserted. To create an impotent plate element, the stiffness properties of the original plate element are multiplied by incredibly small-scale factors such as 10^{-6}. This scaling is the reason for the word dummy in the description. Even though the plate element placed in the soil layer has no contribution to the support system, it facilitates the determination of the internal forces and deformation in this soil layer (see Figure 3.1b).

3.1.1.3. Individual Pipe (IP) Approach. In the individual pipe (IP) approach, unlike the assumptions made in the other two approaches, the contribution of the pipes is not accounted for in the weighted average while calculating the elastic modulus of the improved zone. They are modeled separately using the engineering properties of the steel pipes. Therefore, the elastic modulus (E) of this improved zone is calculated according to the weighted average of the elastic moduli of only the original ground surrounding the tunnel before the UA application and the injected grout that fills the voids (see Figure 3.1c). In this approach, while modeling the temporary lining, it is handled like the plate (P) approach and a plate element having not scaled stiffness parameters is located along the tunnel radial surface.

3.2. Instrumented Case Studies Investigated for the Validation Study

In order to ensure the validity of the tunnel modeling technique, two case studies were investigated using similar assumptions. The cases belong to two different locations on the Çekmeköy-Sancaktepe-Sultanbeyli Metro Line project. To determine the case study locations, the metro line and the ongoing construction activities are filtered first for the existence of UA application. The UA applied locations were further grouped based on tunnel types (Type A, B, P, T, etc.). Type A tunnel, that is commonly constructed along the project which has a section close to a circular section, was determined as suitable for the validation analysis. In essence, at the selected project locations, the excavation and support stages of construction should be completed, and the displacements induced by tunneling should be diminished. Therefore, the locations having ongoing ground movements have been eliminated to avoid misinterpreting of the comparison between displacement results obtained from numerical analysis and field observations. The borders of inspection areas have been narrowed further to ensure the isolation of the selected project locations from the effects of ongoing excavations, such as station excavations. Based on this criteria, two specific inspection areas on the metro line were determined, as shown in Figure 3.2. Thus, the twin tunnel sections with similar ground and loading conditions are generalized for modeling.

As sketched in Figure 3.2a and Figure 3.2b, the plan view of the inspected area covers approximately 50 m and 110 m in the excavation advancement (longitudinal) direction for Case1 and Case2, respectively. In the lateral direction, the width was limited to 100 m on each side of the centerline of the twin tunnel in the numerical model to cover the stated specification of the project and to satisfy enough distance for the alleviation of settlement, although the influence width determined in the project specifications is not so wide. Due to the project route, the clear distances between twin tunnels are not constant. They are approximately 19.8 m and 23.5 m for Case1 and Case2, respectively. In these plan views, there are 13 and 15 settlement bolts in the first and second inspection areas, respectively. Their locations used for the field measurements are indicated with their distances to the centerline of the twin tunnels. Throughout the project, the displacements of these settlement bolts were recorded using laser measuring instruments.

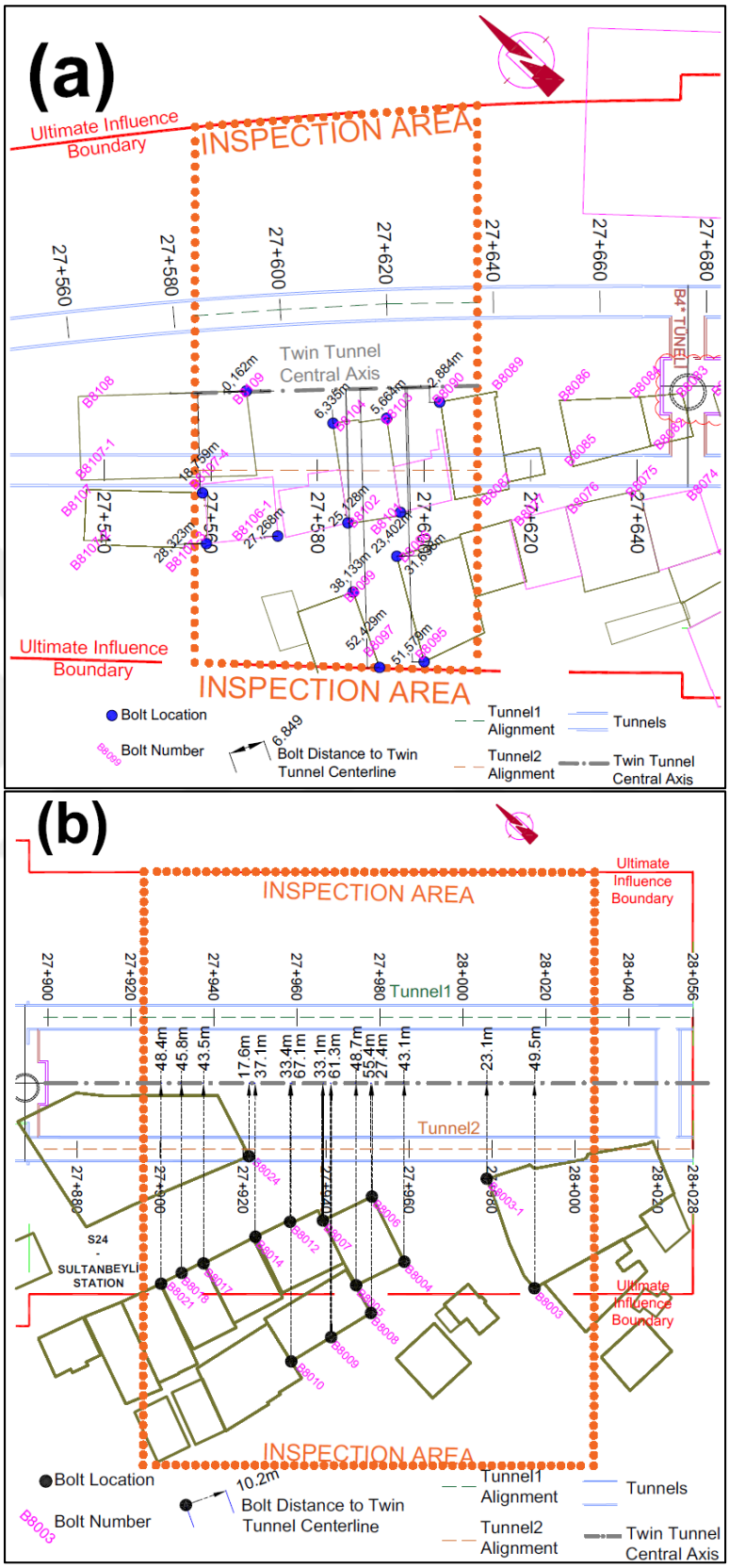


Figure 3.2. The plan views of the specified inspection areas for validation study (a) Case1 (modified after Ergincan et al., 2023) and (b) Case2 (modified after Ergincan et al., 2024).

The idealized soil profiles used for these inspection areas of the two cases are tabulated in Table 3.1 and Table 3.2 for Case1 and Case2, respectively. Hardening soil constitutive model was utilized for these layers. The properties of the improved zones simulating UA application are tabulated in Table 3.3 and Table 3.4 for Case1 and Case2, respectively.

Table 3.1. Idealized soil profile of Case1 selected for validation study (adopted from Ergincan et al., 2023).

Layers	**Ground Layers**	**γ (kN/m³)**	**E' (MPa)**	**c' (kPa)**	**ϕ (°)**
Surface - 3.5 m	Fill	18	15	1	28
3.5 m - 24.0 m	Clayey silty sand	20	70	10	35
24.0 m - 50.0 m	Highly weathered sandstone (Arkose)	24	65	61	39

Table 3.2. Idealized soil profile of Case2 selected for validation study (adopted from Ergincan et al., 2024).

Layers	**Ground Layers**	**γ (kN/m³)**	**E' (MPa)**	**c' (kPa)**	**ϕ (°)**
Surface - 5.0 m	Fill	18	15	1	28
5.0 m - 24.0 m	Highly weathered sandstone	24	65	61	39
24.0 m - 50.0 m	Moderately weathered sandstone	24	95	73	39

Table 3.3. Calculated properties of the improved zone in Case1 (adopted from Ergincan et al., 2023).

Modeling Approaches		**Plate (P) and Dummy Plate (DP) Approaches**				**Individual Pipe (IP) Approach**			
Material	Area (m^2)	E (GPa)		γ (kN/m^3)		E (GPa)		γ (kN/m^3)	
		Gross	W.P.(%)	Gross	W.P.(%)	Gross	W.P.(%)	Gross	W.P.(%)
Soil	2.961	0.065	1.58	24.0	87.64	0.065	30.49	24.0	87.64
Injection	0.219	2.0	3.60	25.0	6.76	2.0	69.51	25.0	6.76
Steel Pipe	0.058	200.0	94.82	78.6	5.60	–		78.6	5.60
Improved Zone		3.760		25.0		0.199		25.0	

Table 3.4. Calculated properties of the improved zone in Case2 (adopted from Ergincan et al., 2024).

Modeling Approaches		**Plate (P) and Dummy Plate (DP) Approaches**				**Individual Pipe (IP) Approach**			
Material	Area (m^2)	E (GPa)		γ (kN/m^3)		E (GPa)		γ (kN/m^3)	
		Gross	W.P.(%)	Gross	W.P.(%)	Gross	W.P.(%)	Gross	W.P.(%)
Soil	3.080	0.095	2.38	24.0	88.06	0.095	39.07	24.0	88.06
Injection	0.219	2.0	3.57	25.0	6.53	2.0	60.93	25.0	6.53
Steel Pipe	0.058	200.0	94.04	78.6	5.40	–		78.6	5.40
Improved Zone		3.657		25.0		0.226		25.0	

In Table 3.3 and Table 3.4, W.P., E, and γ symbols represent weighted percentage, elastic modulus, and unit weight, respectively. The improved zone thickness, pipe thickness, pipe inner diameter, pipe spacing, and pipe outer diameter were assumed as 35 cm, 6.3 mm, 101.7 mm, 30 cm, and 114.3 mm, respectively. UA applied tunnel sections are constructed with rising steps and they also have an enlarging nature due to the shape of an umbrella. The last excavation step (until the next overlapping) was accepted as the most critical section, that has an 8.2 m-equivalent-diameter for the selected Type A tunnel. This critical section was selected for modeling.

3.2.1. Assumptions

To model the staged construction of a tunnel case using 2D finite element software, some assumptions are required. The following assumptions were made in this study:

- Since the project is located in an urban area, there are road embankments and building loads over the sections of the validation cases. These loads by determined using AASHTO (2002), Faheem & Hassan (2014), and Norouzi (2020); and were applied on the plate elements simulating foundations.
- The groundwater level was lowered as it is applied frequently in NATM excavations.

- The interactions between soil and structural material were defined with the R_{inter} factor in PLAXIS 2D software to reduce the strength and stiffness of interface. In this study, R_{inter} =0.70 was used for the interfaces for the ground materials following Ağbay (2019).
- As explained in FHWA (2009), since the fresh and hardened phases of shotcrete do not have the same strength, they were defined separately in the software, and the strength was increased in steps together with the deconfinement process. One-third of the shotcrete strength was accepted for the fresh phase, and it was increased to full strength in the hardened phase following the study by Ishida et al. (2009).
- As explained in PLAXIS Tutorial Manual (2022), in order to simulate the 3D effects in PLAXIS 2D, the deconfinement option can be used. Deconfinement relies on preserving the initial stress partly in phases. The remaining stress is set to zero in the proceeding phases by fully deactivating (i.e. increasing the deconfinement ratio up to 100%) the soil cluster. Deconfinement ratios were determined as 40%-60%-100% for the upper half excavation phases of tunnels and 20%-40%-100% for the lower half excavation phases of tunnels consistent with the ranges stated by FHWA (2009), Zelger (2012), and Güneş (2021).

3.2.2. Excavation Stages

As addressed in Section 2.2., NATM is a cyclic (sequential) excavation method. The cycles have different stages in sequence, so they are modeled according to staged construction principles. For the conducted validation studies of twin tunnels, 17 phases were appointed for the corresponding construction stages. The first 11 construction stages are presented in Figure 3.3. The construction stages (phases in PLAXIS) performed for the first tunnel (T1) are repeated for the excavation of the second tunnel (T2). These 11 construction stages are briefly explained below.

0. Initial Phase: The self-load of the soil layers is applied with K_0 procedure.
1. Surface Loading: The loads are applied prior to the excavation.
2. Dewatering: The groundwater level is lowered before the excavation.
3. Activation of the zone improved by UA: Since UA application is performed in the advancement direction, the improved zone is created before the excavation reaches

this specific section. The surrounding layer above the tunnel crown is replaced with an improved layer before the excavation started.

4. Upper half excavation – unsupported phase: After the UA application, the upper half of the tunnel is excavated, and the tunnel starts to converge. In this phase, there are no support elements, but a deconfinement ratio is applied to the deactivated soil cluster.
5. Upper half excavation – partially supported (fresh shotcrete) phase: Shortly after the advancement of excavation, the excavation surface is supported with temporary support elements like shotcrete lining and soil nails. A lining element is activated on the radial surface of the tunnel to simulate shotcrete application. Soil nails are activated in this phase. Also, temporary invert lining is activated and the deconfinement ratio is increased.
6. Upper half excavation – fully supported (hardened shotcrete) phase: With the hardening of the shotcrete, the lining element was replaced with the element having full strength of shotcrete. Also, the temporary invert lining element is replaced due to the same reason, and the deconfinement ratio reaches 100%.
7. Invert excavation – unsupported phase: The temporary invert lining is deactivated, and the invert area is excavated by deactivating the soil cluster with a low deconfinement ratio for this phase.
8. Invert excavation – partially supported (fresh shotcrete) phase: In this phase, a lining element having the fresh condition of shotcrete is activated on the radial surface of the invert excavation area, and the deconfinement ratio is raised.
9. Invert excavation – fully supported (hardened shotcrete) phase: With the hardening of the shotcrete, the lining element is replaced with the element having full strength of shotcrete, and the deconfinement ratio reaches 100%.
10. Start of the second tunnel excavation by activating the improved zone: The excavation of the second tunnel starts after the UA application by replacing the zone above the tunnel crown with the improved layer. After that, starting from the 4th to 9th stages, the steps are repeated for the second tunnel (T2), sequentially.

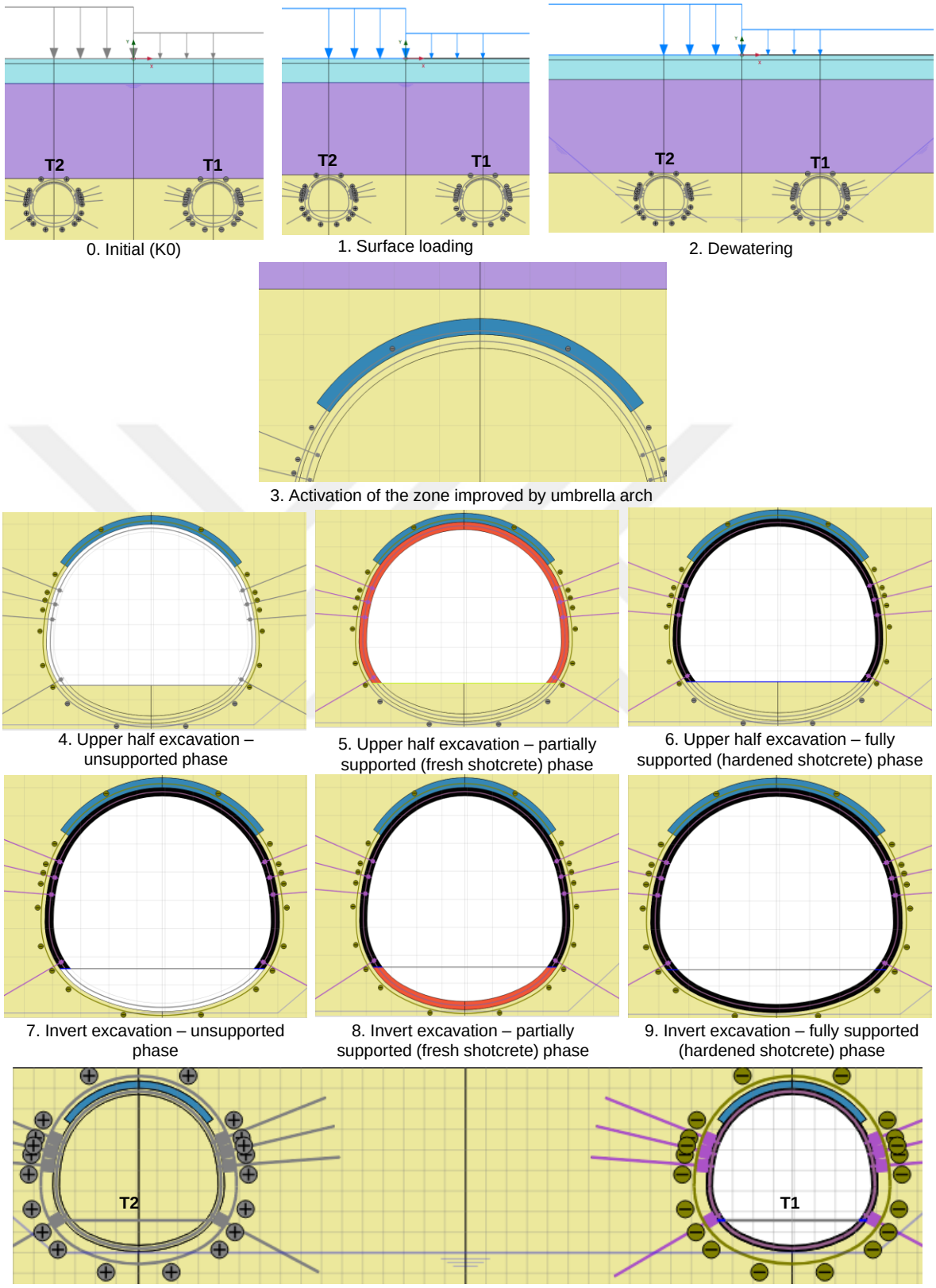


Figure 3.3. The numerical modeling phases appointed for the UA applied twin NATM tunnel sections in the validation studies (adopted from Ergincan et al., 2024).

3.3. Results of the Validation Studies

The two cases selected for the validation study were examined in terms of convergence, inner tunnel volume loss (V_L), surface volume loss (V_S), and settlement profile. The numerical results were compared with the field measurements. The results assessed for each case are presented in Ergincan et al. (2023) and Ergincan et al. (2024) in detail. For this thesis, they are summarized below, together with the comparative discussion at the end.

3.3.1. Results of the Analysis for the Instrumented Studies

For Case1 and Case2, displacement and volume loss results are summarized in Table 3.5 and Table 3.6, respectively. The surface settlement profiles obtained from the numerical analysis of these cases are presented in Figure 3.4 and Figure 3.5, respectively. The settlement profiles are projected together with the measurements obtained from the sensors. The results obtained from the analysis performed for the inspection areas of both cases are summarized below:

- The maximum vertical displacement ($u_{y,max}$) and the maximum resultant displacement (u_{max}) in the twin tunnels are very close to each other, indicating that the maximum horizontal displacement ($u_{x,max}$) has minimal effect on the maximum total displacements.
- The volume loss values are within the acceptable ranges provided in the literature. The most loss is observed in the individual pipe approach, while the least loss is observed in the dummy plate approach.
- Consistent with the volume loss results, the dummy plate approach resulted in lower displacements than those obtained with the other two approaches.
- An increase in surface volume loss (V_S) is observed with the increase in inner tunnel volume loss (V_L).
- For Case1, in all approaches, the second tunnel (T2) converged more than the first tunnel (T1). Therefore, the location of S_{max} is closer to T2 for Case1. On the other hand, for Case2, opposite indications are observed in the case where the dummy plate approach is used. Consequently, for Case2, the location of S_{max} is closer to T1 in the

case with the dummy plate approach, but it is closer to T2 in the cases with the plate and individual pipe approaches.

- All three approaches predicted the settlement with allowable error margins. For any of the three approaches, the difference between the results obtained from the numerical analysis and field measurements is not more than 1 cm.
- The settlement values predicted by the dummy plate approach are very close to the ones measured in the field.
- For Case1, the settlement profile exhibits one peak and the shift of the settlement profile from the centerline is visible and closer to the second tunnel. Additionally, the shift is more distinguishable using the dummy plate approach. However, for Case2, the settlement profile exhibits two peaks and a distinctive shift is not observed.
- For the investigated cases, a unique advantage of using the individual pipe approach is not figured out in comparison with the plate or dummy plate approaches.

Table 3.5. Displacement and volume loss results of Case1 (adopted from Ergincan et al., 2023).

Modeling Approach		**P (Plate)**		**DP (Dummy Plate)**		**IP (Individual Pipe)**	
Twin Tunnels		T1	T2	T1	T2	T1	T2
$u_{x,max}$ (mm)		8.1	8.5	3.0	6.4	7.9	8.8
$u_{y,max}$ (mm)		25.0	24.9	15.7	21.7	25.2	25.6
u_{max} (mm)		25.1	25.0	15.7	21.7	25.3	25.7
V_L	(%)	0.57	0.58	0.37	0.57	0.58	0.60
	(m^3/m)	0.303	0.311	0.181	0.283	0.307	0.321
Total volume loss in the twin tunnels, $\sum V_L$ (m^3/m)		0.614		0.464		0.628	
V_S (m^3/m)		1.377		0.907		1.385	

Table 3.6. Displacement and volume loss results of Case2 (adopted from Ergincan et al., 2024).

Modeling Approach		P (Plate)		DP (Dummy Plate)		IP (Individual Pipe)	
Twin Tunnels		T1	T2	T1	T2	T1	T2
$u_{x,max}$ (mm)		7.3	7.8	4.6	3.9	7.5	7.6
$u_{y,max}$ (mm)		22.3	22.7	19.8	18.9	22.7	23.0
u_{max} (mm)		22.3	22.8	19.8	18.9	22.7	23.0
V_L	(%)	0.483	0.491	0.433	0.420	0.494	0.500
	(m^3/m)	0.26	0.26	0.21	0.21	0.26	0.27
Total volume loss in the twin tunnels, $\sum V_L$ (m^3/m)		0.518		0.421		0.529	
V_S (m^3/m)		1.165		0.984		1.173	

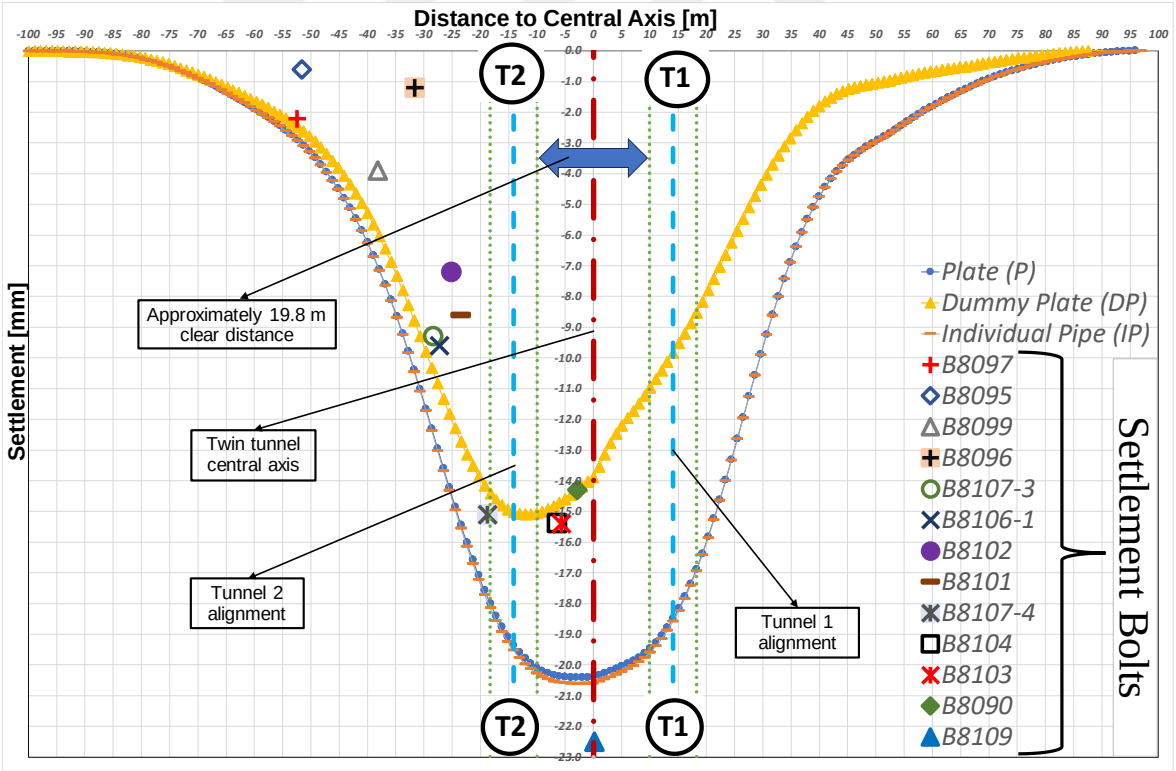


Figure 3.4. The settlement profile obtained from the numerical modeling for Case1 and its comparison with the field measurements shown with settlement bolts (modified after Ergincan et al., 2023).

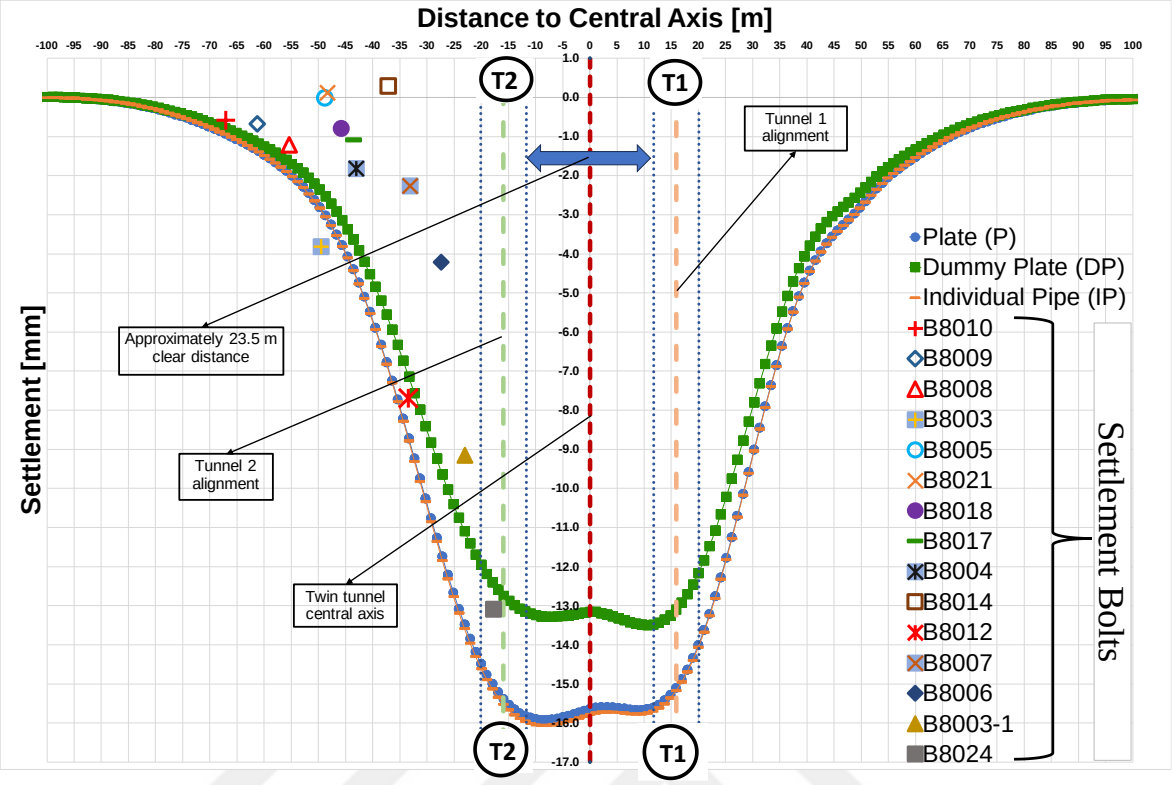


Figure 3.5. The settlement profile obtained from the numerical modeling for Case2 and its comparison with the field measurements shown with settlement bolts (modified after Ergincan et al., 2024).

3.3.2. Discussion of the Comparative Findings

The major findings obtained from the results of the analysis of the two instrumented NATM sections supported by UA (Case1 and Case 2) are generally very similar. The only major difference is the shift of the settlement profile observed in Case 1. This could be mainly because the distances between the twin tunnels were slightly different in Case1 and Case2. Not unifying of the settlement profiles (i.e. two peaks in the profile) is another indication to show the impact of the distance between tunnels. On the other hand, despite the differences in the ground conditions and the clear distance, the predicted settlement profiles are in good agreement with the field measurements for both cases. This repeated prediction success in settlement strongly consolidates the validity of the approach used in the study.

4. RESARCH METHODOLOGY FOR THE PARAMETRIC STUDY

4.1. Approach for the Parametric Study

Based on the results of the validation study, the methodology of the parametric study was established. The dummy plate approach was selected as the most appropriate for the parametric study because this approach provided a better agreement with the settlement profiles of the validation cases compared with the other two approaches (*see* results in Chapter 3). Additionally, dummy plate element that is introduced within the soil does not complicate the assessment of the internal forces on the lining elements.

The construction stages of the parametric study were generally similar to those presented in the validation study. Similar with the validation study, the material properties of the support elements and the deconfinement ratios are kept as those selected in the validation study for the unsupported, partially supported, and fully supported phases of the upper and lower halves of tunnel excavations.

In the parametric study, the investigated geometric parameters included tunnel diameter, overburden depth, and tunnel spacing. Additionally, the effects of ground conditions were investigated using three separate ground conditions. The cases were run for tunnels supported with and without UA support. The ground condition, overburden depth, and tunnel diameter parameters are independent parameters; as such, these were varied directly, independent from the other parameters in the thesis. The tunnel distance, UA improved zone characteristics, length of lining elements, and number of bolt elements can be considered to vary indirectly, as these parameters varied based on either the tunnel diameter or the tunnel diameter and the ground conditions both. The support elements include not only lining elements but also soil nails or rock bolts, and these elements are defined as embedded beams with constant material properties in PLAXIS 2D. These support elements were placed at constant spacing and length for each tunnel, and hence their number varies per tunnel diameter.

As discussed previously, advancement length is not a definable parameter in two-dimensional analysis. Nonetheless, the deconfinement ratio is a tool to simulate the 3D effects in 2D modeling. In PLAXIS 2D, M_{stage} is another tool for this purpose, as stated by Zelger (2012); however, their working principles are different, as explained in PLAXIS Reference Manual (2022). M_{stage} is also not applicable to twin tunnels; accordingly, the deconfinement option was preferred during both the validation and parametric studies conducted for this thesis. In essence, the deconfinement ratio changes depending on the ground conditions, properties of support elements, overburden depth, tunnel diameter, and unsupported advancement length. The deconfinement ratios were adjusted for construction stages in this research; however, the ratios selected for different cases remained constant throughout the parametric study to eliminate the combined effects on the tunnel behavior.

Using constant deconfinement ratios for cases analyzed with different (dependent or independent) parameters indicates the variation of the advancement length implicitly. In other words, the advancement length would be different or arranged so that the deconfinement ratio could remain constant. Consequently, it is important to note that this thesis does not handle tunnel behavior change depending on the variation in deconfinement ratio. This indicates that the three-dimensional effects may not be simulated, and their assessments are ignored from the results of the parametric study.

Based on the experience gained in the validation study, slight changes were also employed in the methodology of the parametric study. The effects of surface loading and groundwater lowering were not considered in the parametric study to eliminate their combined effects with other parameters. The selected R_{inter} is taken as 0.95 in the parametric study. The soil nails or rock bolts are introduced at the upper half excavation – fully supported (hardened shotcrete) phase. The construction stages applied for each case of the parametric study are presented in Figure 4.1, sequentially. The actions performed between the 2^{nd} and the 7^{th} stages are repeated for the second tunnel (T2), starting from the completion of the 8^{th} construction stage.

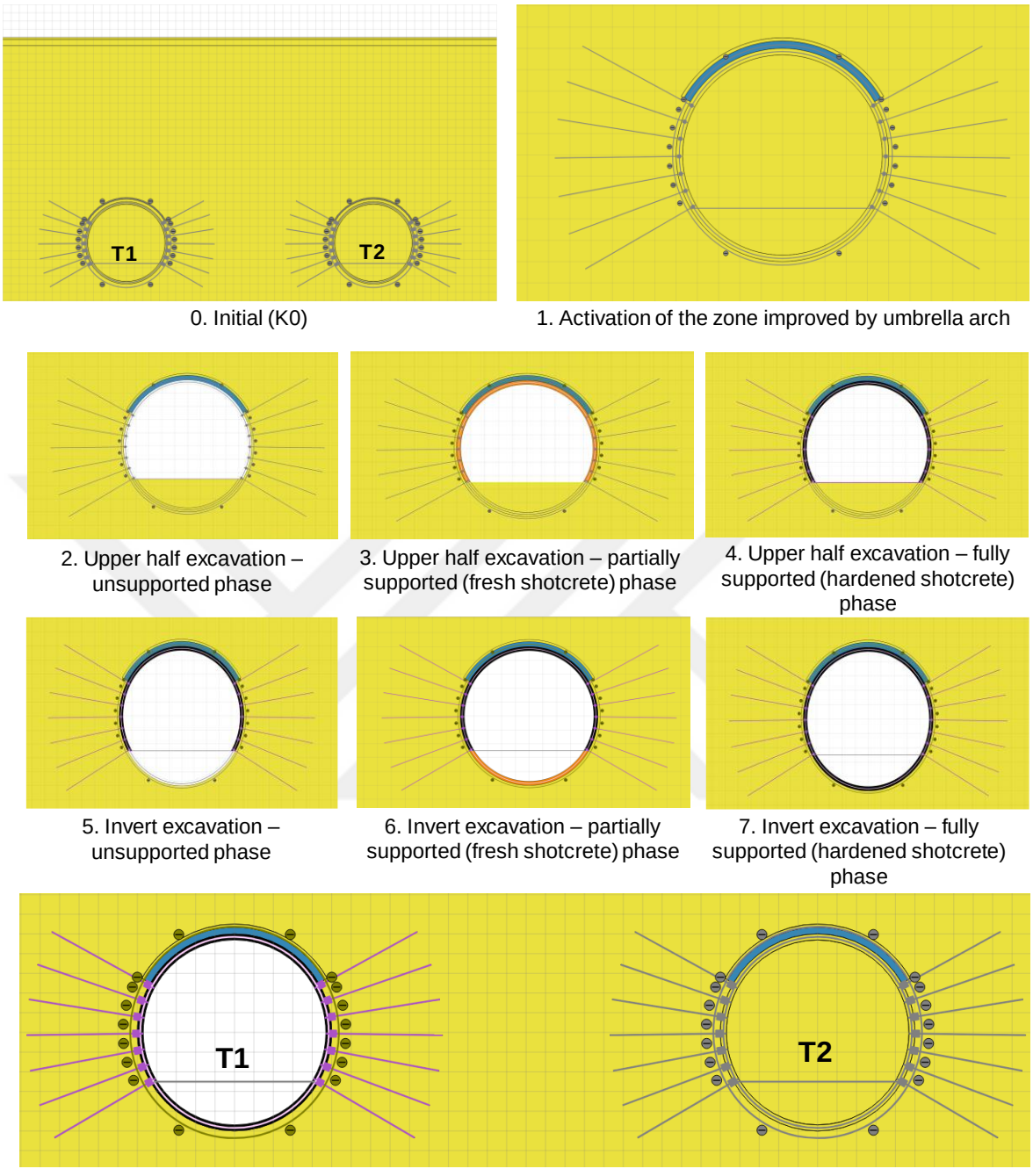


Figure 4.1. The numerical modeling phases appointed for the UA applied twin NATM tunnel sections in the parametric study.

The stress distribution and deformations at the model boundaries should not be affected by tunnel excavation. For the boundaries in 2D modeling, from the tunnel center, 2-3 times the tunnel diameter is suggested for the bottom boundary and 4-5 times the tunnel diameter is suggested for the vertical side boundaries by Meissner (1996). By Möller (2006),

1.3 – 2.2 times the tunnel diameter is suggested for the bottom boundary and the suggestion for the vertical boundaries is correlated with the ratio of overburden depth to tunnel diameter. In the study conducted by Ağbay (2019) for twin tunnels, the bottom and vertical boundaries are accepted as 3 times and 5 times the tunnel diameter, respectively. The boundaries of the models in the parametric study of this thesis were determined based on the validation study experience and the most geometrically critical parametric case in this thesis. The case having the largest tunnel diameter and the largest distance between tunnels is the critical case. In the parametric study, the bottom boundary is fixed to 70 m, which corresponds to 3 times the largest tunnel diameter. In parametric cases of this thesis, the tunnel bottoms are located at 40-m-depth; thus, a 30-m distance has been kept to this boundary for all tunnel diameters. On the other hand, to see the redeemed distribution of the surface settlement, the vertical boundaries are fixed to 100 m in each direction as used in the validation study, which is greater than 5 times the largest tunnel diameter. The bottom, side, and surface boundaries were set as fully fixed, normally fixed, and free constraints, respectively. Thus, zero displacement for the bottom, only vertical displacement for the sides, and free displacement for the surface were satisfied. These boundaries were found enough to see the redeemed stress distribution and deformations in all cases. Before creating the stages of tunnel construction, the discretization and mesh generation of these models were completed with a fine element distribution. An example mesh view of a FE model analyzed in the parametric study is presented in Figure 4.2.

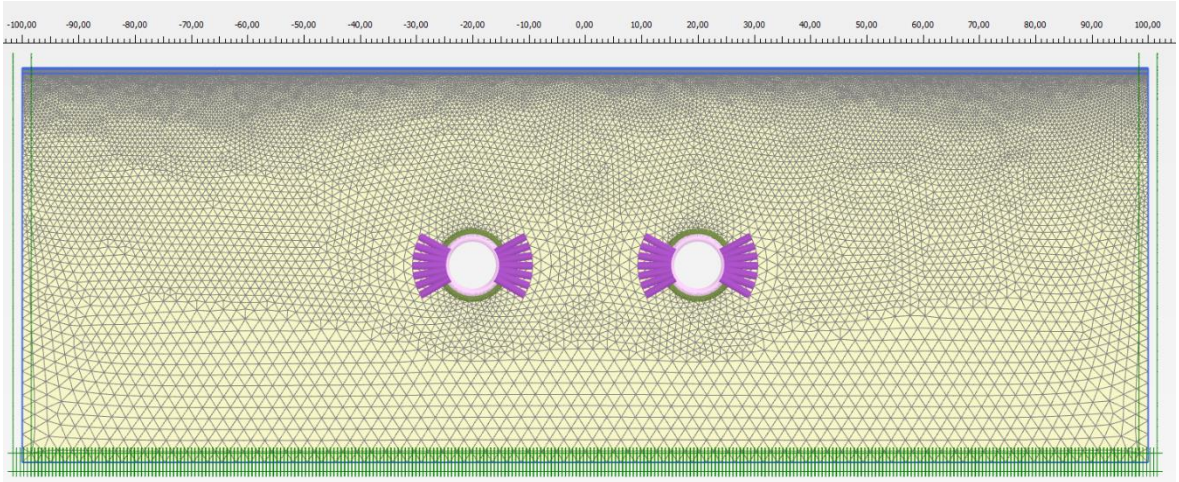


Figure 4.2. A mesh view of a model used in the parametric study.

4.2. Parameter Selection for the Numerical Analysis

4.2.1. Geometric Parameters

The tunnel shape was selected as circular to eliminate unnecessary stress concentration zones and to simplify the parametric study. The excavation sequence is determined based on the number of partitions of the excavation area in NATM excavations. In the validation studies, the partitions were: 1) upper half and 2) invert, and the equivalent diameter (D_{eq}) was 8.2 m. Without increasing the number of partitions, it is difficult to excavate a tunnel with an acceptable volume loss value. As tunnel diameter increases, the required number of partitions increases. Accordingly, the upper bound for tunnel diameter was selected as 10 m. In the case combinations of the parametric study, three tunnel diameters were investigated: 6 m, 8 m and 10 m, represented with D06, D08, and D10, respectively.

To restrict volume loss within acceptable limits and to avoid tunnel collapses, the ratios of cover depth (in other words, overburden depth), to diameter (C/D) are limited to 1 to 5 range. By considering extreme conditions such as the largest diameter tunnel with the shallowest overburden depth and vice versa, the overburden depth was ranged between 10 m and 30 m. Thus, the overburden depths (cover depth) were selected as 10 m, 20 m, and 30 m, represented by C10, C20, and C30, respectively, in case combinations.

The clear distance between twin tunnels, in other words, the pillar width, as stated by Karakus and Fowell (2000) or Li et al. (2020), was also investigated in the study. According to Della Vella and Rodriguez (2014), the pillar width is defined as the center-to-center spacing of the tunnels minus the sum of their radii, and hence it is the clear distance. In this thesis, this parameter was varied or proportioned using the tunnel diameter. In the case combinations of the parametric study, the clear distance between tunnels was selected as one, two, and three times the tunnel diameters, represented by O1, O2, and O3, respectively. As the tunnels are twin and their shapes are circular, these distances correspond to two, three, and four times the tunnel diameter once the center-to-center spacing of the tunnels is considered, respectively.

One of the other important aspects investigated in this research is the UA application. The thickness describing the UA application is 35 cm, as experienced in the validation studies. In the parametric study, it covers 120° of the tunnel crowns geometrically. The bottom-120°-part of the remaining periphery is reserved for the invert of the tunnel, and the 60°-parts on two sides locating between the invert and UA zone are reserved as the bench for rock bolt or soil nail applications. These zones reserved for UA application are designed while creating geometric models of cases, and they are used in cases of existence of UA application by replacing the material of the zone with the improved ones.

4.2.2. Soil and UA Material Properties

In the conducted parametric study, three types of ground conditions were appointed considering hard clay, completely weathered rock, and weathered rock, represented by S1, S2, and S3, respectively. They are considered as ground conditions that require umbrella arch application frequently. The hardening soil constitutive model and drained condition are selected for all types. The properties of the ground condition sets are provided in Table 4.1. In addition to the table:

- Tangent stiffness for primary oedometer loading (E_{oed}^{ref}) is input the same with secant stiffness in standard drained triaxial test (E_{50}^{ref}), unloading / reloading stiffness (E_{ur}^{ref}) is input three times of E_{50}^{ref}, as proposed by default,
- Poisson ratio (v) and Poisson's ratio for unloading - reloading (v_{ur}) are fixed to 0.3 and 0.2, respectively.

Table 4.1. Soil and rock parameters used in the parametric study.

Ground Conditions	**γ (kN/m^3)**	**γ_{sat} (kN/m^3)**	**c (kPa)**	**ϕ (°)**	**E_{50}^{ref} (kN/m^2)**	**ψ (°)**
S1- Hard Clay (HC)	18	19	20	28	37000	0
S2- Highly Weathered Rock (HWR)	18	19	25	34	55000	4
S3 - Weathered Rock (WR)	18	19	40	38	80000	8

The shear strength parameters used for the improved zone are presented in Table 4.2. The elastic modulus and unit weight for the improved zones were calculated with respect to the weighted average of the materials included in the zone that covers 120° of the tunnel crowns. Injection and pipe parameters can be calculated with respect to the number of holes in a unit meter, as explained by Hoek (2004). In this research, a similar approach was adopted, using CAD software. Naturally, the weighted average values of elastic modulus and unit weight vary depending on the tunnel diameter and ground conditions. A calculation example belonging to D10_S1 combinations is presented in Table 4.3, and its variations are summarized in Table 4.4.

Table 4.2. The fixed parameters of improved zones according to ground conditions.

Ground Conditions in the Improved Zone	**c (kPa)**	**ϕ (°)**	**ψ (°)**
S1- Hard Clay (HC)	1,000	35	5
S2- Highly Weathered Rock (HWC)	1,500	40	10
S3 - Weathered Rock (WR)	2,000	42	12

Table 4.3. Calculation example for the elastic modulus and unit weight of improved zone.

D10_S1					
Thickness of improved zone (cm):			35		
Spacing of UA pipes (cm):			30		
Outer diameter of UA pipes (mm):			114.3		
Thickness of UA pipes (mm):			6.3		
Inner diameter of UA pipes (mm):			101.7		
Number of UA pipes:			35		
Drilling diameter (mm):			125		
Material	Area (m^2)	Elastic Modulus (GPa)	Weighted share of the elastic modulus	Unit weight (kN/m^3)	Weighted share of the unit weight
Ground	3.364	0.037	0.124467	18.0	60.552
Injection	0.355	2	0.709401	25.0	8.875
UA pipes	0.075	200	14.962777	78.6	5.895
Total	3.794		15.796646		75.322
Average for the improved zone	-	4.164135	-	19.8	-

Table 4.4. The varied parameters of improved zones according to ground conditions.

Elastic Modulus (kPa)	S1	S2	S3
D10	4,164,135	4,180,097	4,202,266
D06	4,073,166	4,089,173	4,111,404
D08	4,129,612	4,145,591	4,167,784

Varying the parameters presented in this chapter, a total of 162 models were created using three tunnel diameters, three overburden depths, three clear distance ratios, and three ground conditions with or without UA application. For each case, designations were assigned. As an example, the case D10_C30_O3_ S2_T1 refers to a model created with a twin tunnel section having 10 m diameter circular tunnels, 30 m overburden depth, three times the tunnel diameter clear distance between tunnels, under highly weathered rock conditions, supported with UA application. A model section view from the case given as an example and its zoomed in views are presented in Figure 4.3.

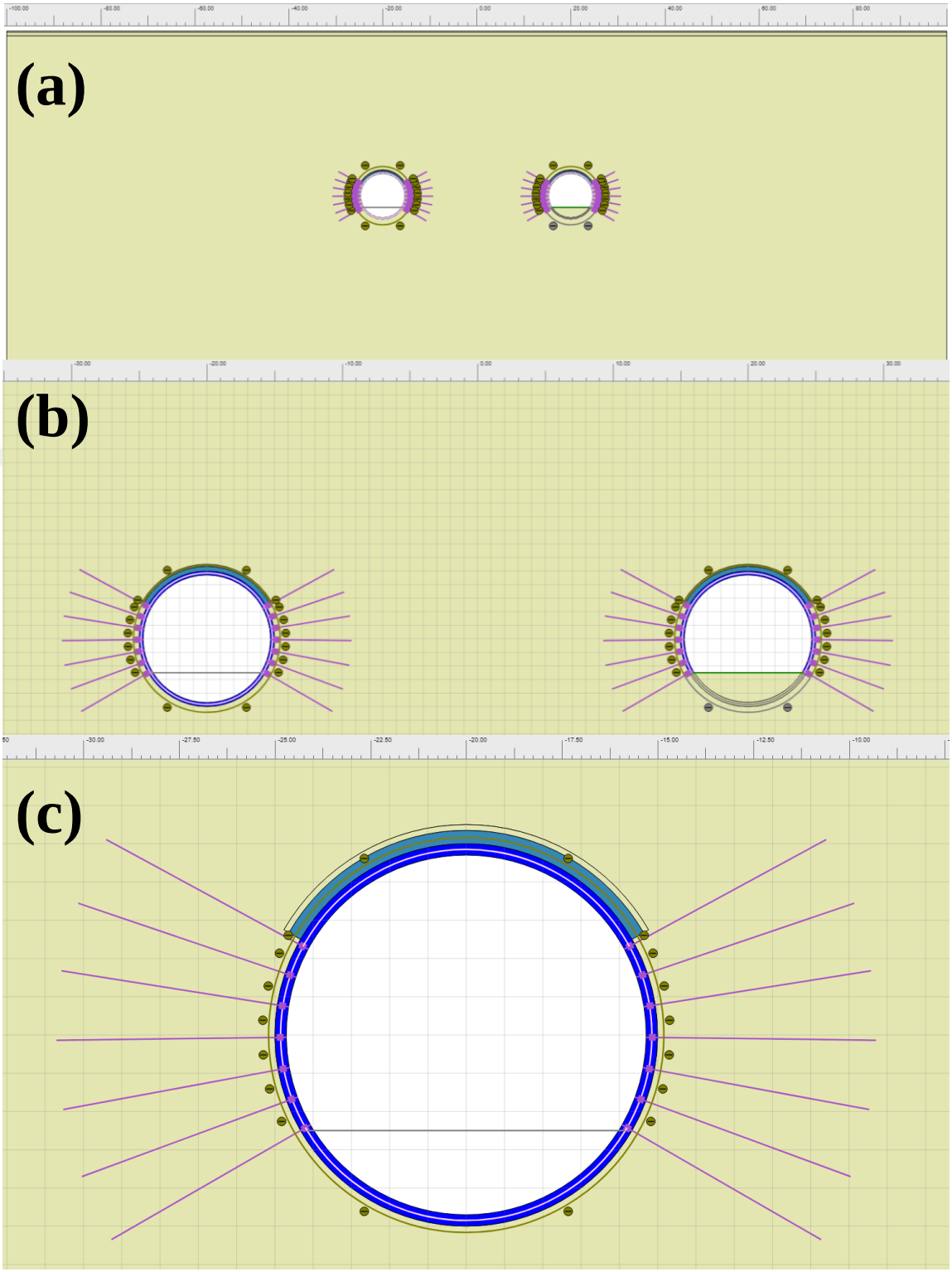


Figure 4.3. Model views belonging to D10_C30_O3_S2_T1 case representing (a) full section, (b) zoomed in section for twin tunnels, and (c) zoomed in section for the left tunnel.

5. RESULTS AND DISCUSSION OF THE PARAMETRIC STUDY

In this chapter, the behaviors of the models are presented and discussed in terms of settlement profile, maximum settlement, coordinate of the maximum settlement, volume loss in the tunnels and on the surface, convergence, and forces on support elements. All the cases are modeled with 200-m transversal length. Additionally, fixed deconfinement ratios are used; these ratios are not adjusted according to UA improvement zone, overburden depth, tunnel diameter, ground conditions, or distance between twin tunnels.

5.1. Umbrella Arch Application

First of all, since the deconfinement ratios used in all models in this thesis remain constant, the difference between the cases with and without umbrella arch application is analyzed. For this comparison, extreme cases are taken into consideration. In terms of UA application, the compared case pairs are D06_C10_O1_S1_T0/T1, D08_C20_O2_S2_T0/T1, D06_C30_O3_S3_T0/T1, D10_C10_O1_S1_T0/T1, and D10_C30_O3_S3_T0/T1. In Figure 5.1, surface settlement profiles of these case pairs are plotted throughout the modeling boundary. As addressed under Section 2.5.1, due to the modeling approach, it is hard to see the impact of the improved zone which represents the UA application in 2D modeling. As expected, the difference is small in terms of settlement profile, as presented in Figure 5.1. The differences between D06_C10_O1_S1_T0/T1 and D08_C20_O2_S2_T0/T1 pairs are somewhat noticeable. However, the differences are not significant for D06_C30_O3_S3_T0/T1 and D10_C30_O3_S3_T0/T1 pairs; it is even indistinguishable for the D10_C10_O1_S1_T0/T1 pair.

In order to see the difference more clearly, they are compared in terms of average volume loss. The volume loss in tunnels is expressed as the percentage difference between the converged and original areas to the original area. In Figure 5.2, these cases are plotted as a bar chart showing the average volume loss of twin tunnels. While there are noticeable quantitative distinctions among them, some exhibit negligible differences. In general, it is

seen that UA application appears to have a positive effect in reducing volume loss despite the fixed deconfinement ratio approach.

To further understand the influence of other parameters, the D08_O2 cases, representing the average cases of the parametric study due to their diameter and clear distance, are taken into consideration. In Figure 5.3, the pairs of D08_O2 cases are plotted in terms of the average volume loss of twin tunnels against varied parameters such as ground conditions and overburden depth. The positive effect of UA application is evident in these cases as well. In addition, it is observed that the average V_L increases as overburden depth increases but the ground conditions worsen. Given these findings, since the impact of UA application is limited due to the fixed deconfinement ratio approach, the subsequent sections of the chapter primarily focus on cases where UA is applied.

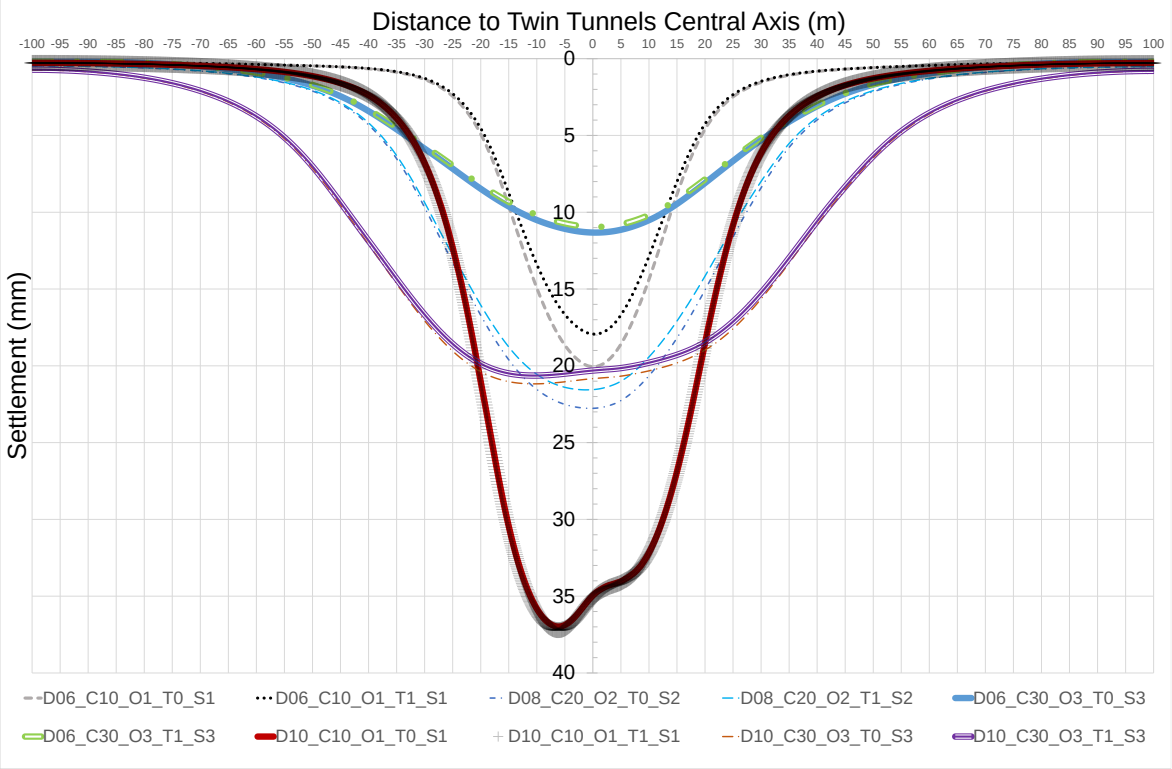


Figure 5.1. Effect of UA application on settlement profiles of extreme cases.

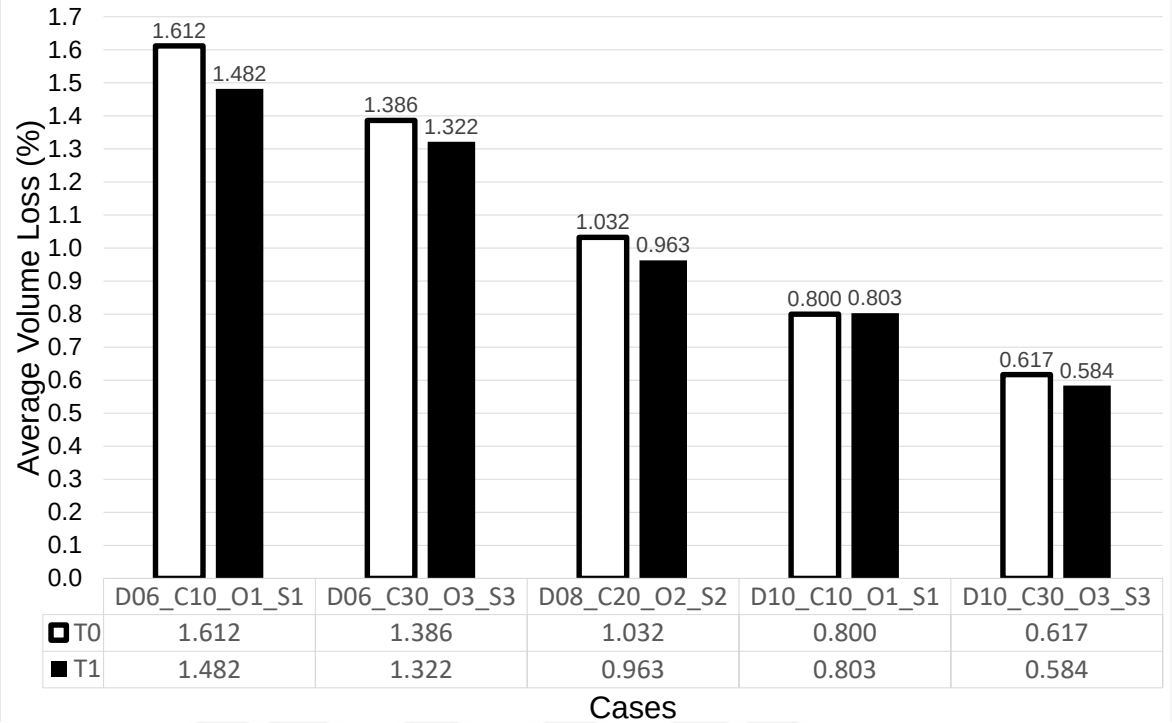


Figure 5.2. Effect of UA application on average volume loss (V_L) of twin tunnels in extreme cases.

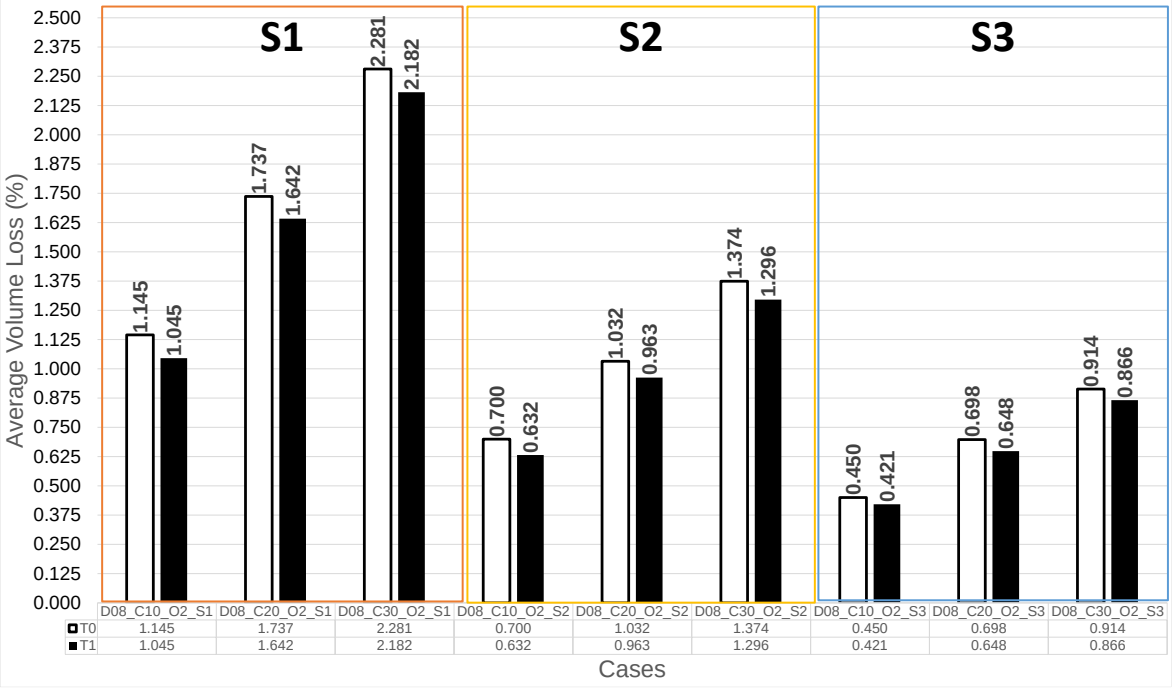


Figure 5.3. Effect of UA application on average volume loss (V_L) of twin tunnels in D08_O2 cases.

5.2. Settlement Profiles

Settlement profiles of all UA-applied cases are presented in this section. In the succeeding nine graphs, tunnel diameter and distance between twin tunnels are fixed, whereas ground conditions and overburden depth are varied.

While the tunnel diameter is 10 m (D10), the settlement profile exhibits two peaks in the cases with 10 m overburden depth (C10), as shown in Figure 5.4. This indicates that unifying of the settlement profiles is challenging when the overburden depth is shallow. As the distance between twin tunnels increases, the occurrence of two settlement peaks start to appear in C20 cases as well, as presented in Figure 5.44c. The peak point of the profile occurs on the left side (close to the first excavated tunnel) for C10 cases, and it shifts towards the right (close to the second excavated tunnel) as the overburden depth increases. On the other hand, as the clear distance increases, the coordinate of S_{max} shifts towards the first excavated tunnel. In addition to that, as expected due to the fixed deconfinement ratio approach, the maximum settlement value (S_{max}) increases as overburden depth increases. Similarly, it increases as the ground conditions worsen even if the overburden depth is constant. Furthermore, a comparative analysis of the graphs reveals that S_{max} decreases and settlement profiles widen as the distance between twin tunnels increases, while other parameters remain fixed. In other words, decreasing the distance between the tunnels results in increased S_{max} and a deeper settlement profile. Therefore, it can be inferred that overburden depth and distance between twin tunnels affect S_{max} and coordinate of S_{max} oppositely.

Similar to the D10 cases, unifying of settlement profiles is challenging in D08 cases when the overburden depth is as shallow as 10 m. However, this phenomenon is not clear when the tunnels are closer to each other as can be seen in Figure 5.5a. This shows that the occurrence of two settlement peaks depends not only on the cover depth and diameter of the tunnels but also on the distance between the twin tunnels. The relationships between overburden depth with S_{max} and its coordinate, clear distance with S_{max} and its coordinate, and ground conditions with S_{max} are similar those in D10 cases as can be seen in Figure 5.5.

On the contrary, the two settlement peaks phenomenon is not clearly seen in D06 cases, even under shallow overburden depth conditions, until the distance between tunnels is

increased, as presented in Figure 5.6. The relationships addressed in the previous paragraph are also valid for D06 cases. Differently, the coordinate of S_{max} has not occurred on the left side of the central axis when the distance between the tunnels is at the closest position for D06 cases. This indicates that under the same overburden depth, a larger tunnel diameter causes S_{max} to shift towards the side of the first excavated tunnel. Furthermore, a comparative analysis of the graph sets belonging to three diameters shows that S_{max} increases as the diameter increases.

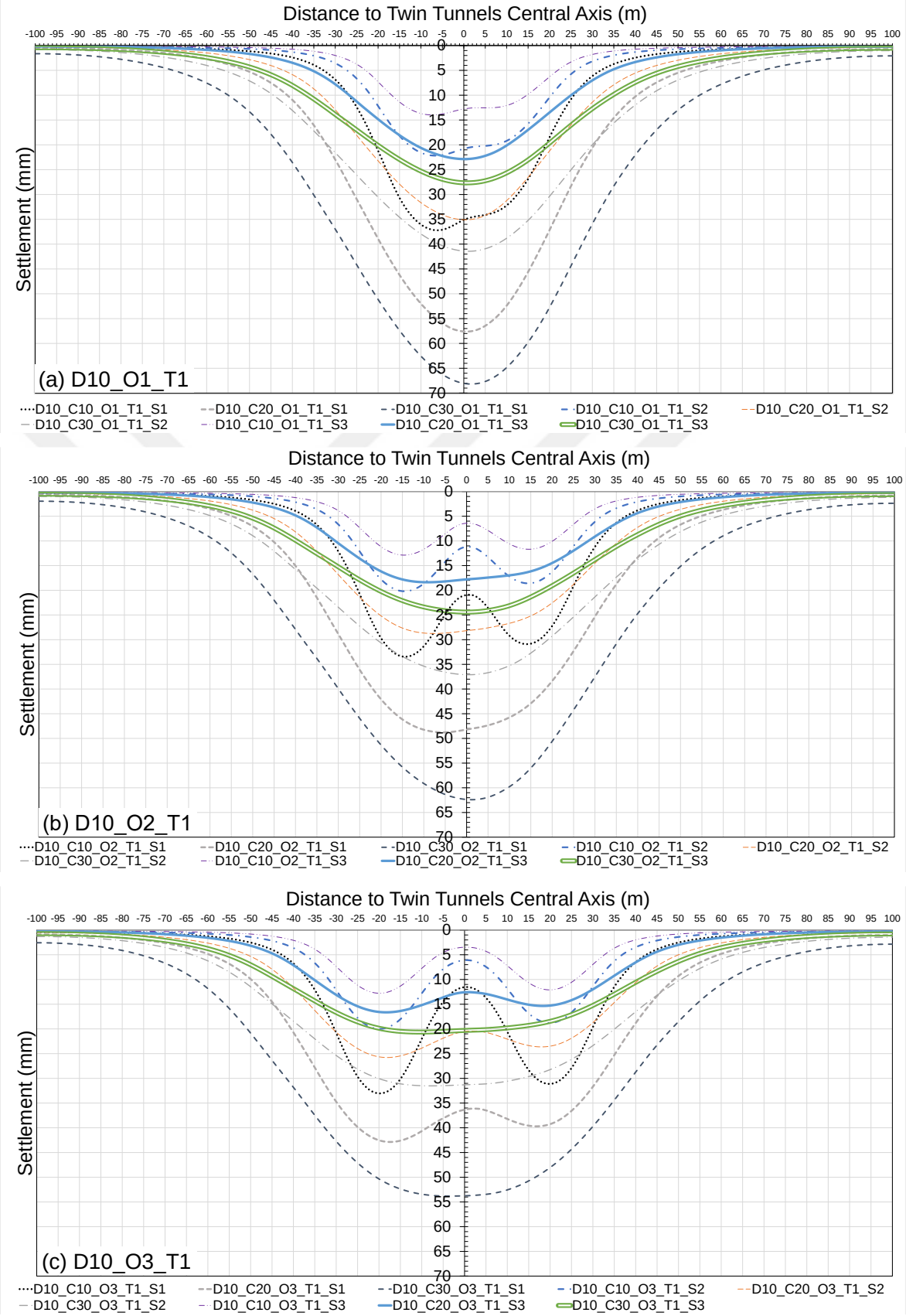


Figure 5.4. Surface settlement profiles of D10_T1 cases for (a) O1, (b) O2, (c) O3.

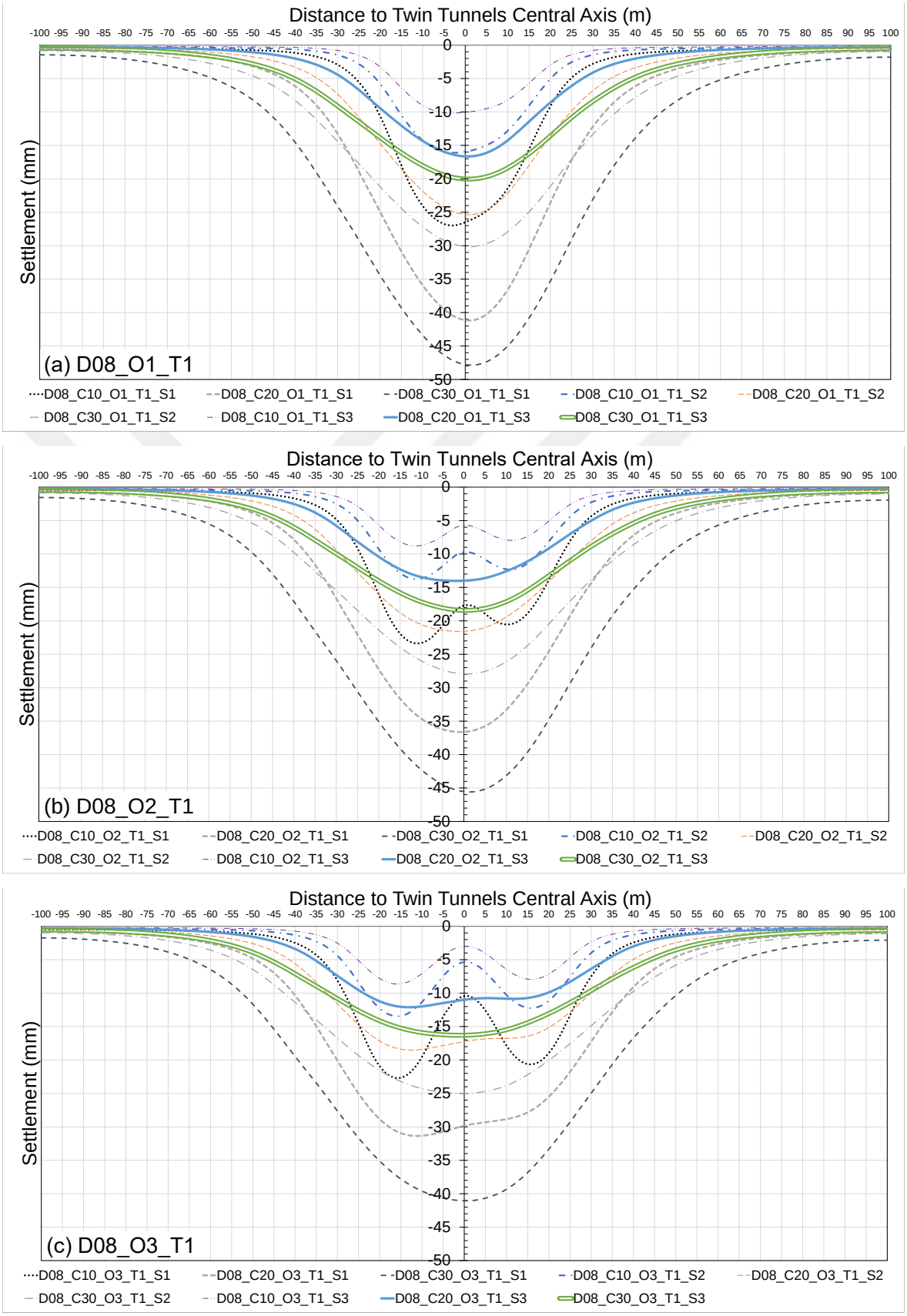


Figure 5.5. Surface settlement profiles of D08_T1 cases for (a) O1, (b) O2, (c) O3.

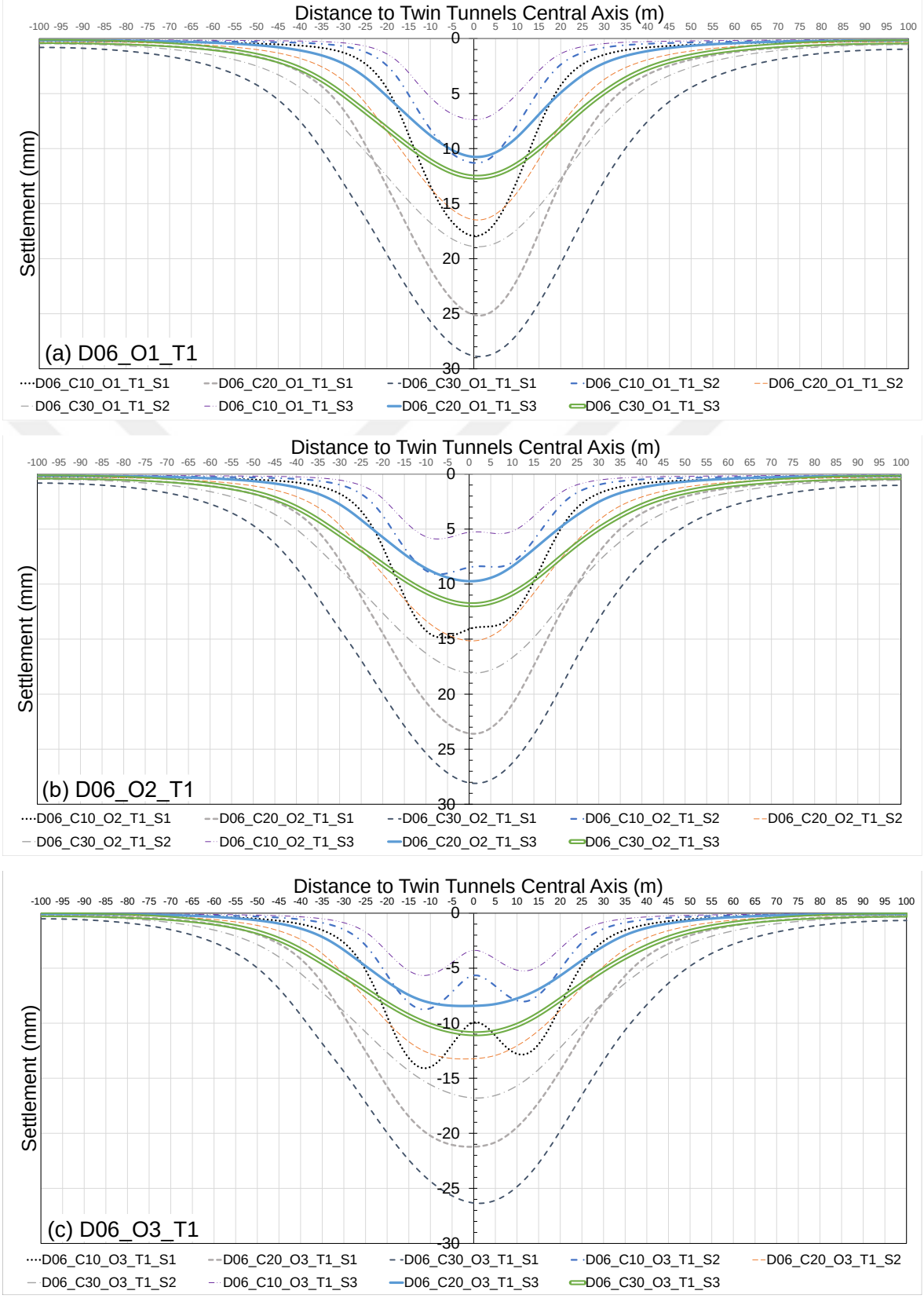


Figure 5.6. Surface settlement profiles of D06_T1 cases for (a) O1, (b) O2, (c) O3.

5.3. Maximum Settlement Value (S_{max}) and Its Coordinate (skewness)

As highlighted in Section 5.2, the settlement profiles exhibit at least one peak point. Nevertheless, depending on geometric conditions, two peaks may be observed. In this thesis, S_{max} is accepted as the larger of the two peaks if they exist. The S_{max} values of all UA applied cases are represented in this section. In the three subsequent graphs in Figure 5.7, tunnel diameters are fixed while overburden depth, clear distance, and ground conditions vary. As identified earlier, S_{max} increases as overburden depth increases, tunnel diameter enlarges, clear distance decreases, or ground conditions worsen, provided that other parameters remain constant.

As an additional example, to see the effect of clear distance on settlement in detail, S_{max} values of C30 cases are plotted in Figure 5.8 with respect to the combinations of tunnel diameter and ground conditions. The slopes of these combinations indicate that the impact of clear distance on S_{max} diminishes as tunnel diameter decreases.

Another observation can be made regarding the coordination of S_{max}. As previously shown in the settlement profiles, the peak points that represent the coordinates of S_{max} are not fixed. Similar observations on eccentric settlement have been made by Della Valle & Rodriguez (2014) for twin tunnels excavated using TBM method. This observed shifting of S_{max} is referred to as skewness in this thesis. For clarity, the coordinates of S_{max} values are represented in horizontal bar charts in Figures 5.9, 5.10, and 5.11. Each figure illustrates the change in skewness with respect to ground conditions, overburden depth, and clear distance while tunnel diameter is kept constant. It is evident that the ground conditions influence skewness, but its effect decreases with reduced overburden depth. Geometric conditions have a more significant impact on skewness than ground conditions. As identified earlier, skewness shifts towards the positive side of the central axis (i.e. the secondly excavated tunnel side) as the clear distance decreases. Furthermore, in C10_O3 cases, regardless of tunnel diameter and ground conditions, skewness emerges nearly on the axis of the first excavated tunnel. Another skewness behavior is observed depending on the cover depth to tunnel diameter (C/D) ratio. As this ratio increases, skewness shifts towards the second tunnel. In other words, it shifts right as tunnel diameter decreases under the same overburden depth or as overburden depth increases for the same tunnel diameter. Skewness can be

beneficial to determine the excavation order of tunnels. For example, the occurrence of S_{max} may be desired under less critical superstructures rather than highly critical ones to avoid failures induced by tunnel excavation.

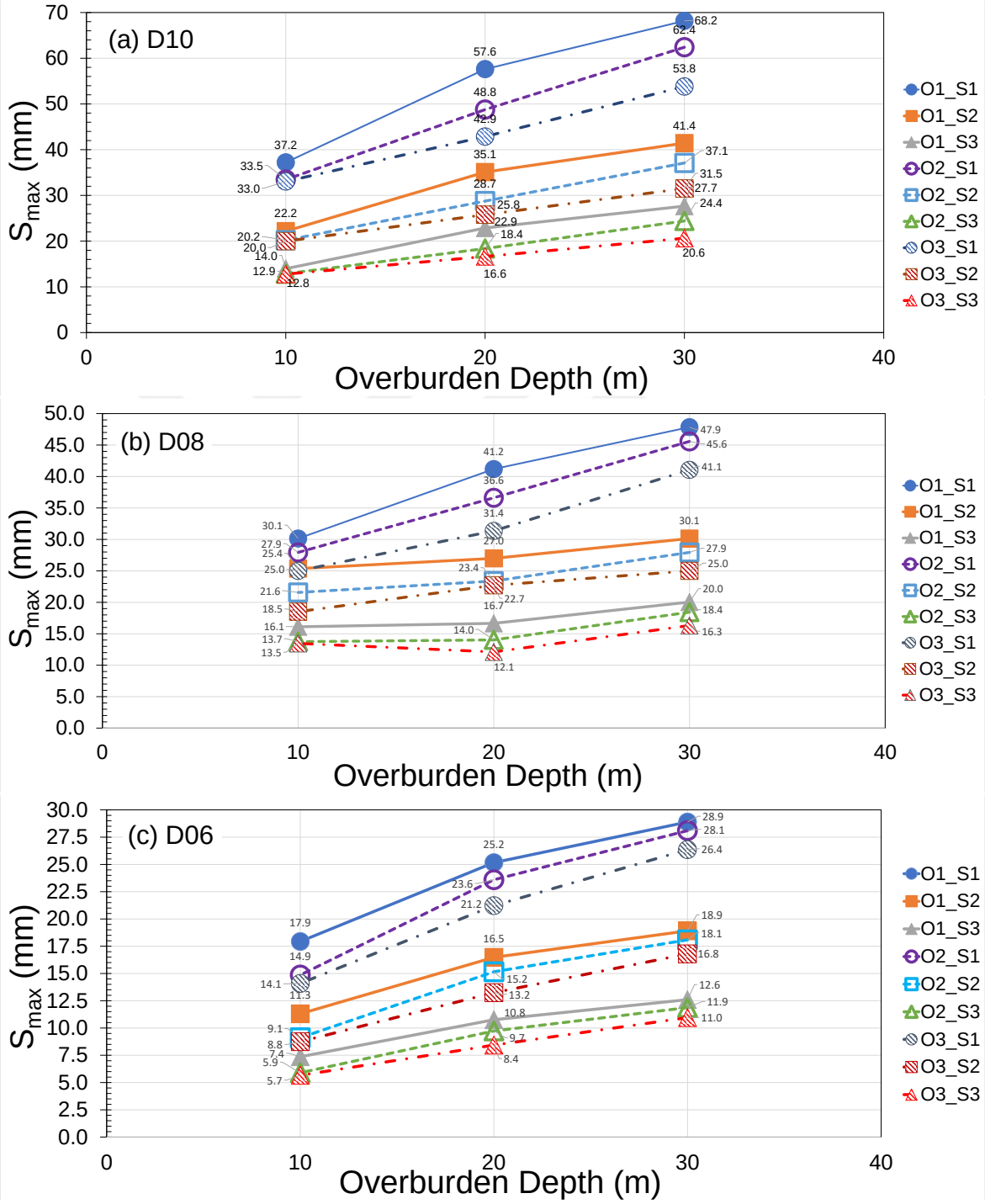


Figure 5.7. Maximum surface settlement (S_{max}) of the UA applied tunnels with respect to overburden depth for (a) D10, (b) D08, and (c) D06 cases.

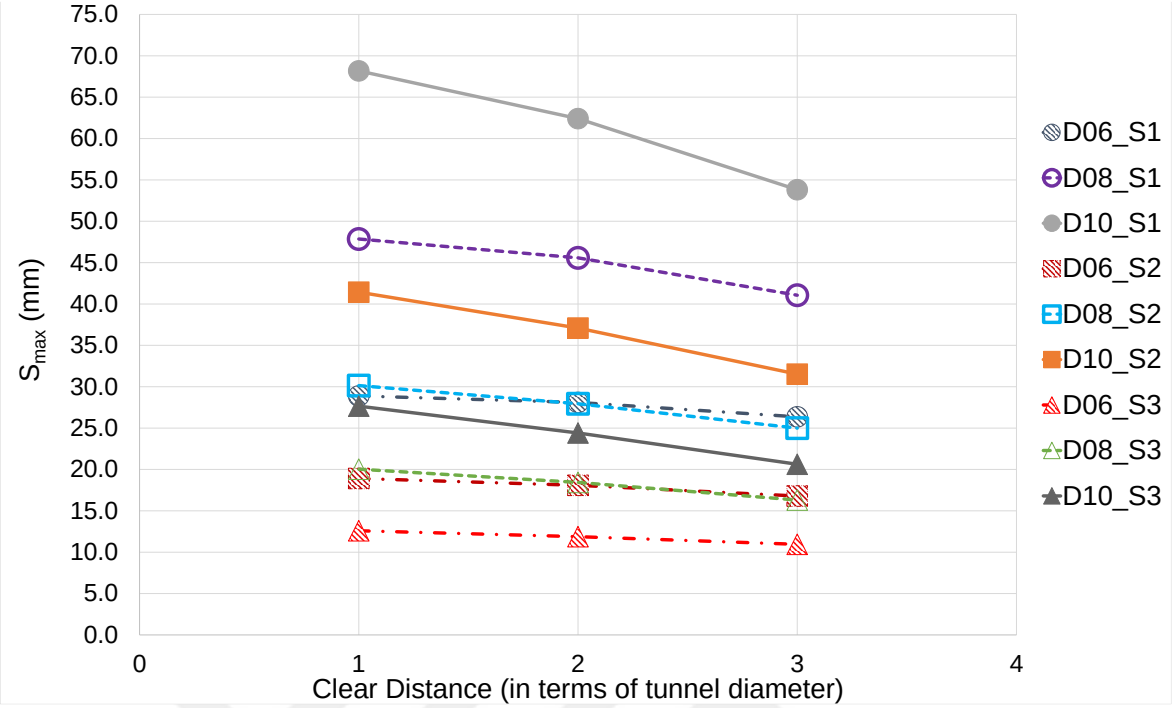
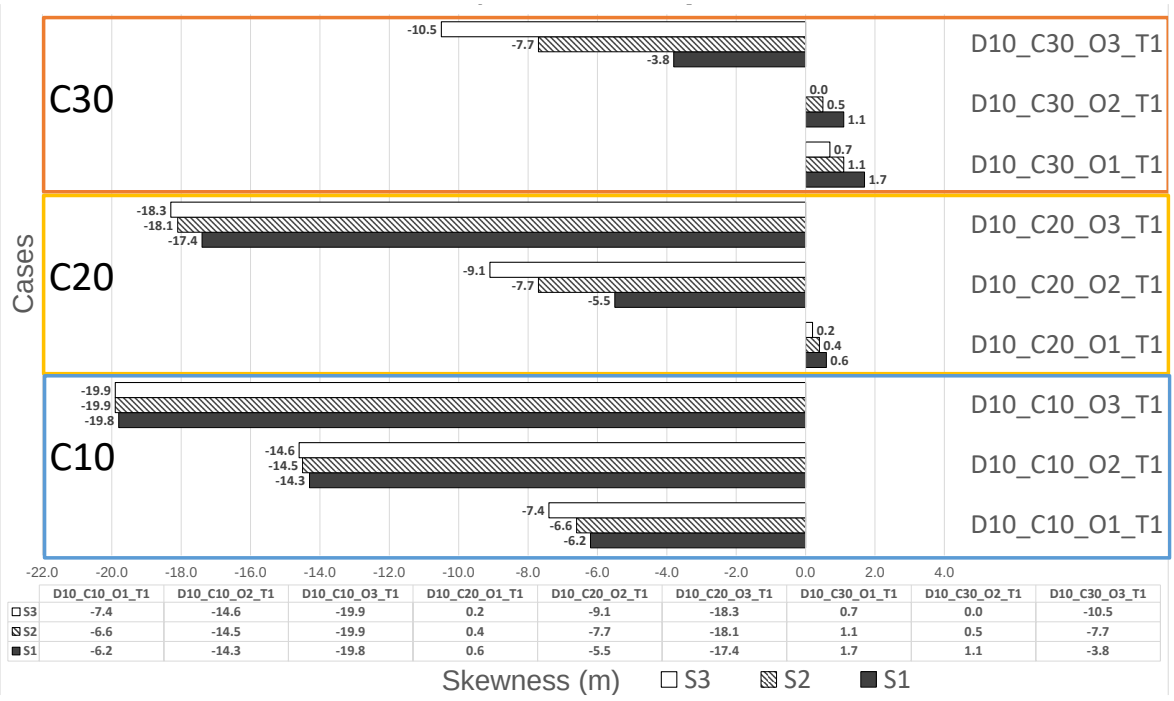
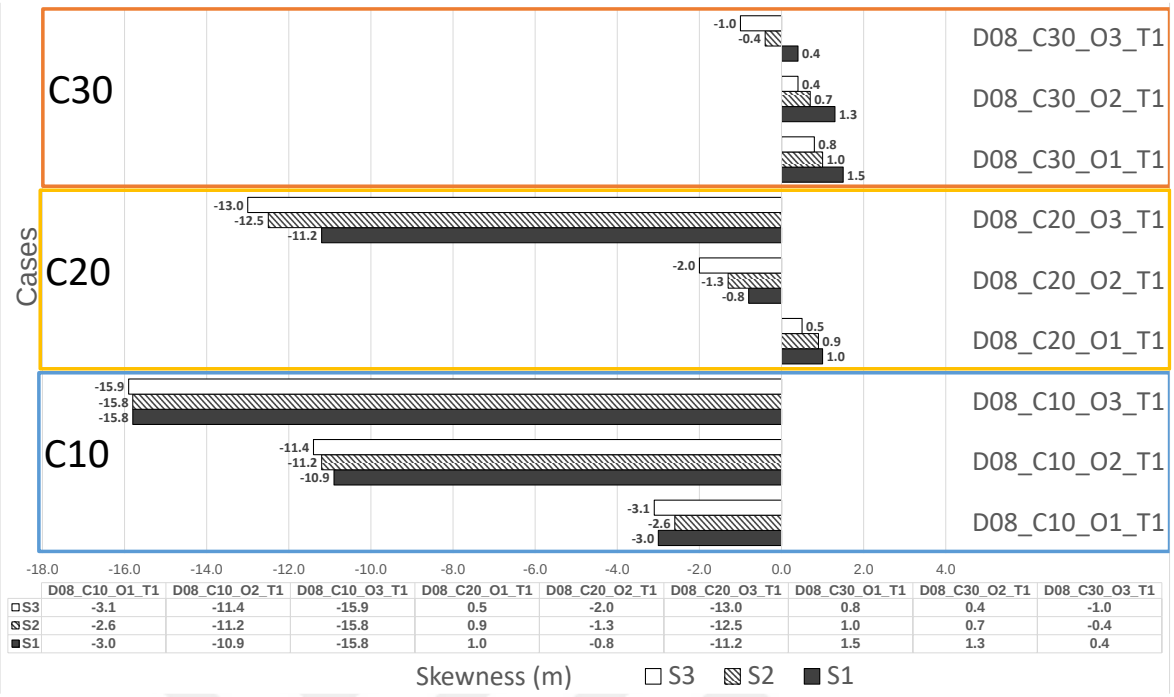


Figure 5.8. Maximum surface settlement (S_{max}) of the UA applied tunnels with respect to clear distance for C30 cases.



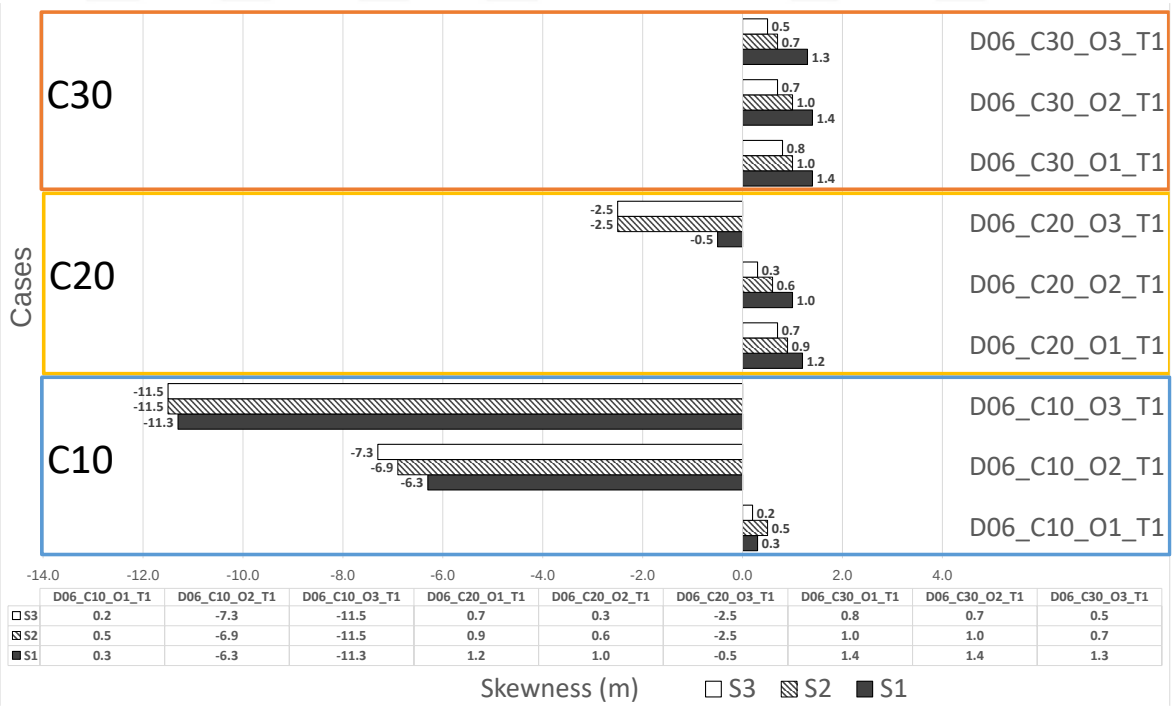
	D10_C10_O1_T1	D10_C10_O2_T1	D10_C10_O3_T1	D10_C20_O1_T1	D10_C20_O2_T1	D10_C20_O3_T1	D10_C30_O1_T1	D10_C30_O2_T1	D10_C30_O3_T1
S3	-7.4	-14.6	-19.9	0.2	-9.1	-18.3	0.7	0.0	-10.5
S2	-6.6	-14.5	-19.9	0.4	-7.7	-18.1	1.1	0.5	-7.7
S1	-6.2	-14.3	-19.8	0.6	-5.5	-17.4	1.7	1.1	-3.8

Figure 5.9. Coordinate of the maximum surface settlement (skewness) of the UA applied tunnels for D10 case.



	D08_C10_O1_T1	D08_C10_O2_T1	D08_C10_O3_T1	D08_C20_O1_T1	D08_C20_O2_T1	D08_C20_O3_T1	D08_C30_O1_T1	D08_C30_O2_T1	D08_C30_O3_T1
S3	-3.1	-11.4	-15.9	0.5	-2.0	-13.0	0.8	0.4	-1.0
S2	-2.6	-11.2	-15.8	0.9	-1.3	-12.5	1.0	0.7	-0.4
S1	-3.0	-10.9	-15.8	1.0	-0.8	-11.2	1.5	1.3	0.4

Figure 5.10. Coordinate of the maximum surface settlement (skewness) of the UA applied tunnels for D08 case.



	D06_C10_O1_T1	D06_C10_O2_T1	D06_C10_O3_T1	D06_C20_O1_T1	D06_C20_O2_T1	D06_C20_O3_T1	D06_C30_O1_T1	D06_C30_O2_T1	D06_C30_O3_T1
S3	0.2	-7.3	-11.5	0.7	0.3	-2.5	0.8	0.7	0.5
S2	0.5	-6.9	-11.5	0.9	0.6	-2.5	1.0	1.0	0.7
S1	0.3	-6.3	-11.3	1.2	1.0	-0.5	1.4	1.4	1.3

Figure 5.11. Coordinate of the maximum surface settlement (skewness) of the UA applied tunnels for D06 case.

5.4. Volume Loss in Tunnels and on Surface

Volume loss is a frequently used term in tunneling, describing the ratio or amount of displacement induced by the tunnel excavation process in the section. In a tunnel it can be calculated as the ratio of the difference between the converged and original tunnel areas to the original area. Since there are twin tunnels in this thesis, the volume loss (V_L) is calculated distinctly for each tunnel but represented by the average of the two tunnels in terms of percentage (%) and the total of the two tunnels in terms of volume per meter (m^3/m). On the other hand, since the surface does not have a closed form, surface volume loss (V_S) is represented by the volume per meter (m^3/m) for two-dimensional sections. For the calculation of V_S, the settlement profile is integrated.

In Figure 5.12, the average V_L (%) change in UA applied cases is plotted with respect to overburden depth and the combinations of ground condition and clear distance, while tunnel diameter is kept constant for each of the sub-figures. As presented in the figure, average V_L (%) increases as the ground conditions worsen and overburden depth increases. However, the effect of clear distance on V_L seems negligible. On the other hand, even though V_L decreases in terms of volume per meter (m^3/m) as tunnel diameter decreases, it increases in terms of percentage since the original area of the tunnel decreases dramatically as the tunnel diameter gets smaller.

Since the effect of clear distance on volume loss is limited, the data is also plotted by fixing the clear distance as O1 conditions in Figure 5.13. The graph showing the change in average V_L with respect to tunnel diameter and the combinations of overburden depth and soil conditions corroborates the implications stated in the above paragraph. In terms of percentage, volume loss decreases as tunnel diameter increases. On the other hand, it increases as the ground conditions worsen and overburden depth increases.

Volume loss reaches a maximum of 3.026% in the case of D06_C30_O1_T1_S1 and a minimum of 0.304% in the case of D10_C10_O2_T1_S3. These values are within the range of 0.2 – 3.3% listed by Mair (1996). When considering the surface volume loss (V_S), similar trends are observed in Figure 5.14 which plots the change in V_S with respect to overburden depth and the combinations of tunnel diameters, clear distances, and ground

conditions. However, since V_S is represented by the volume per meter, not by percentage, it increases as the tunnel diameter increases.

For the relationship between inner tunnel total volume loss (V_L) and surface volume loss (V_S), they are compared in terms of volume per meter (m^3/m). For the comparison, the ratio of V_S to V_L is taken into consideration, and it is referred to as volume loss reflection ratio (V_S/V_L) in this thesis. In Figure 5.15, this ratio is plotted for each tunnel diameter with respect to the change in overburden depth, ground conditions, and clear distance. According to this figure, the reflection ratio increases as overburden depth increases. The clear distance and ground conditions have limited effects on it. In comparing the three diameter charts, it is seen that the reflection ratio decreases as tunnel diameter decreases.

Furthermore, in order to normalize the volume loss, it is represented according to C/D ratios initially as plotted in Figure 5.16. Thereafter, considering the effect of the diameter in terms of area, it is also plotted with respect to the ratio of overburden depth to tunnel area (C/A_T) in Figure 5.17. Since the tunnels analyzed in this thesis are circular, their areas directly depend on the square of tunnel diameter. While the trends depending on the C/D ratio are not clear, the general trend observed is an increase in volume loss as the C/A_T ratio increases. As detected previously, V_L increment due to worse ground conditions is also evident in these charts.

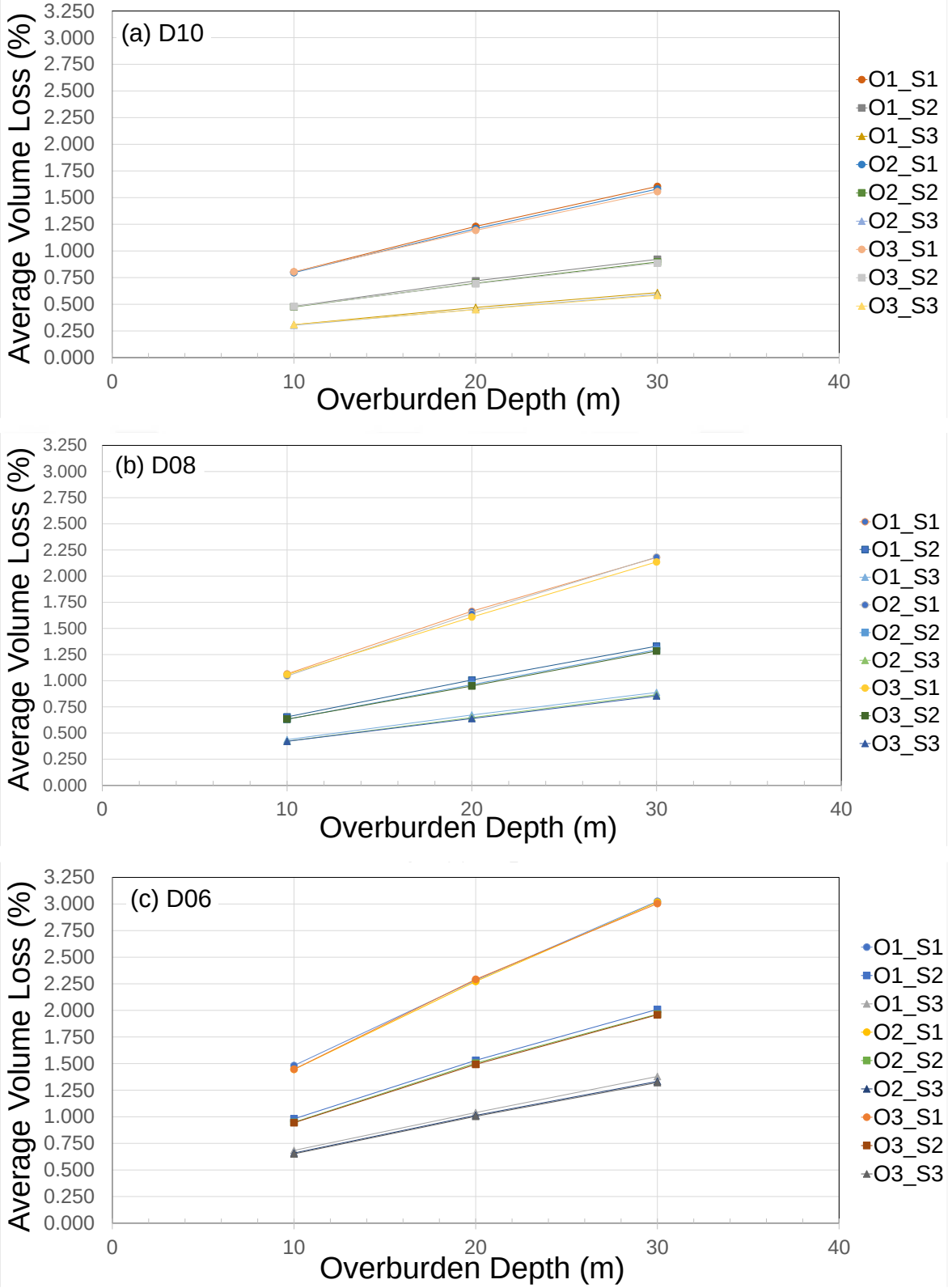


Figure 5.12. Average volume loss percentage (V_L %) of the UA applied tunnels with respect to overburden depth for (a) D10, (b) D08, and (c) D06 cases.

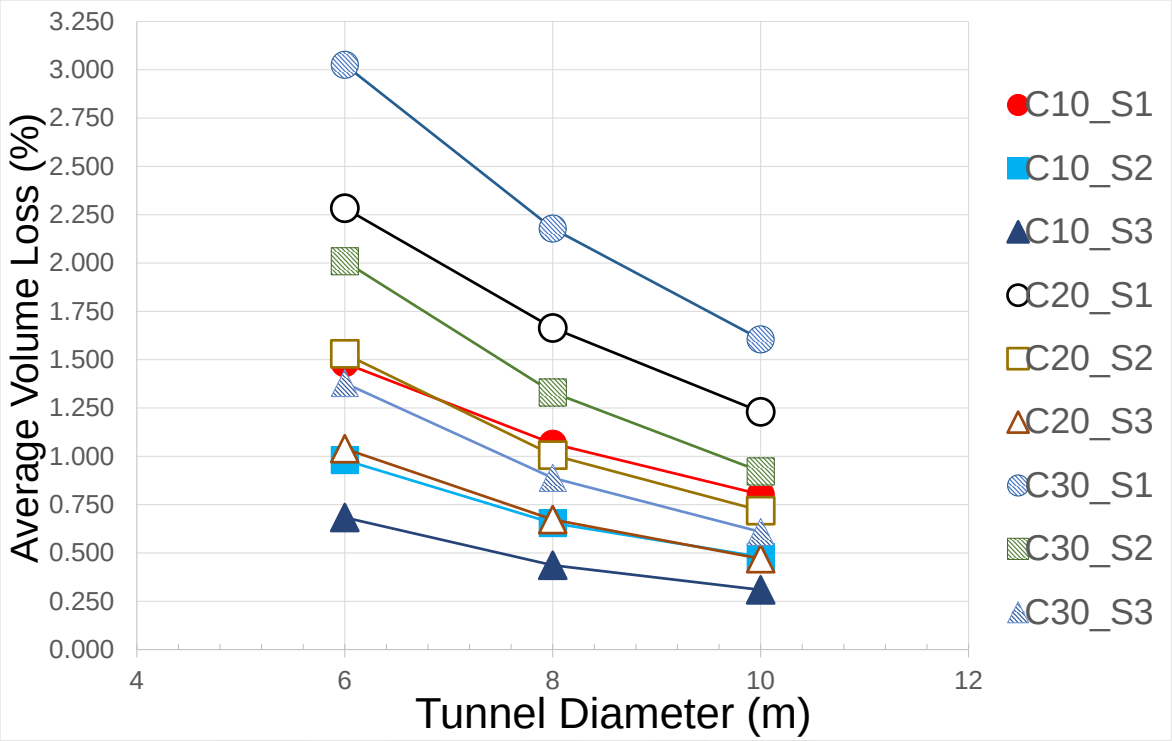


Figure 5.13. Average volume loss percentage (V_L %) of the UA applied tunnels with respect to tunnel diameter for O1 case.

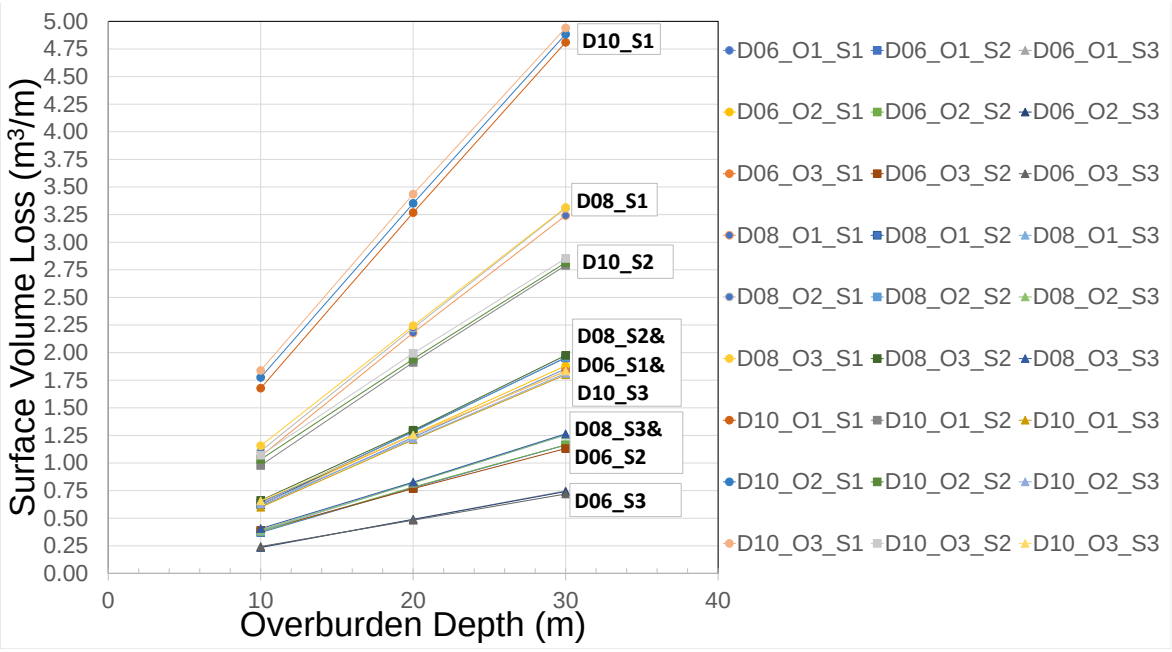


Figure 5.14. Surface volume loss (V_S) of the UA applied tunnels with respect to overburden depth.

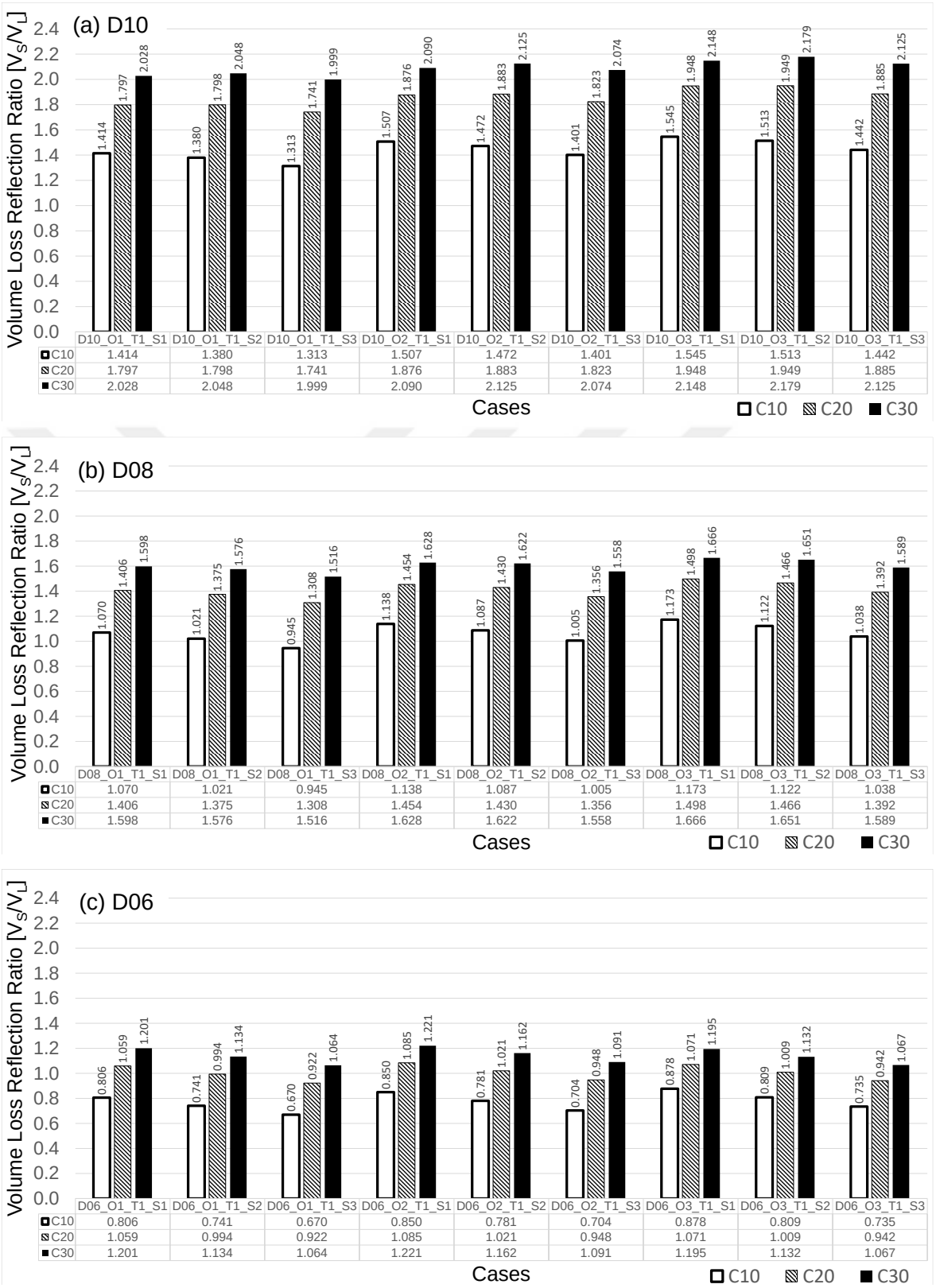
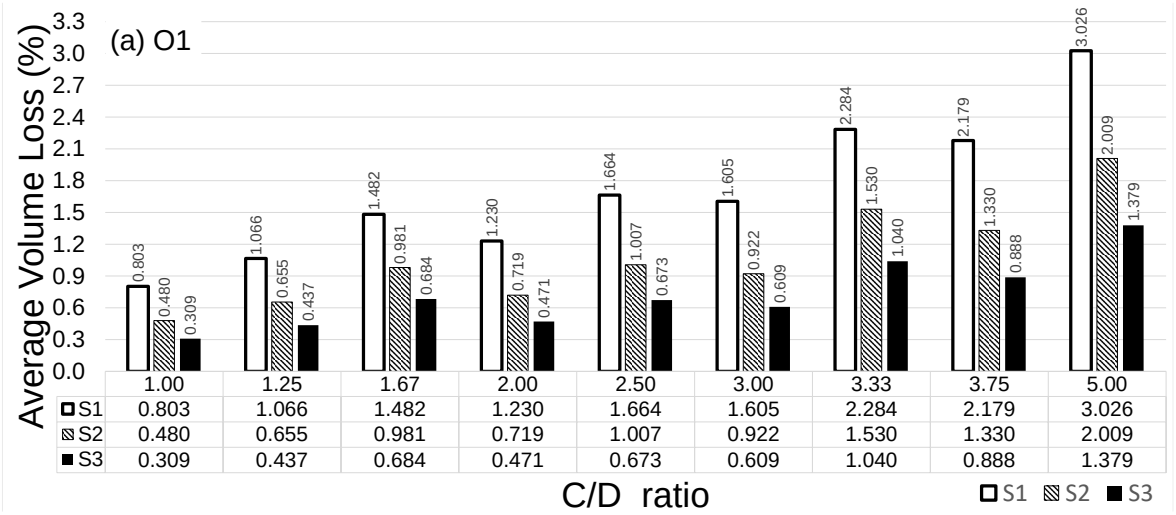
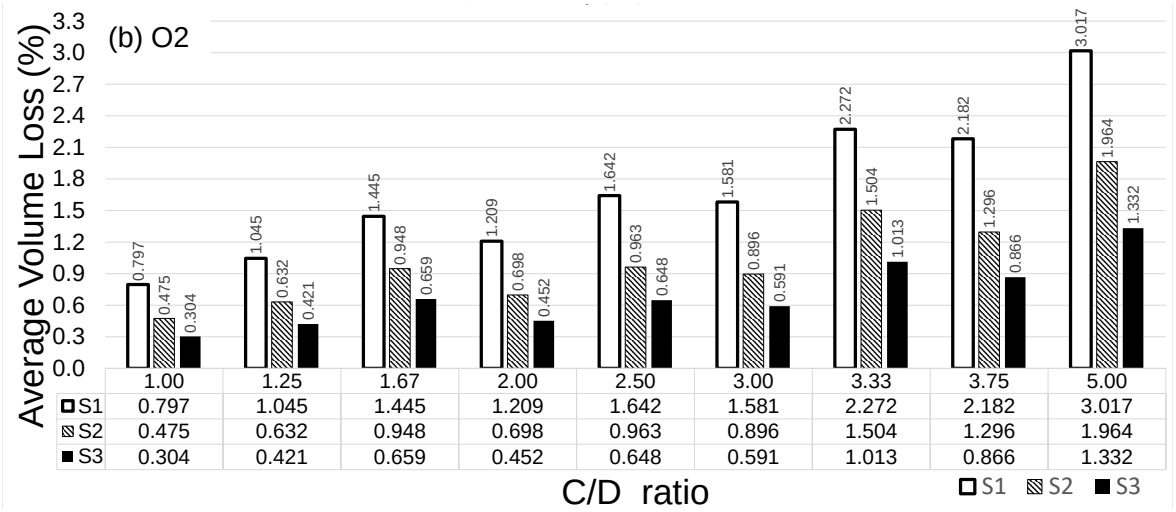


Figure 5.15. Volume loss reflection ratio (V_S/V_L) of the UA applied tunnels for (a) D10, (b) D08, and (c) D06 cases.





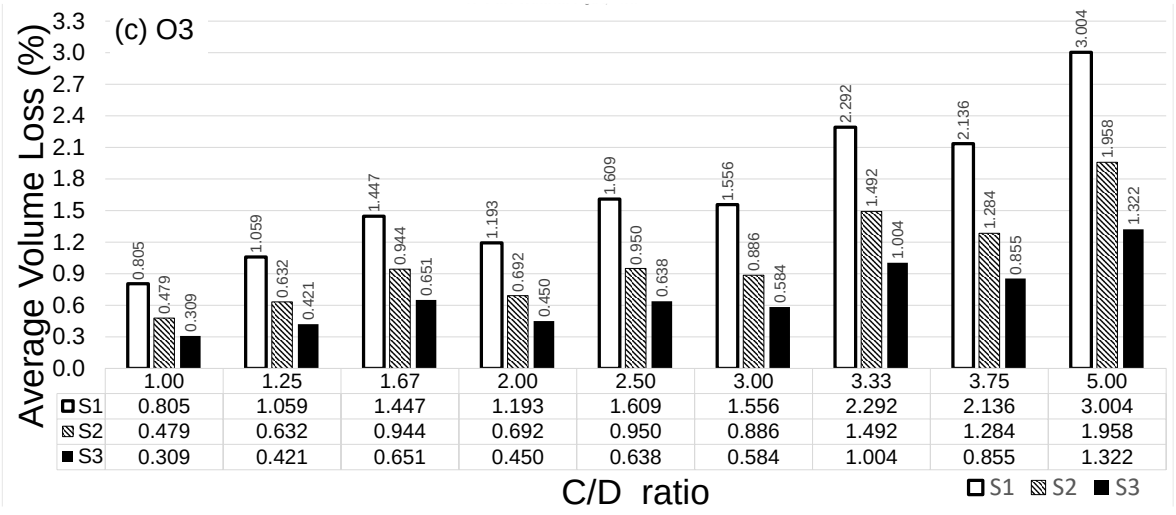


Figure 5.16. Average volume loss percentage (V_L %) of the UA applied tunnels with respect to clear distance to tunnel diameter ratio (C/D) normalization for (a) O1, (b) O2, and (c) O3 cases.

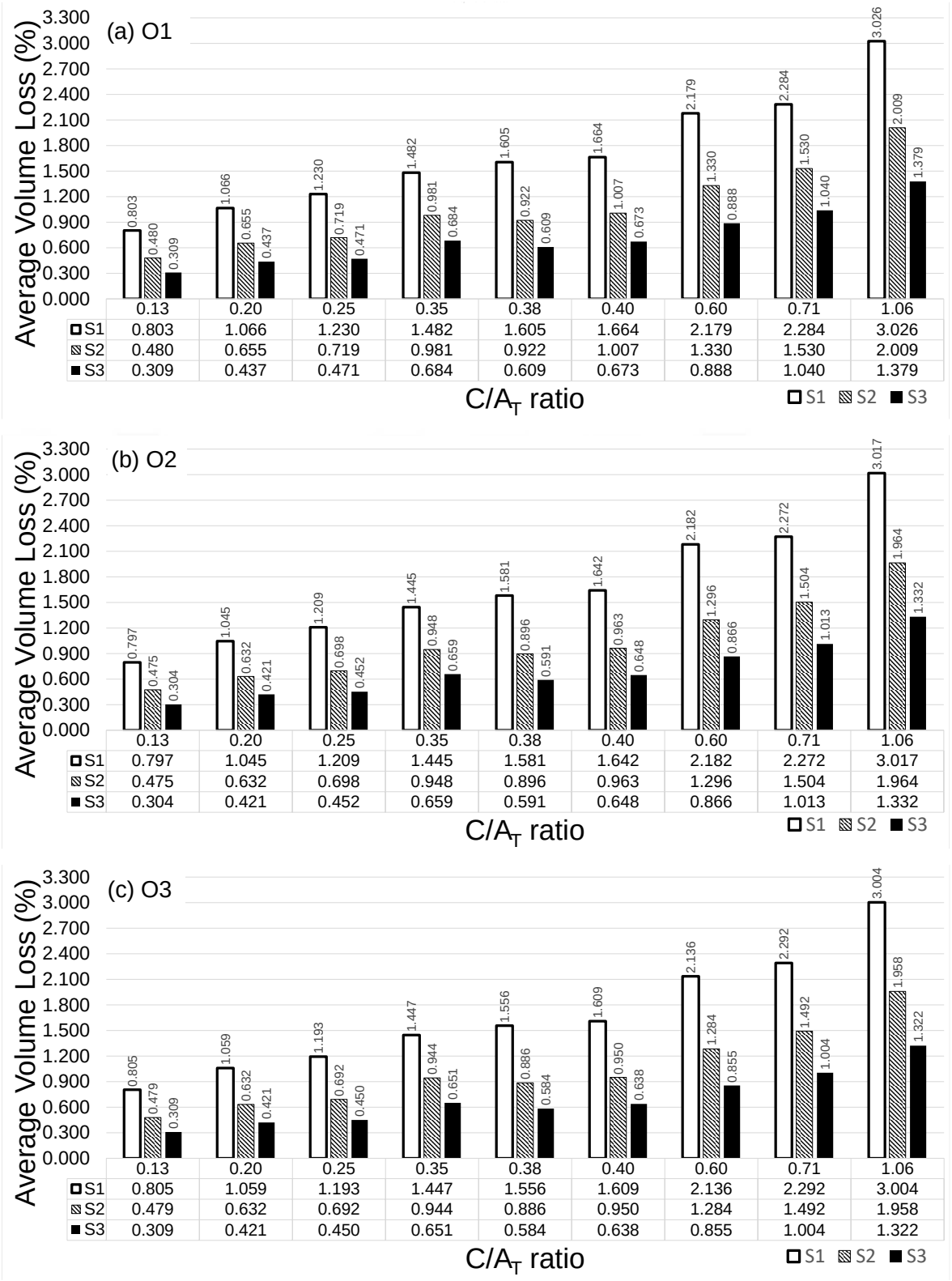


Figure 5.17. Average volume loss percentage (V_L %) of the UA applied tunnels with respect to clear distance to tunnel area ratio (C/A_T) normalization for (a) O1, (b) O2, and (c) O3 cases.

5.5. Convergence

Convergence is a frequently used definition in tunneling, describing the displacement of the tunnel surface due to surrounding stress. It is observed periodically during the excavation process. Since field measurement instruments are installed after the completion of the temporary lining, displacements cannot be measured in the field until the lining is completed. It is known that the actual displacement is always larger than the measured displacement. Therefore, a difference in convergence results between the calculated numerical models and the measured data is inevitable. This difference can be reduced by creating the numeric model in stages and obtaining the results from the corresponding stages. In spite of the fact that the difference is inevitable, convergence values are beneficial in parametric studies to understand the tunnel displacements. For this purpose, the maximum vertical and horizontal displacements of tunnels are plotted in Figure 5.18 and Figure 5.19. In these figures, displacement changes in UA applied cases are plotted with respect to overburden depth and the combinations of ground conditions and clear distance while tunnel diameter is kept constant for each of the sub-figures. Unless the swelling exceeds the downward displacement, the maximum vertical displacement ($u_{y,max}$) is always in the negative direction. However, the maximum horizontal displacement ($u_{x,max}$) can occur negatively or positively relative to the vertical axis. Therefore, it is considered and plotted as absolute values.

According to Figure 5.18, the vertical displacement in tunnels increases as overburden depth increases and ground conditions worsen. Clear distance has a limited effect on $u_{y,max}$. When it is reduced, $u_{y,max}$ increases, but its effect is less distinctive in shallow tunnels. In comparison of the three-diameter graph set, it is seen that $u_{y,max}$ increases as tunnel diameter increases. When considering the results with limitations, for example stated by IMM (2020), in some of the cases, especially those with 10 m tunnel diameter, $u_{y,max}$ exceeds 5 cm which is beyond the limits stated in the specification. Therefore, it can be concluded that the precautions performed in these numerical models are insufficient to meet the limits specified by IMM (2020), but some additional measures such as subdividing the excavation areas can be taken for large tunnels.

In general, similar implications can be observed for $u_{x,max}$ as plotted in Figure 5.19. It can be considered that $u_{x,max}$ has mirrored trends of $u_{y,max}$ with respect to the horizontal axis due to absolute values, but the values are in a narrower range. There are no results beyond the limits in terms of $u_{x,max}$ concerning the limit values stated by IMM (2020), which can be considered as a specification example.

Additionally, resultant displacements can be taken into consideration to understand the convergence of tunnels as plotted in Figure 5.20. In this figure, the change in resultant displacements is plotted with respect to overburden depth and the combinations of ground conditions and clear distance while tunnel diameter is kept constant for each of the sub-figures. It appears as a mirrored version of $u_{y,max}$ with respect to the horizontal axis and the differences are negligible. Also, in terms of values, they are very similar to $u_{y,max}$. Therefore, it is implicated that the vertical movement dominates the displacement of the tunnels. Furthermore, since the difference between $u_{y,max}$ and u_{max} is too small to distinguish, the horizontal displacement at the point where maximum vertical displacement occurred is minimal. Thus, it can be concluded that the most displaced part of the tunnel is its crown.

Since the effect of clear distance on u_{max} is limited and its graph with respect to overburden depth is very similar to the graph of $u_{y,max}$, the change in u_{max} is also plotted in terms of tunnel diameter as shown in Figure 5.21 for O1 cases. The graph showing the change in u_{max} with respect to tunnel diameter and the combinations of overburden depth and soil conditions implies that the maximum resultant displacement increases as tunnel diameter increases, overburden depth increases, and ground conditions worsen.

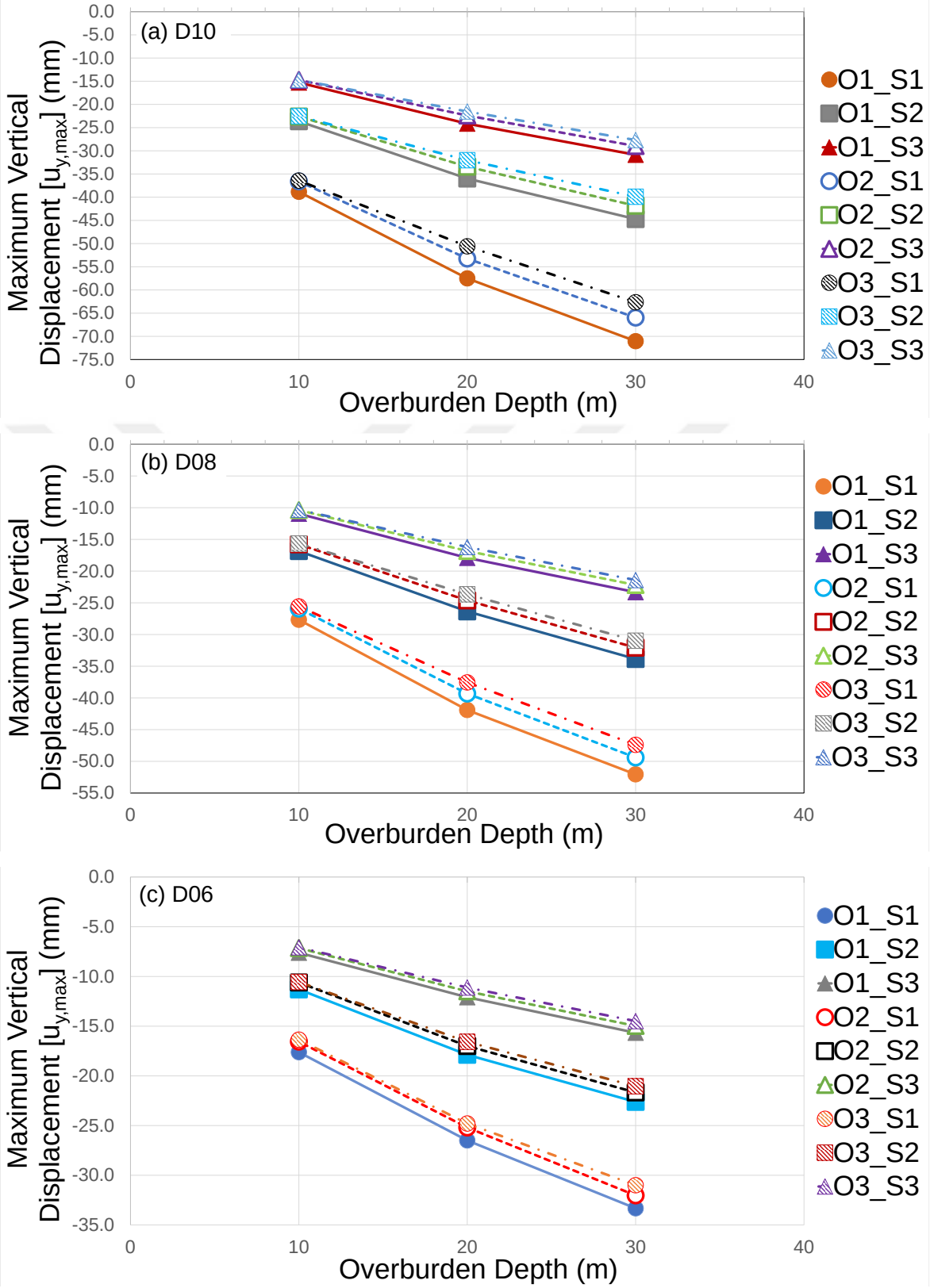


Figure 5.18. Maximum vertical displacement ($u_{y,max}$) of UA applied tunnels with respect to overburden depth for (a) D10, (b) D08, and (c) D06 cases.

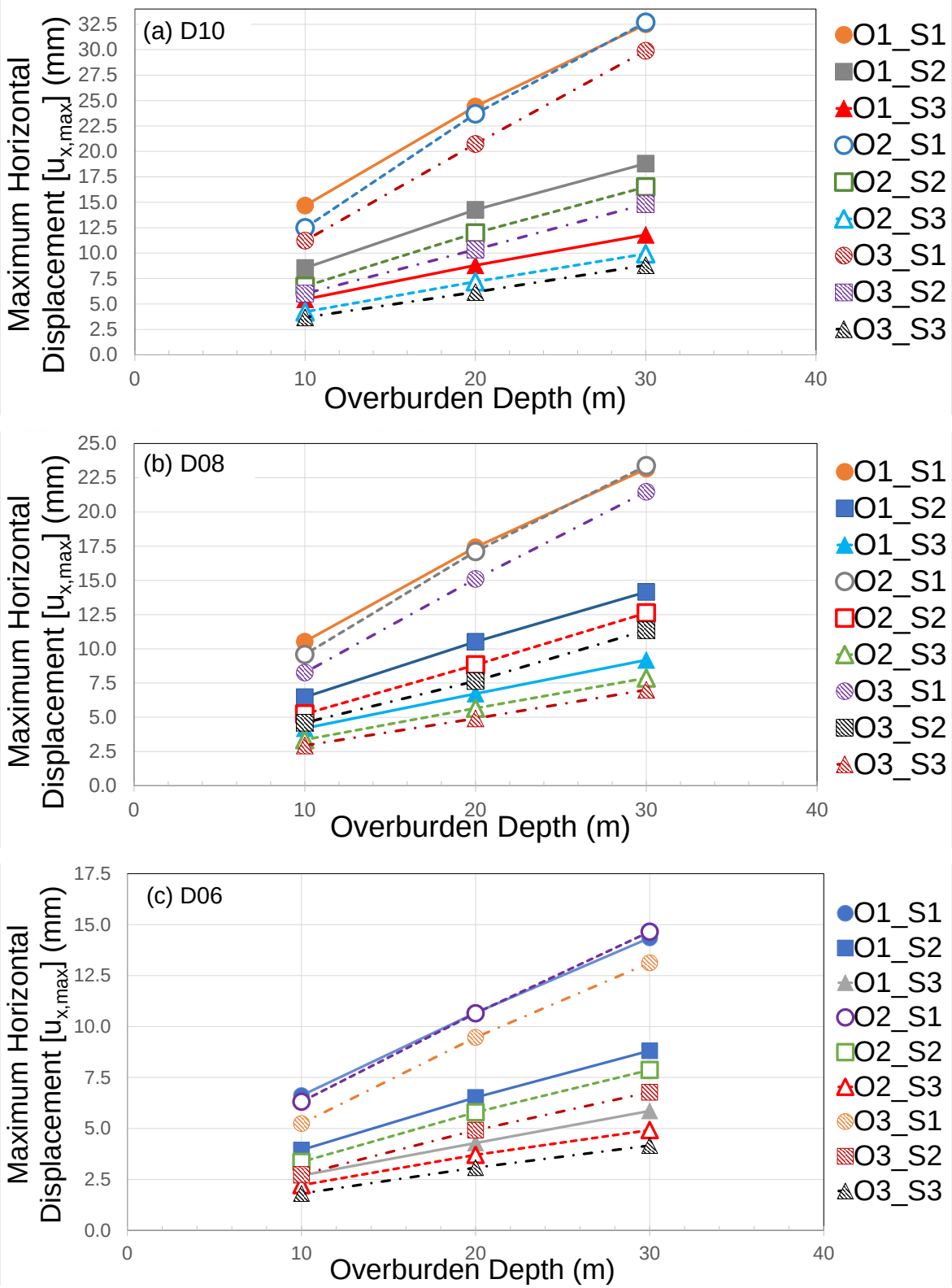


Figure 5.19. Maximum horizontal displacement ($u_{x,max}$) of UA applied tunnels with respect to overburden depth for (a) D10, (b) D08, and (c) D06 cases.

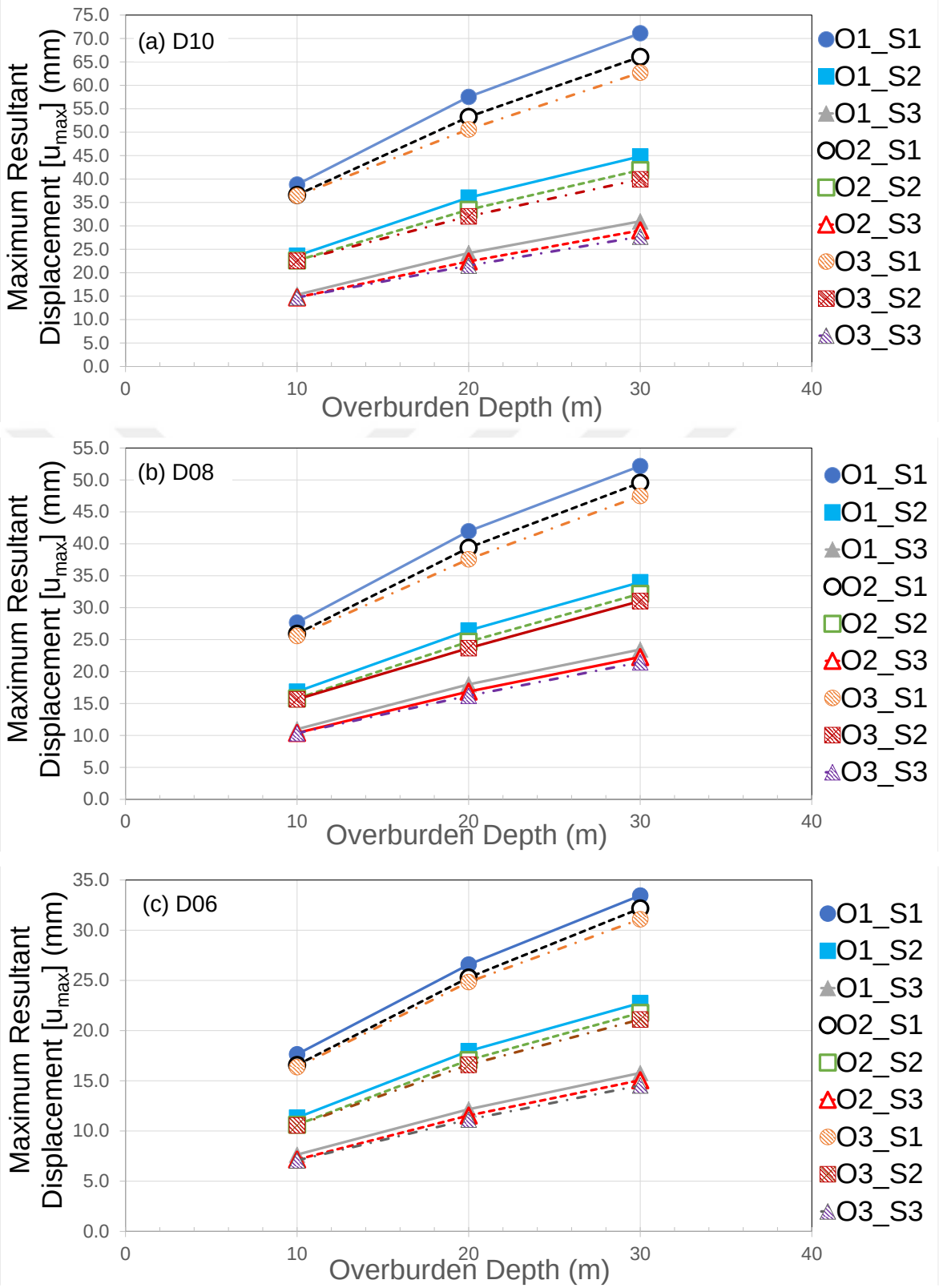


Figure 5.20. Maximum resultant displacement (u_{max}) of UA applied tunnels with respect to overburden depth for (a) D10, (b) D08, and (c) D06 cases.

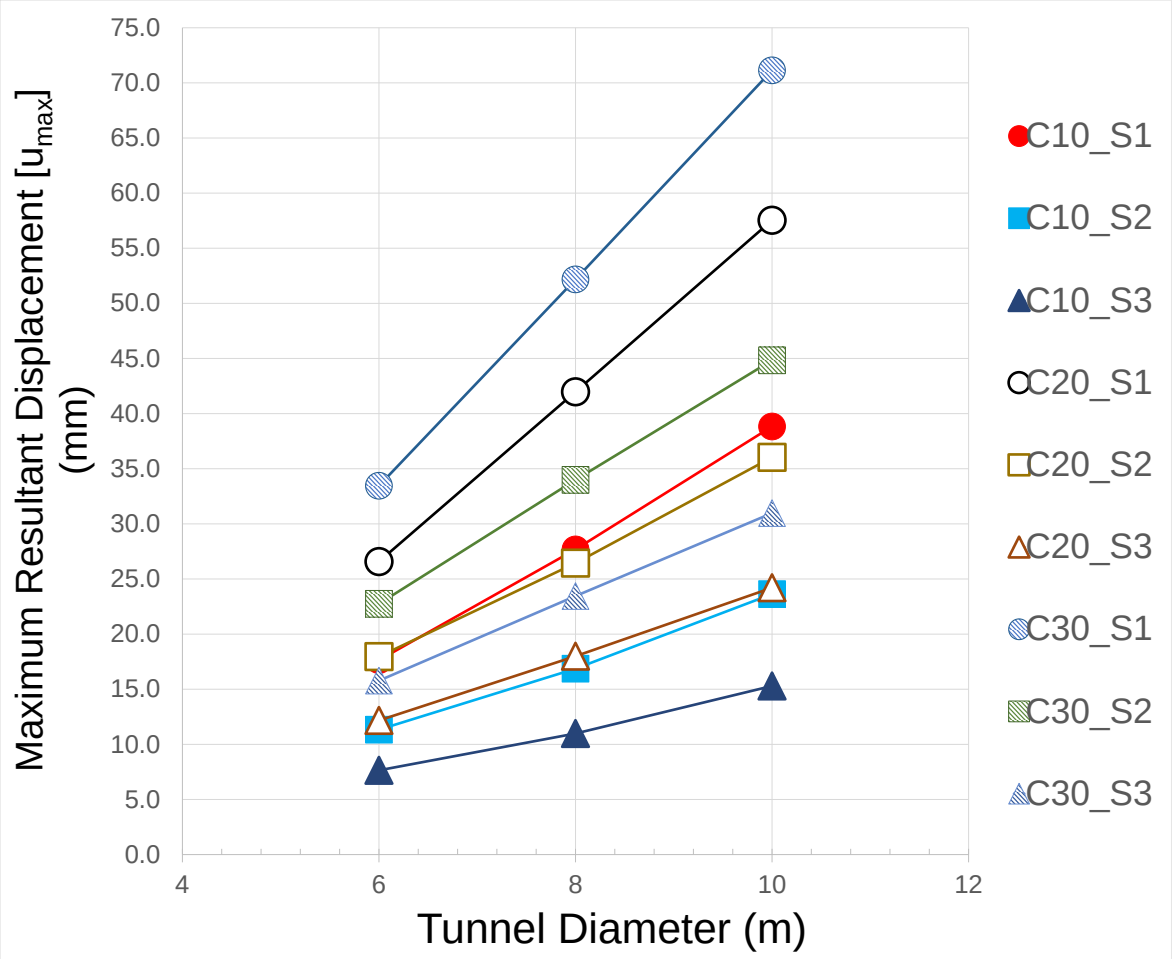


Figure 5.21. Maximum resultant displacement (u_{max}) of UA applied tunnels for O1 cases.

5.6. Forces on Support Elements

Forces on support elements are critical for the safe structural design of a tunnel. Mainly, two support elements are used in the modeling of cases in this thesis: temporary lining and bolts. Since the lining elements are modeled with the dummy plate approach, the obtained results from the software are multiplied by the scale factor used for the approach before plotting. On the other hand, the bolts are modeled without scaling, so the results are obtained and plotted directly. While bolts are inspected in terms of axial force only, lining elements are inspected in terms of axial force, shear force, and bending moment. Thanks to software, the maximum results can be obtained stage by stage or as the one occurring throughout the construction. The maximum results differ from one stage to another stage, and the maximum result in the last stage can be less than the previous stages. Therefore, obtaining the maximum results throughout construction is preferred rather than a specific

stage. Thus, the most critical value is obtained in terms of structural safety. The figures presented for these comparisons are plotted with respect to overburden depth and the combinations of ground condition and clear distance while tunnel diameter is kept constant for each of the sub-figures.

Figure 5.22 shows that the maximum axial force on bolts of twin tunnels throughout the construction ($N_{bolt,max}$) increases as the ground conditions worsen and the overburden depth increases. The force increases slightly as the clear distance decreases, but it has a limited effect. According to the comparison of three-diameter graph set, $N_{bolt,max}$ increases as the tunnel diameter increases. When the maximum axial force on lining elements ($N_{lining,max}$) is analyzed, similar trends are observed as presented in Figure 5.23. However, the effect of ground conditions is not as distinctive as it is for bolts. On the other hand, the force increments due to the increase in diameter are evident.

In order to see the effect of tunnel diameter on the axial force on lining elements, additional graphs are plotted in Figure 5.24 for O1 condition. This graph shows the change in $N_{lining,max}$ with respect to tunnel diameter and the combinations of overburden depth and ground conditions. According to the graph, the force increments due to the increase in tunnel diameter and overburden depth is corroborated. Also, it is seen that $N_{lining,max}$ increases as ground conditions worsen but its impact diminishes as overburden depth decreases.

When the maximum shear force on lining elements ($V_{lining,max}$) is analyzed, the distinct effect of ground conditions is again observed, in addition to the similarity in trends depending on overburden depth, clear distance, and tunnel diameter as plotted in Figure 5.25. In terms of maximum bending moment, ($M_{lining,max}$) similar trends are kept as shown in Figure 5.26. Therefore, if it is considered that the same structural elements having constant strength capacity are used for different cases, then the factor of safety (F_s) decreases as tunnel diameter gets larger, overburden depth gets deeper, clear distance gets narrower, and ground conditions worsen.

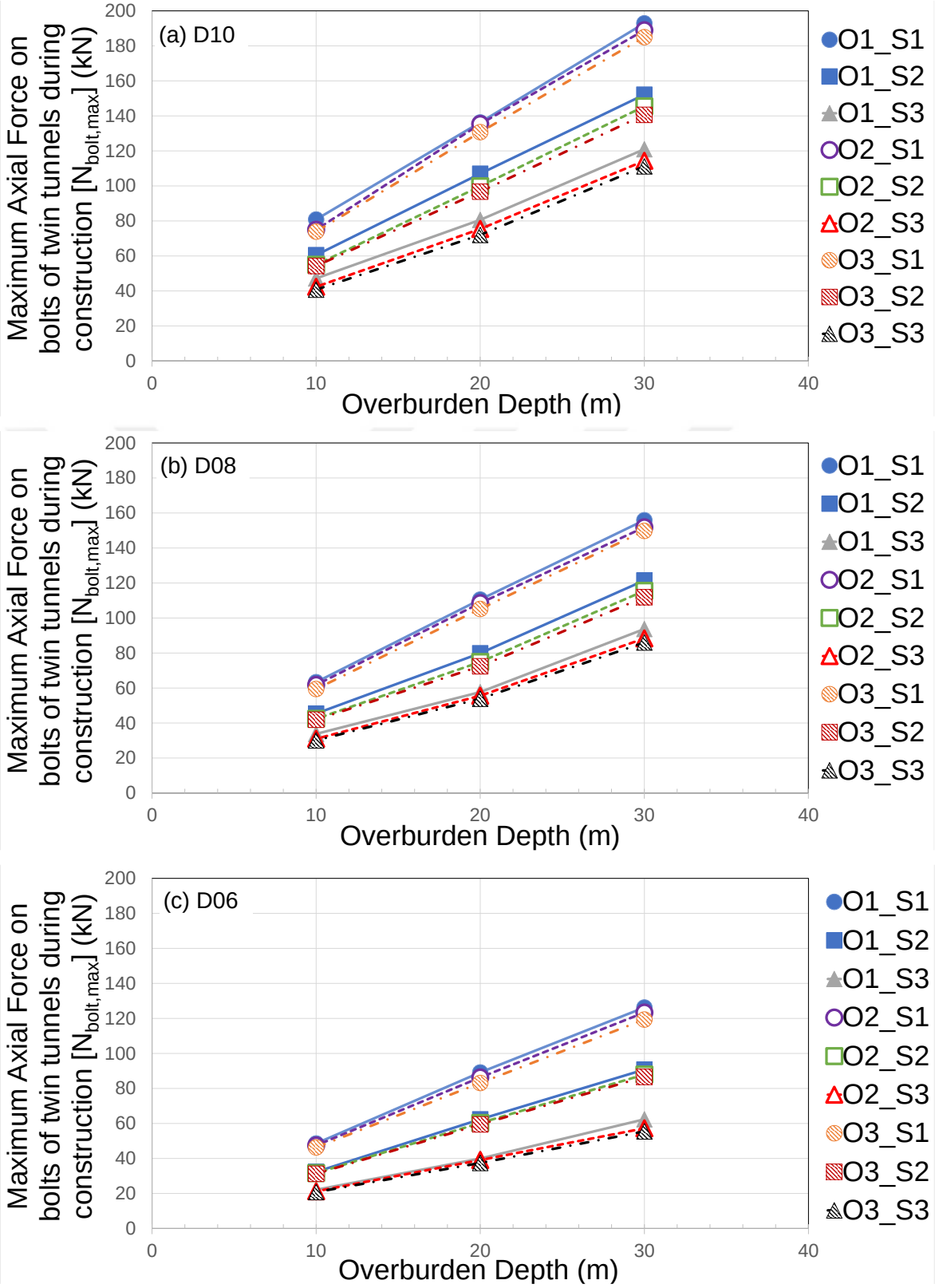


Figure 5.22. Maximum axial force on bolts of UA applied twin tunnels throughout the construction ($N_{bolt,max}$) with respect to overburden depth for (a) D10, (b) D08, and (c) D06 cases.

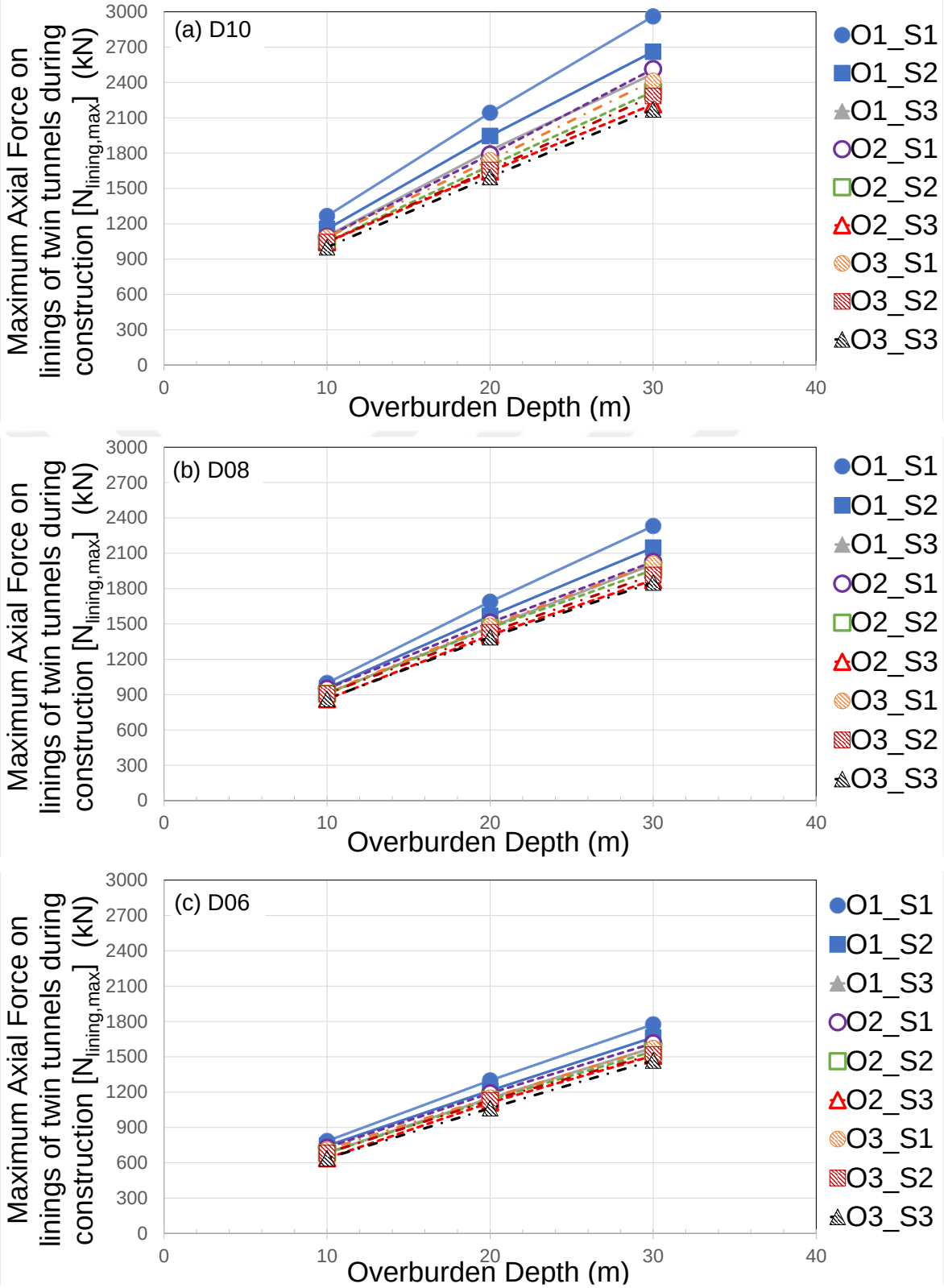


Figure 5.23. Maximum axial force on linings of UA applied twin tunnels throughout the construction ($N_{lining,max}$) with respect to overburden depth for (a) D10, (b) D08, and (c) D06 cases.

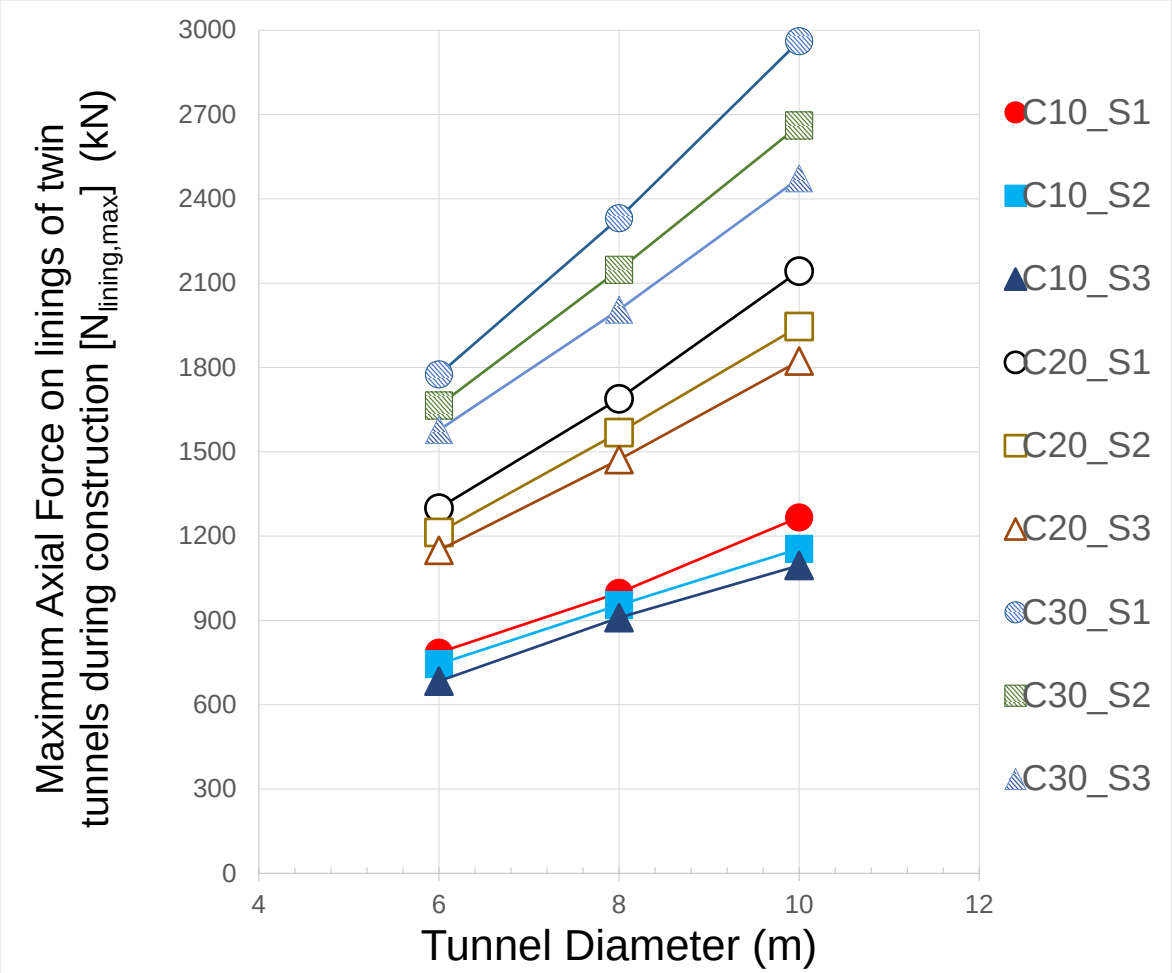


Figure 5.24. Maximum axial force on linings of UA applied twin tunnels throughout the construction ($N_{lining,max}$) with respect to tunnel diameter for O1 cases.

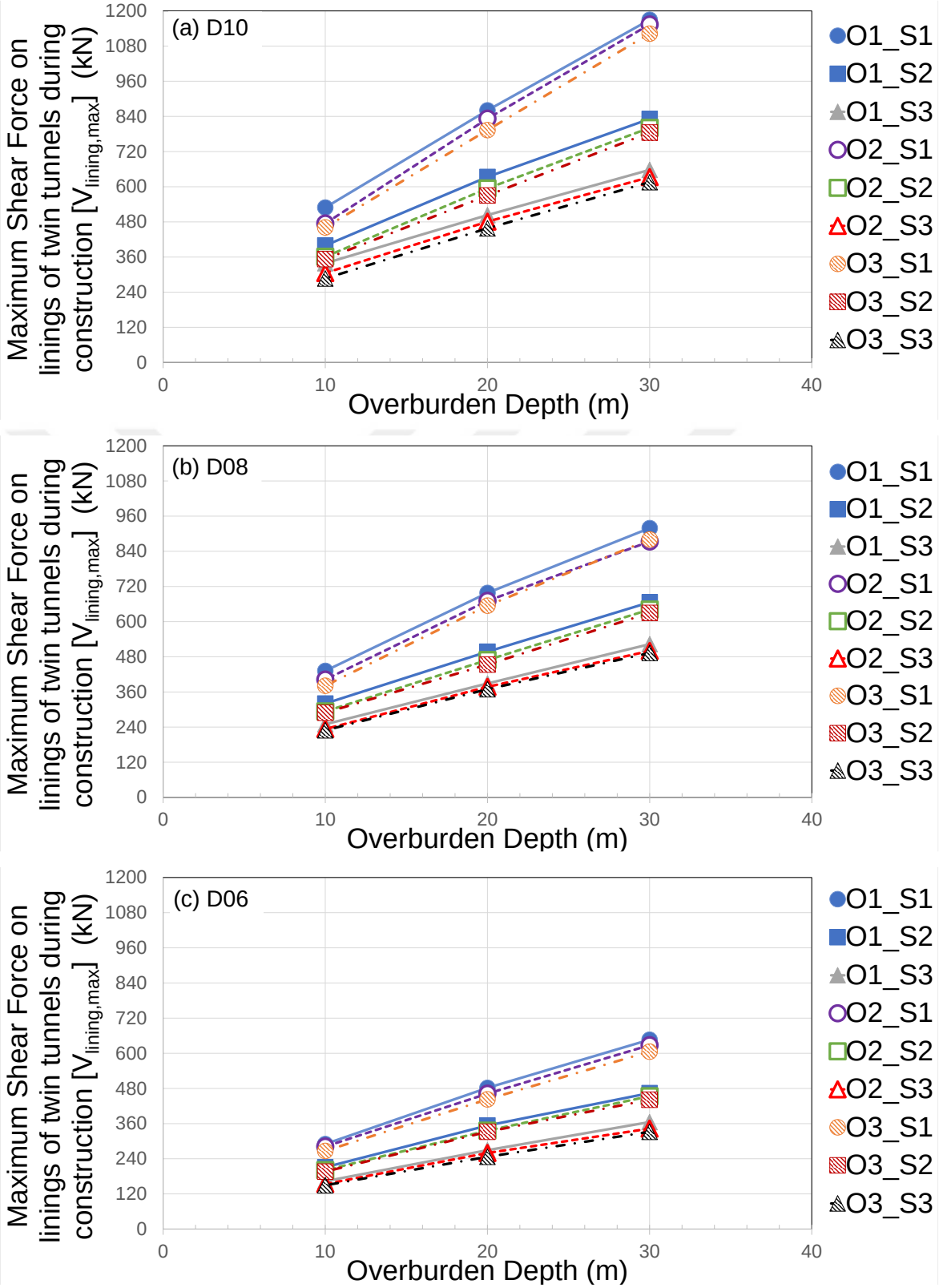


Figure 5.25. Maximum shear force on linings of UA applied twin tunnels throughout the construction ($V_{lining,max}$) with respect to overburden depth for (a) D10, (b) D08, and (c) D06 cases.

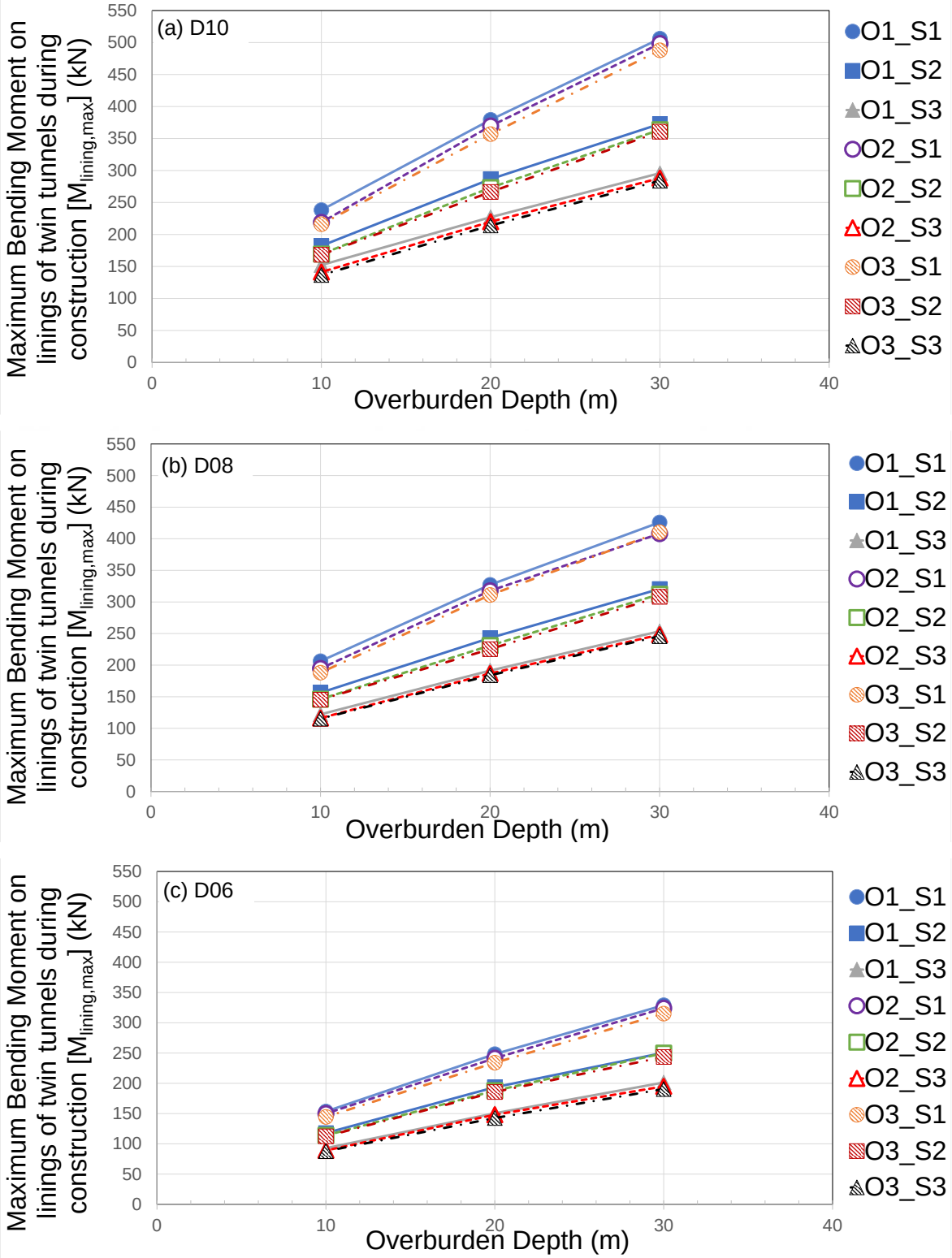


Figure 5.26. Maximum bending moment on linings of UA applied twin tunnels throughout the construction ($M_{lining,max}$) with respect to overburden depth for (a) D10, (b) D08, and (c) D06 cases.

6. CONCLUSION AND RECOMMENDATIONS

This study investigates the behavior of NATM tunnels supported by umbrella arch (UA). For this investigation, a detailed validation study was initially conducted for two different twin tunnel sections of Çekmeköy – Sancaktepe – Sultanbeyli metro line by applying three different UA modeling approaches using 2D numerical analysis. The numerical analysis results were compared with field measurements to identify the most suitable modeling approach. Upon completion of the validation study, a parametric study was conducted. The parametric study investigated the effect of improvement zone thickness, overburden depth, tunnel diameter, ground conditions, and twin tunnel distance on tunnel behavior. Based on the results of the 2D FE analyses conducted on the twin tunnel sections supported by umbrella arch for validation and parametric studies, the following conclusions were drawn:

- The findings in the validation study show that it is possible to estimate surface settlement within an allowable error margin using 2D numerical analysis with different modeling approaches based on the improved zone (plate, dummy plate, and individual pipe; abbreviated as P, DP, IP, respectively). The results indicate that NATM tunnels can be modeled successfully using one of the three approaches.
- Despite its more involved modeling requirements, the IP approach (creating individual pipes in the model) in 2D did not provide a unique advantage compared with the P and DP approaches.
- The DP approach was the best-suited approach among the investigated settlement predictions of the analyzed cases. Therefore, the DP approach was preferred in the parametric study.
- Subsequently, the parametric study was established upon the validated DP approach and constant deconfinement ratios (i.e., fixed values for phases in each parametric case) were used in the 2D numerical modeling by adopting from the validation study. Using constant deconfinement ratios for cases analyzed with different (dependent or independent) parameters implied that the advancement length varied for each analyzed case. This approach was taken to eliminate the combined effects on the tunnel

behavior; however, this constancy also prevented the observation of three-dimensional arching effects.

- The results of the validation and parametric studies underlined the importance of the deconfinement ratio. Using a constant deconfinement ratio irrespective of ground, support, excavation, and geometric conditions inhibited the identification of the effects of the non-existence of UA on the tunnel behavior. Even though the most distinctive difference was observed in terms of volume loss in tunnels (V_L) when the extreme cases were compared with and without UA support, the differences were deemed negligible in some cases.
- On the other hand, all the calculated V_L values were tolerable and coherent with the expected ranges indicated in the literature. As anticipated, V_L (%) was found to be highly dependent on ground conditions, and it increased as ground conditions worsened. V_L (%) also increased with the increase in overburden depth (C). The effect of the clear distance on V_L was deemed negligible. When V_L is quantified as volume per meter (m^3/m) instead of a percentage, even though the absolute volume loss declined with the reduction in tunnel diameter (D), the volume loss in terms of percentage increased since the initial section area of a tunnel drops dramatically with the decrease in tunnel diameter. In order to normalize the effect of geometric conditions on tunnel behavior in terms of volume loss, C/D and overburden depth over tunnel area (A_T) ratios (C/A_T) were introduced. The trends with respect to C/D were not clear, but V_L clearly increased with the increase in C/A_T.
- Surface volume loss (V_S) had similar trends to volume loss in tunnels (V_L). However, V_S can be represented by the volume per meter only; therefore, it increased as tunnel diameters increased. To understand the relationship between V_L and V_S, their ratio (V_S/V_L), which was called volume loss reflection ratio, was introduced. This ratio decreased with the reduction in tunnel diameter and overburden depth.
- Validation results indicated that V_S increases as V_L increases. V_L is also coherent with the convergence of tunnels, which is the displacement of tunnel peripheries, and it is an important criterion for safe construction. In this context, it is observed that the maximum displacement in the vertical direction ($u_{y,max}$) governs the maximum resultant displacement (u_{max}) in tunnels; in other words, the effect of horizontal displacement is negligible where the maximum resultant displacement occurs. The

dominance of $u_{y,max}$ on the u_{max} was verified by the parametric study also, and the crown part was detected as the most critical or displaced part of the tunnel.

- As anticipated, it is seen that $u_{y,max}$ increased as overburden depth increased, tunnel diameter increased, ground conditions worsened, and the distance between the twin tunnels got closer. However, the effect of clear distance diminishes with the drop in overburden depth. The observations for the maximum horizontal displacement ($u_{x,max}$) were similar to those of $u_{y,max}$, but in a narrower range in terms of values.
- When surface settlement shapes are compared, it can be seen that the overlapping of settlement profiles (i.e., observing a single peak) becomes unlikely when overburden depth is shallow. As C/D decreased and the clear distance increased, observing two peaks in the profile became more likely.
- When the cases were compared in terms of the maximum settlement (S_{max}), an increase was observed in S_{max} with the increase in overburden depth. This is likely due to the effects of using a constant (i.e., from one case to another) deconfinement ratio. As expected, S_{max} also increases as ground conditions worsen and tunnel diameter enlarges. Conversely, S_{max} decreases if the clear distance between tunnels increases. However, it is important to note that the increase in the clear distance makes the settlement profile wider. Furthermore, the impact of clear distance on S_{max} diminishes as the tunnel diameter decreases.
- Even though the twin tunnels were modeled symmetrically in the section, the x-coordinate of the S_{max} was not observed on the symmetry axis in validation studies. This result shows that the settlement profile can skew mainly due to geometric conditions, excavation order, and even ground conditions. With the parametric study, it is revealed that geometric conditions are clearly more effective than the ground conditions; however, the results indicate the ground conditions may also impact skewness, but this effect declined as the overburden depth decreased. In the context of geometric conditions, the skewness shifted towards the secondly excavated tunnel as overburden depth increased, but it moved in the opposite direction as clear distance increased. As the C/D ratio increased, skewness shifted towards the second tunnel. Skewness is an important parameter as it allows determining the excavation order of twin tunnels to avoid the occurrence of the S_{max} at an undesired location.
- In the context of safe structural design, the forces on support elements are important. For this parametric study, the support elements are temporary lining and bolts. The

effect of clear distance on the maximum axial force on bolts of twin tunnels throughout the construction ($N_{bolt,max}$) was limited, almost negligible. On the other hand, $N_{bolt,max}$ increased as ground conditions worsened and overburden depth or tunnel diameter increased. Except for the distinctive impact of ground conditions on bolts, similar trends were observed for the maximum axial force on lining elements throughout the construction ($N_{lining,max}$). The limited impact of ground conditions on $N_{lining,max}$ became negligible as overburden depth decreased.

- In terms of the maximum shear force on lining elements throughout the construction ($V_{lining,max}$) and the maximum bending moment on lining elements throughout the construction ($M_{lining,max}$), trends depending on overburden depth, clear distance, and tunnel diameter were similar to those observed for $N_{lining,max}$. A distinct effect of the ground conditions on the $V_{lining,max}$ and $M_{lining,max}$ was again realized. Therefore, for tunnels that have the same capacity in terms of the structural elements, the factor of safety increased as tunnel diameter became smaller, overburden depth became shallower, clear distance became larger, and ground condition improved.

For future research on NATM tunnels supported by umbrella arch, three-dimensional (3D) numerical analyses are recommended to observe the mechanistic impact of this forepoling technique (i.e., UA). Thus, the parameters related to the umbrella arch, such as pipe length, pipe diameter, pipe spacing, and overlap length, can be investigated more effectively in 3D. Also, tunnel face displacements can be observed by 3D modeling. Additionally, studies exploring the impact of deconfinement ratios should be performed in order to better simulate the third dimension in 2D modeling. Finally, long-term analysis of tunnels under seismic conditions should be investigated for their safety in earthquake zones.

REFERENCES

Ağbay, E., 2019, *Assessment of Twin Tunnel Induced Ground Deformation by Empirical and Numerical Analyses (Eurasia Tunnel: NATM Part, Istanbul, Turkey)*, Ph. D. Thesis, Middle East Technical University.

Aksoy, C. O., and T. Onargan, 2010, "The Role of Umbrella Arch and Face Bolt as Deformation Preventing Support System in Preventing Building Damages", *Tunnelling and Underground Space Technology*, Vol. 25, No. 5, pp. 553-559.

Aygar, E. B., and C. Gokceoglu, 2020, "Problems Encountered During a Railway Tunnel Excavation in Squeezing and Swelling Materials and Possible Engineering Measures: A Case Study from Turkey", *Sustainability*, Vol. 12, No. 3.

Bae, G. J., H. S. Shin, C. Sicilia, Y. G. Choi, and J. J. Lim, 2005, "Homogenization Framework for Three-Dimensional Elastoplastic Finite Element Analysis of a Grouted Pipe-Roofing Reinforcement Method for Tunnelling", *International Journal for Numerical and Analytical Methods in Geomechanics*, Vol. 29, No. 1, pp. 1-24.

Bagherzadeh, P., K. Goshtasbi, and M. Kashef, 2020, "Umbrella Arch Method Performance, Structural Behavior and Design Elements Utilizing in Collapsing Zones", *Environmental Earth Sciences*, Vol. 79, No. 23.

Barış, C., and Y. Mahmutoğlu, 2018, "Türkiye'de Yeni Avusturya Tünel Açma Yöntemiyle (NATM) Açılan Metro Tünellerinde Tercih Edilen Kaya Sınıflamaları", *Yer Mühendisliği Dergisi*, No. 11, pp. 24-32.

Barton, N., R. Lien, and J. Lunde, 1974, "Engineering Classification of Rock Masses for the Design of Tunnel Support", *Rock Mechanics*, Vol 6, No. 4, pp. 183-236.

Bauer, F., Daller, J. and Proprenter, M., 2005. “Tunnel ‘Wienerwald’”, *International Symposium on Design, Construction and Operation of Long Tunnels*, Taipei, P.R. China, pp. 999-1008.

Bieniawski, Z. T., 1973, “Engineering Classification of Jointed Rock Masses", *Transaction of the South African Institution of Civil Engineers*, Vol.15, No. 12, pp. 335-344.

Bieniawski, Z. T., 1976, "Rock Mass Classifications in Rock Engineering”, *Symposium on Exploration for Rock Engineering*, edited by Z. T. Bieniawski, Rotterdam, Holland, pp. 7-106.

Bieniawski, Z. T., 1990, *Tunnel Design by Rock Mass Classifications*; U.S. Army Engineer Waterways Experiment Station, Vicksburg, MS, United States of America.

Birincioğlu, A., 2017, Tünel Kazı - Desteklemeleri ve Hasır Çelik Yerine Sentetik Fiber Donatı Kullanımı, M.S. Thesis, Karadeniz Technical University.

Bizjak, K.F. and B. Petkovšek, 2004, “Displacement Analysis of Tunnel Support in Soft Rock Around a Shallow Highway Tunnel at Golovec”, *Engineering Geology*, Vol. 75, No. 1, pp. 89-106.

Carrieri, G., P. Grasso, A. Mahtab, and S. Pelizza, 1991, “Ten Years of Experience in the Use of Umbrella-Arch for Tunnelling”, *The Congress on Soil and Rock Improvement in Underground Works*, Milano, Italy, Vol. 1, pp. 99-111.

Croce P., G. Modoni, G. Russo, 2004, "Jet-grouting Performance in Tunnelling”, *Geosupport 2004: Drilled Shafts, Micropiling, Deep Mixing, Remedial Methods, and Specialty Foundation Systems*, Orlando, FL, United States of America, pp. 910-922.

Çeçen, E. E., 2007, *Kent İçi Tünellerinde Uygulanan Şemsiye Kemer ve Ayna Donatılama Tekniklerinin Gerilme-Deformasyon Üzerine Etkilerinin Sayısal Analizi*, Ph. D. Thesis, İstanbul Technical University.

Çekmeköy-Sancaktepe-Sultanbeyli Metro Line Construction and Electromechanical Systems Procurement, Installation, and Commissioning Work Final Lining Calculation Report for the Type A Tunnel Subtype4, 2022, Anatolian Side Rail Systems Section Directorate of Department of Rail Systems of İstanbul Metropolitan Municipality (IMM), Istanbul.

Çekmeköy-Sancaktepe-Sultanbeyli Metro Line Construction and Electromechanical Systems Procurement, Installation, and Commissioning Work Technical Specifications Part 1 - Rough Construction and Finishing Works, 2020, Directorate of Infrastructure Projects of Department of Survey and Projects of Istanbul Metropolitan Municipality (IMM), p. 160.

Da Via`, A., M. Marotta, and G. Peach, 2006, “High Pressure Jet Grouting for a Collapsed Tunnel - A Case Study”. *International Conference and Exhibition on Tunnelling and Trenchless Technology*, Subang, Selangor, Malaysia, pp. 143-155.

Della Valle, N. D., and M. M. Rodriguez, 2014, "Twin Tunnels and Asymmetrical Settlement Troughs in Soft Soils", *40th World Tunnel Congress, Tunnels for Better Life*, Foz do Iguaçu, Brazil.

Elyasi, A., M. Javadi, T. Moradi, J. Moharrami, S. Parnian, and M. Amrac, 2016, "Numerical Modeling of an Umbrella Arch as a Pre-Support System in Difficult Geological Conditions: A Case Study”, *Bulletin of Engineering Geology and The Environment*, Vol. 75, No. 1, pp. 211-221.

Ergincan, H. E., T. Y. Özüdoğru, and I. Z. Yıldırım, 2023, “Şemsiye Kemer Uygulamasındaki Sayısal Modelleme Yaklaşımlarının Karşılaştırılması”, *5th International Underground Excavations Symposium*, İstanbul, Türkiye, pp. 239-250.

Ergincan, H. E., T. Y. Ozudogru, and I. Z. Yildirim, 2024, “Numerical Modeling of NATM Tunnels Pre-supported with Umbrella Arch Method: Comparison with Field Measurements”, *Geo-Congress 2024*, Vancouver, Canada, pp. 140-151.

Gall, V., J. Rudolf, T. O'Brien, 2011, "Considerations for Very Shallow Conventional (SEM) Tunneling in Urban Settings", *Rapid Excavation and Tunneling Conference*, edited by Redmond, S. and V. Romero, San Fransisco, CA, United States of America, pp. 1281-1296.

Ghee, E. H., B. T. Zhu, D. R. Wines, 2011 "Numerical Analysis of Twin Road Tunnels Using Two-and Three-Dimensional Modelling Techniques", *2nd International FLAC/DEM Symposium*, Melbourne, Australia, pp. 105-116.

Gibbs, P. W., J. Lowrie, D. S. Kieffer, L. McQueen, 2002, "M5 East - Design of a Shallow Soft Ground Shotcrete Motorway Tunnel", *28th ITA-AITES World Tunneling Congress*, Sydney, Australia, pp. 1151-1156.

Güneş, A., 2021, *Numerical Assessment of Tunnel Advancement in Problematic Soil Conditions: A Case Study*, M.S. Thesis, Middle East Technical University.

Harazaki, I., H. Aono, A. Matsuda, T. Aoki, and Y. Hakoishi, 1998, "Field Observation of Large Tunnel Supported by Umbrella Method: Case of Maiko Tunnel in Kobe, Japan", *24th World Tunnel Congress 1998 on Tunnels and Metropolises*, edited by Negro Jr, A., A. Ferreira, Sao Paulo, Brazil, pp.1009-1014.

Hefny, A. M., W. L. Tan, P. Ranjith, J. Sharma, and J. Zhao, 2004, "Numerical Analysis for Umbrella Arch Method in Shallow Large Scale Excavation in Weak Rock", *Tunnelling and Underground Space Technology*, Vol. 19, No. 4-5.

Hoek, E., 2001, "Big Tunnels in Bad Rock", *Journal of Geotechnical and Geoenvironmental Engineering*, Vol. 127, No. 9, pp. 726-740.

Hoek, E., 2004, "Numerical Modelling for Shallow Tunnels in Weak Rock", Unpublished Notes, 2024, https://www.rocscience.com, accessed on June 11, 2024.

Info, 2014, Dywidag-Systems International (DSI), No. 20, pp. 18-19.

International Tunneling Association, 1980, “Neue Österreichische Tunnelbaumethode: Definition und Grundsätze”, Schriftenreihe der Forschungsgesellschaft für das Straßenwesem im Österreichischen Ingenieur- und Architekten-Verein, Vol.74.

Jenkins, F., D. Cerulli, S. Barna, 2011, “Construction of the Dulles Corridor Metrorail Project NATM Tunnels at Tysons Corner, Virginia: A Case History”, *Rapid Excavation and Tunneling Conference*, edited by Redmond, S. and V. Romero, San Fransisco, CA, United States of America, pp. 1312-1323.

Juneja, A., A. Hedge, F. H. Lee, and C. H. Yeo, 2010, “Centrifuge Modelling of Tunnel Face Reinforcement Using Forepoling”, *Tunnel Underground Space Technology*, Vol. 25, No.4, pp. 377-381.

Kahyaoğlu, H., 1998, “TAG Otoyolu Özelinde Tünel İşleri ve Yeni Avusturya Tünel Açma Yöntemi”, *4. Ulaştırma Kongresi*, Ankara, Türkiye, pp. 49-64.

Kamal, H., M. Hussein, and A. Akl, 2021, “Parametric Study of Twin Tunnel Under Seismic Loads for Cairo Metro Line No. 4”, *HBRC Journal*, Vol. 17, No. 1, pp. 137-156.

Kanik, M., 2019, “Evaluation of the Limitations of RMR_{89} System for Preliminary Support Selection in Weak Rock Class”, *Computers and Geotechnics*, Vol. 115.

Karahan, E., 2010, *Design of Excavation and Support Systems for the Çubukbeli Tunnel in Antalya*, M.S. Thesis, Middle East Technical University.

Karakus, M., and R. J. Fowell, 2000, "FEM Analysis for the Effects of the NATM Construction Technique on Settlement Above Shallow Soft Ground Tunnels”, *ISRM International Symposium*, Melbourne, Australia.

Karakuş, M., and R. J. Fowell, 2004, “An Insight into The New Austrian Tunnelling Method (NATM)”, *7th Regional Rock Mechanics Symposium*, Sivas, Türkiye.

Kaya, A., and F. Bulut, 2013, “Zayıf Kaya Kütlelerinde Açılan Tünellerde Ampirik ve Nümerik Yöntemlerle Duraylılık Analizi”, *Jeoloji Mühendisliği Dergisi*, Vol. 37, No. 3, pp. 103-117.

Kaya, A., and F. Bulut, 2017, "Engineering Geological Assessment and Preliminary Support Design for Cankurtaran Tunnel, NE Turkey”, *MT Bilimsel*, No. 11, pp. 3-11.

Kaya, A., and F. Bulut, 2019, "Geotechnical Studies and Primary Support Design for a Highway Tunnel: A Case Study in Turkey”, *Bulletin of Engineering Geology and the Environment*, Vol. 78, No. 8, pp. 6311-6334.

Kaya, Y., 2021, *Eklemli Kayalarda NATM Tünellerin Yol Açtığı Yüzey Oturmalarının Sayısal Analizlerle İncelenmesi*, M.S. Thesis, Yıldız Technical University.

Kim, S., 2008, “Some Experience from the Soft Ground Tunnelling in Urban Area”, *Seminar on: The State-of-the-art Technology and Experience on Geotechnical Engineering in Korea and Hong Kong*, Hong Kong, P. R. China, pp. 71-109.

Klotoé, C.H. and Bourgeois, E., 2019, “Three Dimensional Finite Element Analysis of the Influence of the Umbrella Arch on the Settlements Induced by Shallow Tunneling”. *Computers and Geotechnics*, Vol. 110, pp. 114-121.

Krenn, F., R. Galler, A. Junker, B. Stacherl, 2008, “Shallow Tunnelling in Soft Ground – Influence of the Chosen Support System on the System Behaviour”, *Geomechanik und Tunnelbau*, Vol.1, No. 3, pp. 207–213.

Küçük, K., 2011, "Influence of Ground Water Effect on Shallow Tunnel: A Case Study”, *Journal of Mining Science*, Vol. 47, No.1, pp. 47-54.

Le, B.T., and R. N. Taylor, 2016, “A Study on the Reinforcing Capabilities of Forepoling Umbrella System in Urban Tunnelling”, *3rd European Conference on Physical Modelling in Geotechnics*, Nantes, France.

Li, R., D. Zhang, P. Wu, Q. Fang, A. Li, and L. Cao, 2020, "Combined Application of Pipe Roof Pre-Support and Curtain Grouting Pre-Reinforcement in Closely Spaced Large Span Triple Tunnels", *Applied Sciences*, Vol. 10, No. 9.

Lunardi, P., 2000, "The Design and Construction of Tunnels Using the Approach Based on the Analysis of Controlled Deformation in Rocks and Soils", *Tunnels & Tunneling International*, pp. 3-30.

Maidl, B., M. Thewes, and U. Maidl, 2013, *Handbook of Tunnel Engineering Volume I: Structures and Methods*, First Edition, Wilhelm Ernst & Sohn, Berlin.

Mair, R. J., 1996, "Settlement Effects of Bored Tunnels", *International Symposium on Geotechnical Aspects of Underground Construction in Soft Ground*, London, United Kingdom, pp. 43-53.

Marotta, M., 2013, *Pre-Supports for Conventional Tunnelling in Soft Ground: Review and Development of Analytical Method of Analysis*, M.S. Thesis, Heriot-Watt University.

Meissner, H., 1996, "Tunnelbau unter Tage - Empfehlungen des Arbeitskreises 1.6 'Numerik in der Geotechnik' Abschnitt 2*"*, *Geotechnik*, Vol. 19, No. 2, pp. 99-108.

Miura, K., 2003, "Design and Construction of Mountain Tunnels in Japan", *Tunnelling and Underground Space Technology*, Vol. 18, No. 2-3, pp. 115-126.

Miwa, M., and M. Ogasawara, 2001, "Constructing a Tunnel Through the Embankment of National Road No. 4 Using the AGF Method", *International Symposium on Modern Tunnelling Science and Technology*, edited by Adachi T., K. Tateyama, and M. Kimura, Vol.1, Kyoto, Japan, pp. 487-492.

Miwa, M., and M. Ogasawara, 2005, "Tunnelling Through an Embankment Using All Ground Fasten Method", *Tunnelling and Underground Space Technology*, Vol. 20, No. 2, pp. 121-127.

Möller, S., 2006, *Tunnel Induced Settlements and Structural Forces in Linings*, Ph. D. Thesis, Universitat of Stuttgart.

Muraki, Y., 1997, *The Umbrella Method in Tunnelling*, M.S. Thesis, Massachusetts Institute of Technology.

Müller, L., and E. Fecker, 1978, "Grundgedanken und Grundsätze der 'Neuen Österreichischen Tunnelbauweise'", *Felsmechanik Kolloquium Karlsruhe: Grundlagen und Anwendungen der Felsmechanik*, edited by Natau, O., E. Fecker, and G. Reik, Karlsruhe, Germany, pp. 247-262.

Nitschke, A., V. Gall, V. Ahuja, 2009, "Modeling of Pipe Arch Canopies in Shallow Soft Ground Tunnels Constructed by Sequential Excavation Methods". *EURO: TUN 2009 2nd International Conference on Computational Methods in Tunnelling*, Bochum, Germany, pp. 9-11.

Norouzi, H., 2020, "The Effect of Loading Type on The Amount of Effect of Loading on The Surface Settlement During Forepoling Tunnel Excavation in Different Geotechnical Conditions", *Journal of Applied Engineering Sciences*, Vol. 10, No. 1, pp. 55-60.

Ocak, İ., and E. Selçuk, 2017, "Comparison of NATM and Umbrella Arch Method in Terms of Cost, Completion Time, and Deformation", *Arabian Journal of Geosciences*, Vol. 10, No. 7.

Oke, J. D. S. H., 2016, *Determination of Nomenclature, Mechanistic Behaviour, and Numerical Modelling Optimization of Umbrella Arch Systems*, Ph. D. Thesis, Queen's University.

Oke J, N. Vlachopoulos, M. Diederichs, 2012, "Sensitivity Numerical Analysis of Orientations and Sizes of Forepoles for Underground Excavations in Weak Rock", *46th US Rock Mechanics / Geomechanics Symposium*, Chicago, United States of America.

Oke, J., N. Vlachopoulos, M. S. Diederichs, 2014b, “The Reduction of Surface Settlement by Employing Umbrella Arch Systems for Different Excavation Methods”, *EUROCK International Symposium*, Vigo, Spain.

Oke, J., N. Vlachopoulos, V. Marinos, 2014a, “Umbrella Arch Nomenclature and Selection Methodology for Temporary Support Systems for the Design and Construction of Tunnels”, *Geotechnical and Geological Engineering*, Vol.32, No. 1, pp. 97-130.

ÖNORM B 2203-1, 1994, Underground Works – Works Contract. Part 1: Cyclic Driving (Conventional Tunnelling), Österreichisches Normungsinstitut.

Özer, S. C., 2011, *Tünel Kazılarında Optimum Çelik Boru Kemer Boyutunun Nümerik Modelleme İle Tayini*, M.S. Thesis, Dokuz Eylül University.

Pacher, F., 1964, “Deformationsmessungen im Versuchsstollen als Mittel zur Erforschung des Gebirgsverhaltens und zur Bemessung des Ausbaues”, *Grundfragen auf dem Gebiete der Geomechanik: XIV. Kolloquium der Österreichischen Regionalgruppe (i. Gr.) der Internationalen Gesellschaft für Felsmechanik*, Salzburg, Austria, pp. 149-161.

Pashaye, N.S. F. Moradinia, and A. Ferdousi, 2021, “Using Umbrella Arch Method in Design of Tunnel Lining, Case Study: Water Transfer Tunnel of Kani-Sib, Urmia Lake”, *Numerical Methods in Civil Engineering*, Vol. 6, No. 2, pp. 1-13.

Peila, D., C. Marchino, C. Todaro, and A. Luciani, 2017, “Comparison of the Results of Analytical and Numerical Models of Pre-Reinforcement in Shallow Tunnels”, *Archives of Civil Engineering*, Vol. 18, No. 4.

Pelizza, S. and D. Peila, 1993, “Soil and Rock Reinforcements in Tunnelling”, *Tunnelling and Underground Space Technology*, Vol. 8, No. 3, pp. 357-372.

Perveroğlu Şat, T., A. Türkoğlu, and H.İ. Şahin, 2023, “The Effect of Single and Double umbrella Arch Applications on Surface Settlement in NATM Technics with the Same

Geological Formation; Çekmeköy – Sultanbeyli Subway Example", *5th International Underground Excavations Symposium*, İstanbul, Türkiye, pp. 195-209.

PLAXIS 2D CONNECT Edition V22.00 - Tutorial Manual, 2021, Bentley Systems Incorporated, Exton, PA, United States of America.

PLAXIS 2D CONNECT Edition V22.02 - Reference Manual, 2022, Bentley Systems Incorporated, Exton, PA, United States of America.

Proctor, R.V. and T. L. White, 1946, *Rock Tunneling with Steel Supports*, The Youngstown Printing Co., Youngstown, Ohio, United States of America.

Rabcewicz, L. v., 1964a, "The New Austrian Tunnelling Method, Part One", *Water Power*, Vol. 16, No. 11, pp. 453-457.

Rabcewicz, L. v., 1964b, "The New Austrian Tunnelling Method, Part Two", *Water Power*, Vol. 16, No. 12, pp. 511-515.

Rabcewicz, L. v., 1965, "The New Austrian Tunnelling Method, Part Three", *Water Power*, Vol. 17, No. 1, pp. 19-24.

RocSupport Tutorial Manual: Rock Support Interaction and Deformation Analysis for Tunnels in Weak Rock, 2004, RocScience Incorporated.

Rostami, A., P. K. Dehkordi, M. A. Ziarati, S. Jahani, K. Lotfi, 2016, "The Types of Tunnels Maintenance in Umbrella Arch Method". *Open Journal of Civil Engineering*, Vol. 6, No. 2, pp. 156-162.

Rutledge, J.C., and R.L. Preston, 1978, "New Zealand Experience with Engineering Classifications of Rock for the Prediction of Tunnel Support". *International Tunnel Symposium*, Tokyo, Japan, pp. A3.1-7.

Sarıgül, G., 2018, *Terzili ve Ulubey T1 Tünelleri Killerinin Şişme Davranışının İncelenmesi*, M.S. Thesis, Bülent Ecevit University.

Sauer, G., 1988, "Further Insights into the NATM", *Tunnelling '88*, London, United Kingdom.

Sauer, G., 1990, "Design Concept for Large Underground Openings in Soft Ground Using NATM", *International Symposium on Unique Underground Structures*, Denver, Colorado, United States of America.

Sauer, G., and H. Gold, 1989, "NATM Ground Support Concepts and Their Effect on Contract Practices", *Rapid Excavation and Tunneling Conference*, Los Angeles, CA, United States of America.

Schubert, W., 2015, "Development and Background of NATM", *Austrian Tunnelling Seminar*, Ankara, Türkiye.

Schubert, W., and H. Lauffer, 2012, "NATM – from a Construction Method to a System / NÖT – von der Bauweise zum System", *Geomechanik und Tunnelbau*, Vol. 5, No. 5, pp. 455-463.

Selçuk, E., 2016, *Tünelcilikte NATM ve Boru Kemer Yönteminin, Zaman, Maliyet ve Deformasyon Açısından Karşılıştırılması*, M.S. Thesis, İstanbul University.

Shin, J.-H., Y.-K. Choi, O.-Y. Kwon, and S.-D. Lee, 2008, "Model Testing for Pipe-Reinforced Tunnel Heading in a Granular Soil", *Tunneling and Underground Space Technology*, Vol. 23, No. 3, pp. 241-250.

Sojoudi, H., 2015, *Yerleşim Alanlarında Tünel Kazılarına Bağlı Deformasyonların Modellenmesi*, M.S. Thesis, Ankara University.

Song, K. I., G. C. Cho, S. B. Chang, and I. M. Lee, 2013, "Beam–Spring Structural Analysis for the Design of a Tunnel Pre-Reinforcement Support System", *International Journal of Rock Mechanics & Mining Sciences*, Vol. 59, pp. 139-150.

Széchy, K., 1970, *The Art of Tunneling*, First Edition, Akadémiai Kiadó, Budapest, Hungary.

Tan, W. L., 2005, *Numerical Analysis for Shallow Tunnels in Weak Ground Supported by Umbrella Arch Method*, M.S. Thesis, Nanyang Technological University.

Tanaka, Y., 1996, "Longest Two-Face Tunnel in Japan Being Constructed with NATM. Construction of Kozukayama Tunnel For the 2nd Shinmei Highway", *Journal of the Japan Society of Civil Engineers*, Vol. 81, No. 10.

Technical Manual for Design and Construction of Road Tunnels - Civil Elements, 2009, U.S. Department of Transportation Federal Highway Administration (FHWA).

Terzaghi, K., 1943, *Theoretical Soil Mechanics*, J. Wiley and Sons, New York, United States of America.

Terzaghi, K., 1946, "Rock Defects and Loads in Tunnel Supports", *Rock Tunneling with Steel Supports*, edited by Proctor R. V. and T.L. White, The Commercial Shearing and Stamping Co., Youngstown, Ohio, United States of America, pp. 47-91.

Tonon, F., 2011, "ADECO Full-Face Tunnel Excavation of Two 260 m^2 Tubes in Clays with Sub-Horizontal Jet-Grouting Under Minimal Urban Cover", *Tunnelling and Underground Space Technology*, Vol. 26, No. 2, pp. 253–266.

Trunk, U., and F. Winkler, 2013, "Jet Grouting in Tunnelling", *Geomechanik und Tunnelbau*, Vol. 6, No. 3, pp. 274-289.

Türköz, N. D., 2023, *Assessment of Tunnel Stability and Determination of Tunnel Support Systems for a Segment (Km:90+222.10-93+435.70) of Afyonkarahisar – Burdur Railway Line*, M.S. Thesis, Middle East Technical University.

Volkmann, G.M., and W. Schubert, 2007, “Geotechnical Model for Pipe Roof Supports in Tunneling.”, *33rd ITA - AITES World Tunneling Congress, Underground Space - the 4th Dimension of Metropolises*, Prague, Czech Republic, Vol. 1, pp. 755-760.

Wang, H. T., J. Q. Jia, and H. G. Kang, 2009, “Analytical Approach and Field Monitoring for Mechanical Behaviors of Pipe Roof Reinforcement”, *Journal of Central South University of Technology*, Vol.16, No.5, pp. 827-834.

Wang, Y., Z. Hu, Y. Xie, C. Wang, K. Hua, J. Lai, and H. Lai, 2020, “Numerical Experiment for Support Effect of Umbrella Arch in Tunnel”, *6th International Conference on Environmental Science and Civil Engineering*, Nanchang, P.R. China.

Wickham, G. E., H. R. Tiedemann, and E. H. Skinner, 1972, “Support Determination Based on Geologic Predictions", *Rapid Excavation and Tunneling Conference*, Chicago, IL, United States of America, pp. 43-64.

Wijaya, W., P. P. Rahardjo, and A. Lim, 2021, "Investigation of Twin Tunnel Deformation with Umbrella Grouting Protection & NATM Tunneling Using 3D Finite Element: Case Study Cisumdawu Tunnel”, *Universitas Kadiri Riset Teknik Sipil*, Vol. 5, No. 2, pp. 252-267.

Yang, J. S., D. M. Gou, Y. X. Zhang, 2008, “Field Measurements and Numerical Analyses of Double-Layer Pipe Roof Reinforcement in a Shallow Multiarch Tunnel”, *Transportation Research Record,* Vol. 2050, No. 1, pp. 145-153.

Yeo, C.H., F.H. Lee, A. Hegde, and A. Juneja, 2010, “Centrifuge Modelling of a Steel Pipe Umbrella Arch for Tunnelling in Clay”, *7th International Conference on Physical Modelling in Geotechnics*, Zurich, Switzerland, pp. 611-616.

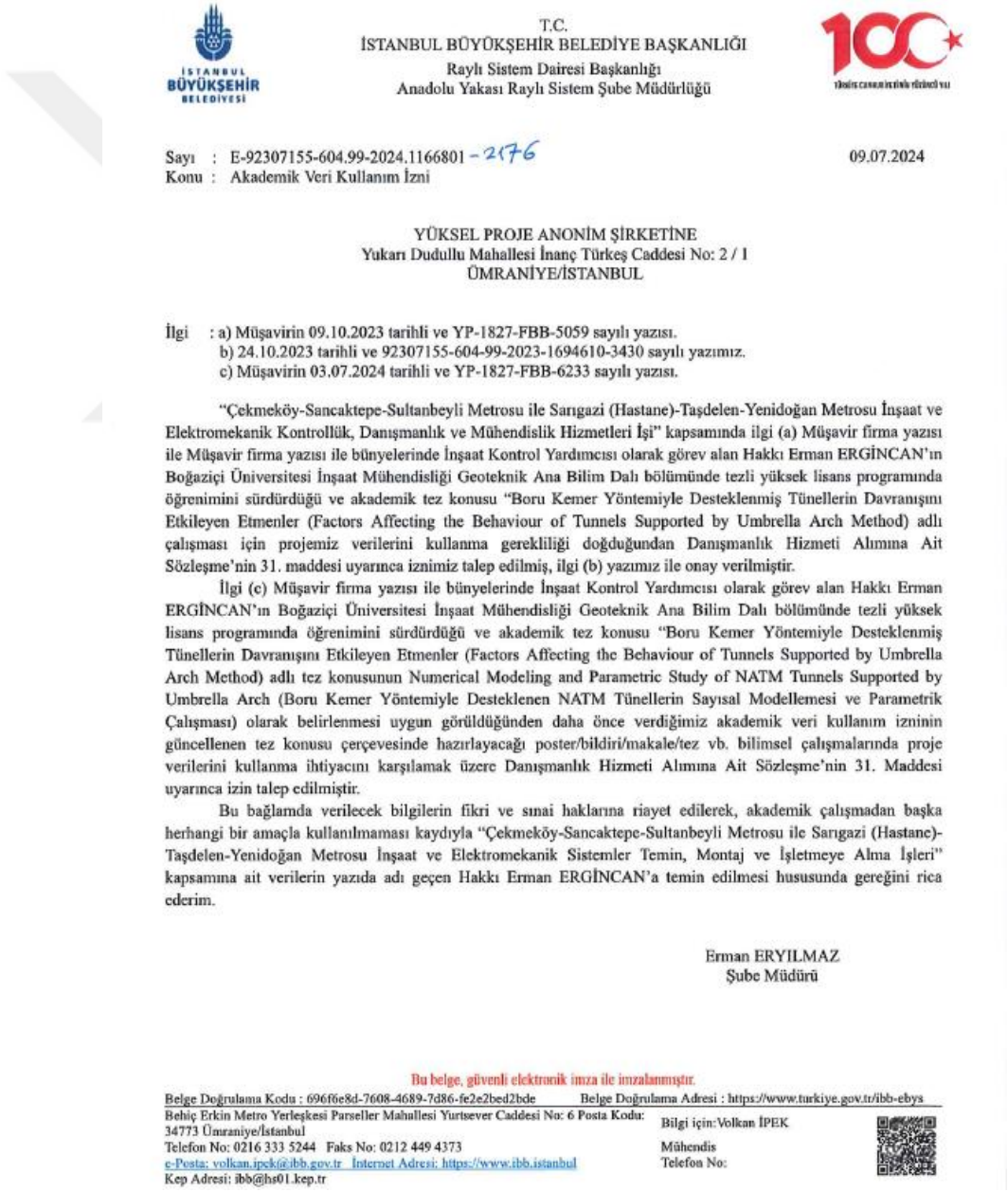
Zarei, H., P. Moarefvand, and E. F. Salmi, 2019, "Numerical Modeling of Umbrella Arch Technique to Reduce Tunnelling Induced Ground Movements", *Environmental Earth Sciences*, Vol. 78, pp. 1-22.

Zelger, J., 2012, *Calibration of 2D Pre-Relaxation Factors in Tunnelling with 3D Finite Element Calculations*, M.S. Thesis, Graz University of Technology.

Zhang, X., M. Wang, Z. Wang, J. Li, S. Zhao, J. Tong, and D. Liu, 2020, "Stability Analysis Model for a Tunnel Face Reinforced with Bolts and an Umbrella Arch in Cohesive-Frictional Soils", *Computers and Geotechnics*, Vol. 124.

APPENDIX A: DATA USE PERMISSION FOR ACADEMIC PURPOSES

For this study, the author has benefitted from the data of the metro project located in İstanbul with permission of Anatolian Side Rail Systems Section Directorate of Department of Rail Systems of İstanbul Metropolitan Municipality, as submitted in Figure A.1.



T.C.
İSTANBUL BÜYÜKŞEHİR BELEDİYE BAŞKANLIĞI
Raylı Sistem Dairesi Başkanlığı
Anadolu Yakası Raylı Sistem Şube Müdürlüğü

Sayı : E-92307155-604.99-2024.1166801 - 2176 09.07.2024
Konu : Akademik Veri Kullanım İzni

YÜKSEL PROJE ANONİM ŞİRKETİNE
Yukarı Dudullu Mahallesi İnanç Türkeş Caddesi No: 2 / 1
ÜMRANİYE/İSTANBUL

İlgi : a) Müşavirin 09.10.2023 tarihli ve YP-1827-FBB-5059 sayılı yazısı.
b) 24.10.2023 tarihli ve 92307155-604-99-2023-1694610-3430 sayılı yazımız.
c) Müşavirin 03.07.2024 tarihli ve YP-1827-FBB-6233 sayılı yazısı.

"Çekmeköy-Sancaktepe-Sultanbeyli Metrosu ile Sarıgazi (Hastane)-Taşdelen-Yenidoğan Metrosu İnşaat ve Elektromekanik Kontrollük, Danışmanlık ve Mühendislik Hizmetleri İşi" kapsamında ilgi (a) Müşavir firma yazısı ile Müşavir firma yazısı ile bünyelerinde İnşaat Kontrol Yardımcısı olarak görev alan Hakkı Erman ERGİNCAN'ın Boğaziçi Üniversitesi İnşaat Mühendisliği Geoteknik Ana Bilim Dalı bölümünde tezli yüksek lisans programında öğrenimini sürdürdüğü ve akademik tez konusu "Boru Kemer Yöntemiyle Desteklenmiş Tünellerin Davranışını Etkileyen Etmenler (Factors Affecting the Behaviour of Tunnels Supported by Umbrella Arch Method) adlı çalışması için projemiz verilerini kullanma gerekliliği doğduğundan Danışmanlık Hizmeti Alımına Ait Sözleşme'nin 31. maddesi uyarınca iznimiz talep edilmiş, ilgi (b) yazımız ile onay verilmiştir.

İlgi (c) Müşavir firma yazısı ile bünyelerinde İnşaat Kontrol Yardımcısı olarak görev alan Hakkı Erman ERGİNCAN'ın Boğaziçi Üniversitesi İnşaat Mühendisliği Geoteknik Ana Bilim Dalı bölümünde tezli yüksek lisans programında öğrenimini sürdürdüğü ve akademik tez konusu "Boru Kemer Yöntemiyle Desteklenmiş Tünellerin Davranışını Etkileyen Etmenler (Factors Affecting the Behaviour of Tunnels Supported by Umbrella Arch Method) adlı tez konusunun Numerical Modeling and Parametric Study of NATM Tunnels Supported by Umbrella Arch (Boru Kemer Yöntemiyle Desteklenen NATM Tünellerin Sayısal Modellemesi ve Parametrik Çalışması) olarak belirlenmesi uygun görüldüğünden daha önce verdiğimiz akademik veri kullanım izninin güncellenen tez konusu çerçevesinde hazırlayacağı poster/bildiri/makale/tez vb. bilimsel çalışmalarında proje verilerini kullanma ihtiyacını karşılamak üzere Danışmanlık Hizmeti Alımına Ait Sözleşme'nin 31. Maddesi uyarınca izin talep edilmiştir.

Bu bağlamda verilecek bilgilerin fikri ve sınai haklarına riayet edilerek, akademik çalışmadan başka herhangi bir amaçla kullanılmaması kaydıyla "Çekmeköy-Sancaktepe-Sultanbeyli Metrosu ile Sarıgazi (Hastane)-Taşdelen-Yenidoğan Metrosu İnşaat ve Elektromekanik Sistemler Temin, Montaj ve İşletmeye Alma İşleri" kapsamına ait verilerin yazıda adı geçen Hakkı Erman ERGİNCAN'a temin edilmesi hususunda gereğini rica ederim.

Erman ERYILMAZ
Şube Müdürü

Bu belge, güvenli elektronik imza ile imzalanmıştır.
Belge Doğrulama Kodu : 696f6e8d-7608-4689-7d86-fe2e2bed2bde Belge Doğrulama Adresi : https://www.turkiye.gov.tr/ibb-ebys
Behiç Erkin Metro Yerleşkesi Parseller Mahallesi Yurtsever Caddesi No: 6 Posta Kodu: 34773 Ümraniye/İstanbul
Telefon No: 0216 333 5244 Faks No: 0212 449 4373
e-Posta: volkan.ipek@ibb.gov.tr İnternet Adresi: https://www.ibb.istanbul
Kep Adresi: ibb@hs01.kep.tr
Bilgi için:Volkan İPEK
Mühendis
Telefon No:

Figure A.1. Official permission to use of the project data for academic purposes.

APPENDIX B: VISUAL REUSE PERMISSION

In the thesis booklet, the visuals created within the validation scope of this thesis and copyrighted to the publisher have been used in accordance with the "current editorial policy on the reuse of self-produced text and graphics" situated on the publisher's web page.